

COMPUTATIONAL ANALYSIS FOR PERFORMANCE PREDICTION OF  
STIRLING CRYOCOOLERS

A THESIS SUBMITTED TO  
THE GRADUATE SCHOOL OF NATURAL AND APPLIED SCIENCES  
OF  
MIDDLE EAST TECHNICAL UNIVERSITY

BY

SEMİH ÇAKIL

IN PARTIAL FULFILLMENT OF THE REQUIREMENTS  
FOR  
THE DEGREE OF MASTER OF SCIENCE  
IN  
MECHANICAL ENGINEERING

DECEMBER 2010

Approval of the thesis:

**COMPUTATIONAL ANALYSIS FOR PERFORMANCE PREDICTION OF  
STIRLING CRYOCOOLERS**

submitted by **SEMİH ÇAKIL** in partial fulfillment of the requirements for the degree of **Master of Science in Mechanical Engineering Department, Middle East Technical University** by,

Prof. Dr. Canan Özgen  
Dean, Graduate School of **Natural and Applied Sciences** \_\_\_\_\_

Prof. Dr. Suha Oral  
Head of Department, **Mechanical Engineering** \_\_\_\_\_

Assoc. Prof. Dr. Cemil Yamalı  
Supervisor, **Mechanical Engineering Dept., METU** \_\_\_\_\_

**Examining Committee Members:**

Prof. Dr. Kahraman Albayrak  
Mechanical Engineering Dept., METU \_\_\_\_\_

Assoc. Prof. Dr. Cemil Yamalı  
Mechanical Engineering Dept., METU \_\_\_\_\_

Asst. Prof. Dr. Almıla Güvenç Yazıcıoğlu  
Mechanical Engineering Dept., METU \_\_\_\_\_

Dr. Tahsin Çetinkaya  
Mechanical Engineering Dept., METU \_\_\_\_\_

Asst. Prof. Dr. İbrahim Atılğan  
Mechanical Engineering Dept., Gazi University \_\_\_\_\_

**Date: 16.12.2010**

**I hereby declare that all information in this document has been obtained and presented in accordance with academic rules and ethical conduct. I also declare that, as required by these rules and conduct, I have fully cited and referenced all material and results that are not original to this work.**

Name, Last name : SEMİH ÇAKIL

Signature :

## **ABSTRACT**

### **COMPUTATIONAL ANALYSIS FOR PERFORMANCE PREDICTION OF STIRLING CRYOCOOLERS**

Çakıl, Semih

M.Sc., Department of Mechanical Engineering

Supervisor: Assoc. Prof. Cemil Yamalı

December 2010, 101 pages

Stirling cryocoolers are required for a wide variety of applications, especially in military equipment, due to their small size, low weight, long lifetime and high reliability considering their efficiency. Thus, it is important to be able to investigate the operating performance of these coolers in the design stage.

This study focuses on developing a computer program for simulating a Stirling cryocooler according to the second order analysis. The main consideration is to simulate thermodynamic, fluid dynamic and heat transfer behavior of Stirling cryocoolers. This goal is achieved by following the route of Urieli (1984), which was focused on Stirling cycle engines.

In this research, a simulation for performance prediction of a Stirling cryocooler is performed. In addition to that, the effects of system parameters are investigated. This attempt helps to understand the real behavior of Stirling cryocoolers using porous regenerator material. Results implied that first order analysis methods give optimistic predictions where second order method provides more realistic data compared to first order methods. In addition to that, it is shown that regenerator porosity has positive effect on heat transfer characteristics while affecting flow friction negatively.

As a conclusion, this study provides a clear understanding of loss mechanisms in a cryocooler. Performed numerical analysis can be used as a tool for investigation of effects of system parameters on overall performance.

Key words: Stirling cryocooler, simulation, computer analysis, second order, porous regenerator

## ÖZ

### STİRLİNG KRİYOJENİK SOĞUTUCUSU İÇİN PERFORMANS TAHMİNİ AMAÇLAYAN YAZILIM GELİŞTİRİLMESİ

Çakıl, Semih

Yüksek Lisans, Makina Mühendisliği Bölümü

Tez Yöneticisi: Doç. Dr. Cemil Yamalı

Aralık 2010, 101 sayfa

Stirling kriyojenik soğutucuları, yüksek verimliliklerinin yanı sıra küçük boyutlu, hafif, uzun ömürlü ve güvenilirlerdir. Bu özellikleri ile başlıca askeri donanımlarda olmak üzere çok geniş bir kullanım alanına sahiptirler. Bu sebeple, bu soğutucuların çalışma performanslarının henüz tasarım aşamasında dikkatlice incelenmesi gerekmektedir.

Bu çalışma, Stirling kriyojenik soğutucuların simülasyonu için, ikinci dereceden analiz yöntemlerine göre bir bilgisayar programı geliştirmeyi amaçlamıştır. Burada asıl kaygı bu soğutucuların termodinamik, akışkanlar dinamiği ve ısı transferi özelliklerini canlandırmaktır. Bu hedef Urieli'nin (1984) Stirling döngülü motorlar için geliştirdiği yöntem izlenerek gerçekleştirilmiştir.

Bu arařtırmada Stirling kriyojenik sođutucusunun performans tahminini amalayan bir simulasyon gerekleřtirilmesi amalanmıřtır. Buna ek olarak sistem deđiřkenlerinin sistem üzerindeki etkileri incelenmiřtir. Bu inceleme gzenekli rejeneratr ihtiva eden Stirling kriyojenik sođutucularını anlamada yardımcı olmaktadır. Sonular, ikinci dereceden analiz metodu gereki deđerler verirken birinci dereceden analiz metodlarının ok iyimser kaldıđını gstermektedir. Buna ek olarak, rejeneratr gzenekliliđinin ısı transfer zelliklerini olumlu etkilediđi, ancak aynı zamanda srtnmeden kaynaklanan kayıpları arttırdıđı gzlemlenmiřtir.

Bu alıřma bir kriyojenik sođutucudaki kayıp mekanizmalarının iyi bir řekilde anlařılmasını sađlanmıřtır. Gerekleřtirilen sayısal analiz sistem parametrelerinin toplam performans üzerindeki etkilerinin incelenmesinde kullanılabilir.

Anahtar Kelimeler: Stirling kriyojenik sođutucu, simulasyon, bilgisayar analizi, ikinci derece, gzenekli rejeneratr

*To my family*

## ACKNOWLEDGMENTS

I would like to express my deepest gratitude to my supervisor Assoc. Prof. Dr. Cemil Yamalı for his guidance, support and valuable suggestions in preparing this thesis.

I feel great appreciation to Alper Ünsoy for his helpful advices, support and encouragement.

The examining committee members Prof. Dr. Kahraman Albayrak, Asst. Prof. Dr. Almıla Güvenç Yazıcıoğlu, Asst. Prof. Dr. İbrahim Atılğan and Dr. Tahsin Çetinkaya greatly acknowledged for their participation, comments and suggestions.

I am deeply thankful to my colleagues for their friendship, moral support and suggestions throughout this study.

I would like to express my endless gratitude to my parents for their love, endless support and trust throughout my life.

Last but not least, I would like to thank to Yaprak Dönmez for her precious support, care, love and patience.

## TABLE OF CONTENTS

ABSTRACT .....	iv
ÖZ .....	vi
ACKNOWLEDGMENTS .....	ix
TABLE OF CONTENTS .....	x
LIST OF TABLES .....	xii
LIST OF FIGURES .....	xiii
NOMENCLATURE.....	xvi
CHAPTERS	
1 INTRODUCTION .....	1
1.1. Cryogenic cooling .....	1
1.2. Cryocoolers .....	3
1.2.1 Recuperative Cryocoolers .....	4
1.2.2 Regenerative Cryocoolers .....	5
1.3 Stirling Cryocoolers .....	7
1.3.1 Stirling Cycle .....	9
1.3.1.1 Work input to an ideal Stirling-cycle refrigerator or heat-pump .....	11
1.3.1.2 Heat flow in an ideal Stirling-cycle refrigerator or heat-pump.....	13
1.3.1.3 Performance of an ideal Stirling-cycle refrigerator or heat-pump ....	15
1.3.2 The Regenerator .....	16
1.3.3 Types of Stirling Cryocoolers .....	17
1.3.3.1 Rotary Compressor & Mechanically Driven Expander .....	17
1.3.3.2 Rotary Compressor & Pneumatically Driven Expander .....	18
1.3.3.3 Linear Compressor & Linear Motor Driven Expander .....	19
1.3.3.4 Linear Compressor & Pneumatically Driven Expander .....	19
1.3.4 Theoretical Analysis of Stirling Cryocoolers.....	20
1.3.4.1 Zeroth Order Analysis.....	20

1.3.4.2 First Order Analysis .....	21
1.3.4.3 Second Order Analysis Methods.....	23
1.3.4.4 Third Order or Nodal Analysis Methods .....	25
1.4 Scope of the Thesis .....	26
2 COMPUTATIONAL ANALYSIS OF STIRLING CRYOCOOLERS .....	27
2.1 The Schmidt Analysis .....	27
2.2 Ideal Adiabatic Analysis .....	33
2.3. Simple analysis .....	39
2.3.1. Regenerator simple analysis.....	40
2.3.2. Heat exchanger simple analysis .....	44
2.3.3. Pressure drop simple analysis .....	46
2.3.4. Correlations used in simple analysis .....	49
2.3.4. Performance of the cryocooler .....	50
2.4 Solution method .....	52
3 ANALYSIS AND RESULTS .....	54
3.1. Cryocooler dimensions and operational data used in the analysis.....	54
3.2. Schmidt Analysis Results.....	56
3.3. Ideal adiabatic Analysis Results.....	58
3.4. Simple Analysis Results.....	64
3.5. Effect of system parameters on the performance .....	67
3.5.1. Effect of porosity.....	67
3.5.2. Effect of operating frequency.....	71
3.5.3. Effect of operating temperatures .....	75
3.5.3. Effect of charging pressure .....	77
3.5.4. Effect of phase angle.....	79
4 CONCLUSION .....	81
4.1 Interpretation of the results of the three analysis .....	81
4.2 Future work and recommendations.....	82
REFERENCES.....	83
APPENDICES	
A.....	88

## LIST OF TABLES

### TABLES

Table 1. 1 Cryocooler Applications (Radebaugh, 1995; Timmerhaus, 1996). .....	2
Table 1. 2: Specific gas constants (Wyllen et al., 1994). .....	13
Table 3. 1 Cryocooler dimensions and operating parameters.....	55
Table 3. 2 Comparison of three analysis methods .....	67

## LIST OF FIGURES

### FIGURES

Figure 1. 1 Most important recuperative (A) and regenerative (B) cycles used in cryocoolers. (Radebaugh, 2000). .....	3
Figure 1. 2 Stirling-cycle machine block diagrams: (A) Engine (B) Refrigerator or heat-pump (Haywood, 2008). .....	8
Figure 1. 3 Four sizes of Stirling cryocoolers with dual-opposed linear compressors (Radebaugh, 2000). .....	9
Figure 1. 4 P-V and T-s diagrams of stirling refrigerator (Haywood, 2008). .....	10
Figure 1. 5 The four steps in the Stirling Cycle (Willems, 2007). .....	11
Figure 1. 6 Rotary kinematic Stirling cryocooler (Riabzev, 2002). .....	18
Figure 1. 7 Rotary pneumatic stirling cryocooler (Riabzev, 2002). .....	18
Figure 1. 8 Linear kinematic stirling cryocooler (Riabzev, 2002). .....	19
Figure 1. 9 Linear pneumatic stirling cryocooler (Riabzev, 2002). .....	20
Figure 1. 10 Ideal isothermal model (Urieli) (Dyson et al., 2004). .....	22
Figure 1. 11 Closed Form Solution Process (Urieli) reproduced: ideal isothermal model set of equations (Dyson et al., 2004). .....	22
Figure 2. 1 Trigonometric substitution of $\beta$ and c (Schmidt, 1871). .....	29
Figure 2. 2 Regenerator linear temperature profile (Creswick 1965) .....	32
Figure 2. 3 Conditional interface temperature .....	34
Figure 2. 4 Temperature distribution in a non-ideal regenerator .....	41
Figure 2. 5 Newton's conceptual model for defining the viscosity of a real fluid....	46
Figure 2. 6 Algorithm of numerical simulation by simple analysis .....	53
Figure 3. 1 Cryocooler schematics .....	54
Figure 3.2 PV diagram obtained by Schmidt analysis .....	57
Figure 3. 3 Volume variations with respect to crank angle.....	58
Figure 3.4 PV diagram obtained by ideal adiabatic analysis .....	59
Figure 3.5 Pressure by ideal adiabatic analysis with respect to crank angle (j).....	60

Figure 3.6 Mass variations with respect to crank angle in compression space(c), expansion space(e), regenerator(r), freezer(h),and cooler(k) sections.....	60
Figure 3. 7 Temperature with respect tocrank angle in compression (c) and expansion (e) spaces.....	61
Figure 3. 8 Heat transfer in the cooler ( $Q_H$ ), freezer ( $Q_L$ ), regenerator ( $Q_r$ ) and expansion work ( $W_e$ ), compression work ( $W_c$ ) and.....	62
Figure 3.9 Heat transfer in the cooler (K), freezer (H) and expansion work (e), with respect to crank angle.....	63
Figure 3.10 PV diagram obtained by simple analysis and ideal adiabatic analysis..	64
Figure 3.11 Pressure drop variations with respect to crank angle in regenerator (r), in cooler (k) and in freezer(h) .....	65
Figure 3.12 Temperature variation with respect to crank angle (i) in expansion (e) and in compression (c) spaces after simple analysis.....	66
Figure 3.13 Regenerator effectiveness $\varepsilon$ versus porosity $\psi$ at different mesh wire diameters plot.....	68
Figure 3.14 Coefficient of performance COP versus porosity $\psi$ at different mesh wire diameters plot.....	69
Figure 3.15 Pressure drop in the regenerator with respect to crank angle at porosity values between 0.5 and 0.9 .....	70
Figure 3.16 Regenerator loss $Q_{Rloss}$ versus porosity $\psi$ plot at different mesh wire diameters.....	71
Figure 3.17 Coefficient of performance at different cold side temperatures versus operating frequency at different cold side temperatures plot.....	73
Figure 3.18 Loss due to pressure drop $\Delta W$ [W] at different cold side temperatures versus operating frequency plot .....	74
Figure 3.19 Cooler gas temperature at different cold side temperatures versus frequency plot.....	74
Figure 3.20 Heat rejected at different cold side temperatures vs frequency plot.....	75
Figure 3.21 Coefficient of performance at different hot side temperatures versus freezer wall temperature.....	76

Figure 3.22 Heat removed at different temperatures versus freezer wall temperature .....	77
Figure 3.23 Coefficient of performance at different cold side temperatures versus charge pressure plot.....	78
Figure 3. 24 Heat removed at different cold side temperatures versus charge pressure plot .....	79
Figure 3.25 Coefficient of performance and heat removed [W] versus phase angle plot .....	80
Figure 3.26 Coefficient of performance and work input [W] versus phase angle plot .....	80

## NOMENCLATURE

- $A$  = free flow area in the heat exchanger
- $A_r$  : Free flow area of regenerator
- $A_{wg}$  = wetted surface area in the heat exchanger
- $A_{wgh}$  = wetted surface area in the freezer
- $A_{wgc}$  = wetted surface area in the cooler
- $C_p$  : Specific heat capacity at constant pressure
- $C_v$  : Specific heat capacity at constant volume
- $COP$  : Coefficient of performance
- $d_H$  : Hydraulic diameter
- $E$  : Total energy of the gas
- $f$  = angular frequency,
- $F$  : Frictional drag force
- $f_f$  : Fanning friction factor
- $f_R$  : Friction factor
- $h$  : Convective heat transfer coefficient
- $k$  : thermal conductivity
- $k_{rw}$  : Thermal conductivity of the regenerator wall
- $L$  : Length
- $L_r$  : Length of the regenerator
- $M$  : Total mass of the gas in the cryocooler
- $m$  : Working gas mass
- $m_c$  : Working gas mass in the compression space
- $m_k$  : Working gas mass in the cooler

$m_r$  : Working gas mass in the regenerator  
 $m_h$  : Working gas mass in the freezer  
 $m_e$  : Working gas mass in the expansion space  
 $\dot{m}$  : Mass flow rate  
 $\dot{m}_{ck}$  : Mass flow rate between compressor and cooler  
 $\dot{m}_{kr}$  : Mass flow rate between cooler and regenerator  
 $\dot{m}_{rh}$  : Mass flow rate between regenerator and freezer  
 $\dot{m}_{he}$  : Mass flow rate between freezer and expansion space  
 $P$  : Working gas pressure  
 $P_{mean}$  : Mean working gas pressure  
 $Q$  : Heat transferred  
 $Q_H$  : Heat transferred from the working gas in the cooler space  
 $Q_L$  : Heat transferred to the working gas in the freezer space  
 $Q_r$  : Heat transferred in the regenerator space  
 $Q_{R_{loss}}$  : Regenerative loss  
 $Q_{R_{ideal}}$  : Heat transfer in the regenerator evaluated by ideal adiabatic analysis  
 $Q_{L_{ideal}}$  : Heat transferred to the working gas in the freezer space evaluated by  
     ideal adiabatic analysis  
 $Q_{H_{ideal}}$  : Heat transferred from the working gas in the cooler space evaluated by  
     ideal adiabatic analysis  
 $S$  : Entropy  
 $T$  : Temperature  
 $T_H$  : Hot side temperature  
 $T_L$  : Cold side temperature  
 $T_h$  : Freezer wall temperature  
 $T_k$  : Cooler wall temperature

$T_{gh}$  : Temperature of the gas in the freezer  
 $T_{gk}$  : Temperature of the gas in the cooler  
 $T_r$  : Temperature of the gas in the regenerator  
 $T_c$  : Temperature of the gas in the compression space  
 $T_e$  : Temperature of the gas in the expansion space  
 $T_{hc-in}$  : Temperature of the gas entering to the regenerator from the freezer  
 $T_{hc-out}$  : Temperature of the gas entering to the cooler from the regenerator  
 $T_{ch-in}$  : Temperature of the gas entering to the regenerator from the cooler  
 $T_{ch-out}$  : Temperature of the gas entering to the freezer from the regenerator  
 $u$  : Velocity of the gas  
 $V$  : Volume  
 $V_{swe}$  : Expansion space swept volume  
 $V_{swc}$  : Compression space swept volume  
 $V_{clc}$  : Compression space clearance volume  
 $V_{cle}$  : Expansion space clearance volume  
 $V_r$  : Volume of the regenerator  
 $V_c$  : Volume of the compression space  
 $V_e$  : Volume of the expansion space  
 $V_h$  : Volume of the freezer  
 $V_k$  : Volume of the cooler  
 $V_r$  : Volume of the regenerator  
 $V$  : Total energy of the gas  
 $V$  : Total energy of the gas  
 $W$  : Work done  
 $W_c$  : Work done in compression space  
 $W_e$  : Work done in expansion space  
 $W_{in}$  : Net work input

ST : Stanton number

RE : Reynold's number

Pr : Prandtl number

$\rho$  : density

$\gamma$  : Ratio of specific heat capacity at constant pressure to specific heat capacity at constant volume

$\theta$  = crank angle

$\alpha$  = angular phase advance of the expansion space volume variations with respect to the compression space volume variations

$\varepsilon$  : Effectiveness of the regenerator

$\phi$  : mass flux

$\psi$  : porosity

$P_{mean}$  = mean pressure of the system

$\mu$  : dynamic viscosity

$\sigma$  : shear stress in the flow field

## CHAPTER 1

### INTRODUCTION

#### 1.1. Cryogenic cooling

Cryogenics (production of cold) can be described as the branch of physics dealing with the production of very low temperatures and the methods to measure such temperatures (Ventura and Risegari, 2008). Although 'very low temperatures' are not specifically defined, the boiling points of nitrogen (77 K), air (79 K), or natural gas (111 K) are commonly preferred as the limit. In addition to these, the limit of 100 K and lower is often used. Cryogenic cooling can be described as a cooling that requires more advanced techniques in order to reach and maintain those temperatures. Cryogenic cooling can be carried out by means of cryocoolers, which are also called cryogenic refrigerators (Willems , 2007).

Cryogenic cooling is usually the preferred design solution for applications requiring substantial cooling over an extended period (Aerospace, 2009). Main applications where cryogenic cooling namely cryocoolers are needed are given in Table 1.1.

Table 1. 1 Cryocooler Applications (Radebaugh, 1995; Timmerhaus, 1996).

Military	<ol style="list-style-type: none"> <li>1) Infrared sensors for missile guidance</li> <li>2) Infrared sensors for surveillance (satellite based)</li> <li>3) Superconducting magnets for mine sweeping</li> </ol>
Industrial and Commercial	<ol style="list-style-type: none"> <li>1) Superconductors for high-speed communication</li> <li>2) Semiconductors for high-speed computers</li> <li>3) Cryopumps for semiconductor manufacture</li> <li>4) Low-level moisture sensors for ultrapure gases</li> <li>5) Infrared sensors for process monitoring</li> </ol>
Medical	<ol style="list-style-type: none"> <li>1) Superconducting magnets for MRI systems</li> <li>2) SQUID magnetometers for heart and brain studies</li> <li>3) Blood and semen storage</li> <li>4) Cryosurgery</li> </ol>
Energy	<ol style="list-style-type: none"> <li>1) LNG production at remote gas wells and for peak shaving</li> <li>2) Infrared sensors for thermal-loss measurements</li> <li>3) SMES for peak shaving and power conditioning</li> </ol>
Environment	<ol style="list-style-type: none"> <li>1) Infrared sensors for atmospheric studies of ozone hole and greenhouse effect</li> <li>2) Infrared sensors for pollution monitoring</li> <li>3) Cryotrapping air samples at remote locations</li> </ol>
Transportation	<ol style="list-style-type: none"> <li>1) Infrared sensors for aircraft night vision</li> <li>2) LNG for fleet vehicles</li> </ol>
Agriculture and Biology	Biological specimens storage
Law Enforcement	Infrared sensors for night vision

## 1.2. Cryocoolers

The working principle of cryocoolers depends on a working gas that goes through a specific thermodynamic cycle. These cycles include compression and expansion of gasses to transport energy from one state to the other. When the working gas is compressed, this leads it to heat up. This heat is removed and expansion of the gas causes it to cool down. This reduction of temperature is used for refrigeration (Willems , 2007).

One of the earliest applications of cryocoolers appeared about 50 years ago, which was for cooling infrared sensors to about 80 K for night vision capability of the military. Until 1998, the number of Stirling cryocoolers for this tactical military application has expanded over 125,000 (Dunmire, 1998). Refrigeration powers are in the range of about 0.15 W to 1.75 W (Radebaugh, 2000). The classification of cryocoolers can be based on the thermodynamic cycle that is followed. However, there is now general agreement that there are only two types: recuperative or regenerative units as shown in Figure 1.1 (Timmerhaus, 1996).

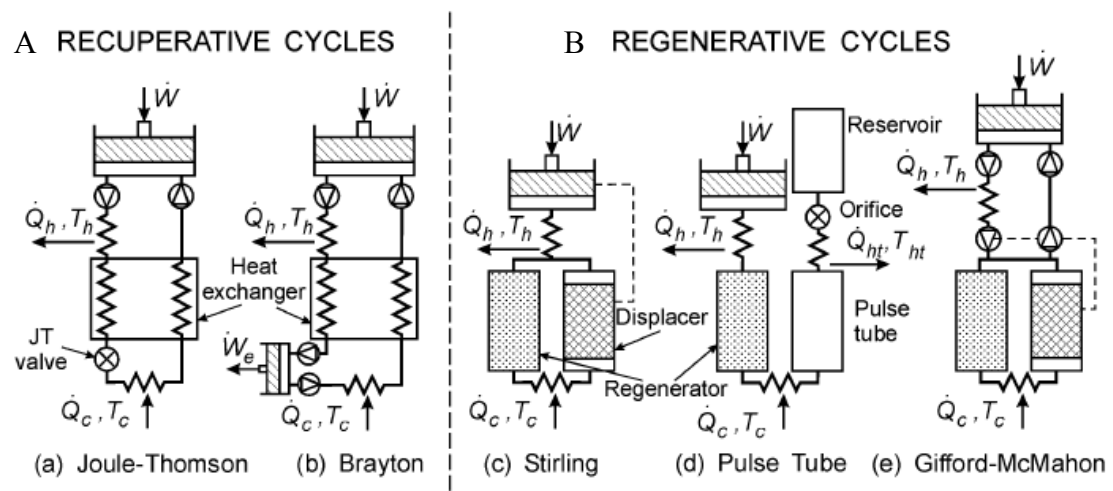


Figure 1. 1 Most important recuperative (A) and regenerative (B) cycles used in cryocoolers. (Radebaugh, 2000).

### 1.2.1 Recuperative Cryocoolers

A recuperative type cryocooler uses recuperative heat exchangers and operate with a steady flow of refrigerant through the system (Radebaugh, 2003). The recuperative heat exchangers provide two separate flow channels for the refrigerant, thus the flow for the latter is always continuous and in one direction. This is analogous to a dc electrical system. In these types of coolers, valving with reciprocating compressors and expanders or rotary or turbine compressors and expanders are required. (Timmerhaus, 1996). Common recuperative cryocoolers are the Joule-Thomson and the Brayton devices, as demonstrated in Figure 1.1 A.

Joule- Thomson cryocoolers use Joule-Thomson (J-T) effect. They employ a J-T expansion or isenthalpic expansion of the working gas to achieve cryogenic temperatures (Hu, 2007). Timmerhaus (1996) explained refrigeration in a J-T cooler in more detail: Cooling is achieved by throttling a nonideal gas which is one of the least efficient methods for attaining cryogenic temperatures. As shown in Figure 1.1 A, first a high-pressure gas is passed down to the countercurrent heat exchanger, where it is cooled through the J-T effect by expansion to a low pressure. Then, the cooled gas is returned through the other side of the exchanger to precool the next incoming high-pressure gas. When this process is repeated until liquefaction of the gas, a stable minimum temperature is reached corresponding to the existing pressure in the reservoir.

Brayton cryocoolers are sometimes referred to as the reverse-Brayton cycle to distinguish it from a heat engine. First Law of Thermodynamics states that the heat absorbed with an ideal gas in the Brayton cycle is equal to the work produced (Radebaugh, 2000). The parts of this type of refrigerator system are a compressor unit, a heat exchanger assembly, an after-cooler unit, and an expansion turbine system. The compressor unit compresses the ambient temperature (300 K) gas, and the heat is rejected to the ambient environmental temperature. Afterwards, the high pressure gas passes through a regenerative heat exchanger. Finally, it expands across the gas turbine and here the heat is extracted (Jha, 2006).

### 1.2.2 Regenerative Cryocoolers

A regenerative cryocooler includes at least one regenerative heat exchanger, or regenerator (Radebaugh, 1991). As demonstrated in Figure 1.1 B, this type of cryocoolers operates with oscillating pressures and mass flows in the cold head. Either a valveless compressor (pressure oscillator) generates the oscillating pressure (Stirling and pulse tube cryocoolers), or a compressor with valves does the work, while valves switch the cold head between a low and high pressure source (Gifford-McMahon cryocooler). The working principle in regenerative cycles is based on an incoming hot gas, which transfers heat to the matrix of the regenerator. Here, the heat is stored for a half cycle in the heat capacity of the matrix. In the second half of the cycle, the returning cold gas, which flows in the opposite direction through the same channel, absorbs heat from the matrix and returns the matrix to its original temperature before the cycle is repeated (Radebaugh, 2000).

Stirling cryocoolers are regenerator type cryocoolers which work on the basis of Stirling cycle (Sahu, 2010). This type of cryocoolers is known for decades. In short, a gas, typically helium, is compressed and expanded to produce cooling in a Stirling cycle. In comparison to simple compression and expansion process, much larger temperature differentials are obtained when the gas shuttles back and forth through a regenerator bed. A displacer is used to force the gas back and forth through a regenerator bed and a piston to compress and expand the gas. Since the regenerator bed is a porous element with a large thermal inertia, it develops a temperature gradient as it operates. As a result, one end of the device becomes hot and the other end becomes cold. The Stirling refrigerator has the highest efficiency of all cryocoolers, very few moving parts and is non-polluting (Kosov, 2003).

Since the scope of this thesis is about Stirling cryocooler, detailed information will be given in following sections.

In Gifford-McMahon cryocooler, a conventional compressor with inlet and outlet valves is used to generate the high- and low-pressure sources as a difference to

stirling cryocoolers. An oil lubricated compressor is usually used and oil removal equipment can be placed in the high-pressure line where there is no pressure oscillation. The use of valves greatly reduces the efficiency of the system (Radebaugh, 2000). These units can achieve temperatures of 65 to 80 K with one stage of expansion and 15-20 K with two stages of expansion (Timmerhaus, 1996).

The moving displacer in the Stirling and Gifford-McMahon refrigerators is eliminated in pulse tube cryocooler due to the following disadvantages:

- a) it is a source of vibration,
- b) it has a limited lifetime,
- c) it contributes to axial heat conduction,
- d) it causes heat loss (Radebaugh, 2000).

In Pulse tube cryocooler, the necessary compression and expansion of the gas is provided by a compressor. The compression work is removed as heat from the first heat exchanger, the after cooler (AC). Between the compressor and the cold end of the pulse tube a regenerator is placed. This regenerator has the same function as in a Stirling cryocooler. Gas flowing from the compressor towards the pulse tube is precooled by the regenerator. When this gas flows back, it is reheated (Willems , 2007).

The mechanism of pulse tube cryocooler follows the following steps:

- 1) The piston moves down to compress the gas (helium) in the pulse tube.
- 2) Compressed gas is at a higher pressure than the average in the reservoir, since it was heated. It flows through the orifice into the reservoir and exchanges heat with the ambient through the heat exchanger at the warm end of the pulse tube. The flow ceases when the pressure in the pulse tube is reduced to the average pressure.
- 3) The piston moves up and expands the gas adiabatically in the pulse tube.
- 4) The cold, low-pressure gas in the pulse tube is forced toward the cold end by the gas flow from the reservoir into the pulse tube through the orifice. As the cold gas flows through the heat exchanger at the cold end of the pulse tube it

picks up heat from the object being cooled. The flow stops when the pressure in the pulse tube increases to the average pressure. The cycle then repeats (Radebaugh, 2000).

### **1.3 Stirling Cryocoolers**

Stirling coolers are based on the Stirling cycle that was invented and patented by Robert Stirling in 1816. In 1834, John Hershel used a closed cycle Stirling engine for making ice. For almost 200 years, the basic concept of the Stirling engine remains unchanged, although the advances in regenerator materials, clearance seal technology, flexure bearing designs etc., have made the Stirling engine a very reliable and robust machine (Riabzev, 2002).

Air was used as the working fluid in the early regenerative systems. Very little development of Stirling refrigerators occurred until 1946 when a Stirling engine at a Dutch company was run in reverse with a motor and was found to liquefy air on the cold tip (Radebaugh, 2000). Pure Helium (99.999%) is the most usable working fluid in a Stirling cooler, due to extremely low liquefaction temperature (4.2°K) and other appropriate characteristics (Riabzev, 2002). For about 40 years, Stirling cryocoolers have been used in cooling infrared sensors for tactical military applications in such equipment as tanks and airplanes (Radebaugh, 2000). Figure 1.3 shows the four sizes of Stirling cryocoolers that are currently used for military tactical applications.

Machines operating on the Stirling cycle are proposed to be the most efficient practical heat engines ever built (Haywood, 2008). Stirling cryocoolers are based on the Stirling cycle, which ideally consists of two isothermal and two isochoric processes (Sahu, 2010). A Stirling cryocooler consists of five main components as shown in Figure 1.2:

- 1) Working gas: various thermodynamic processes are performed, when a working gas is trapped within the system.

- 2) Heat-exchangers – two heat exchangers are used to transfer heat across the system boundary. While a heat absorbing heat-exchanger transfers heat from outside the system into the working gas a heat rejecting heat-exchanger transfers heat from the working gas to outside the system.
- 3) Displacer mechanism – used to displace the working gas between the hot and cold ends of the machine (via the regenerator).
- 4) Regenerator –used as a thermal barrier between the hot and cold ends of the machine, and also as a “thermal store” for the cycle.
- 5) Expansion/compression mechanism – used to expand and/or compress the working gas. In a refrigerator, a net work input is required to move the heat from a low to a high temperature regime (Second Law of Thermodynamics) (Haywood, 2008).

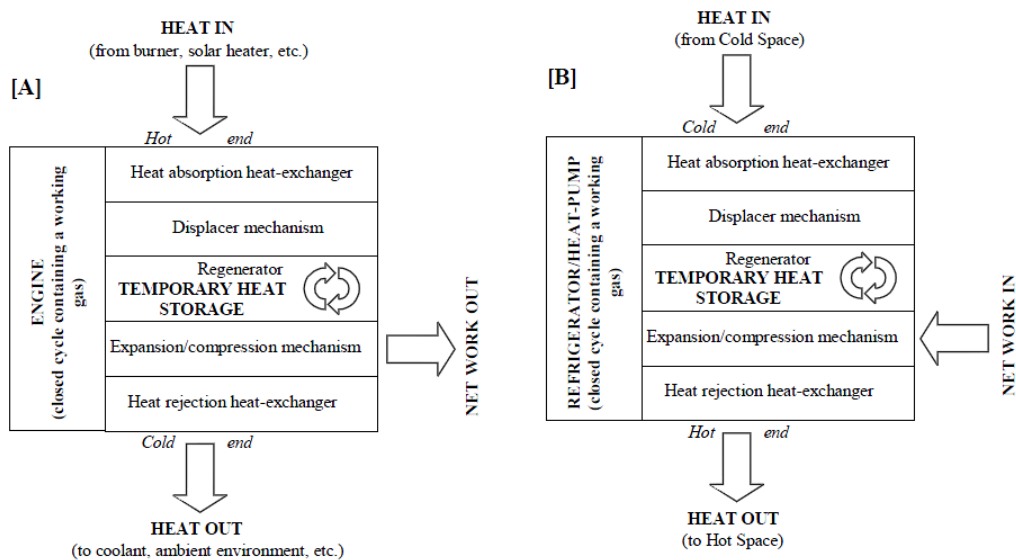


Figure 1. 2 Stirling-cycle machine block diagrams: (A) Engine (B) Refrigerator or heat-pump (Haywood, 2008).

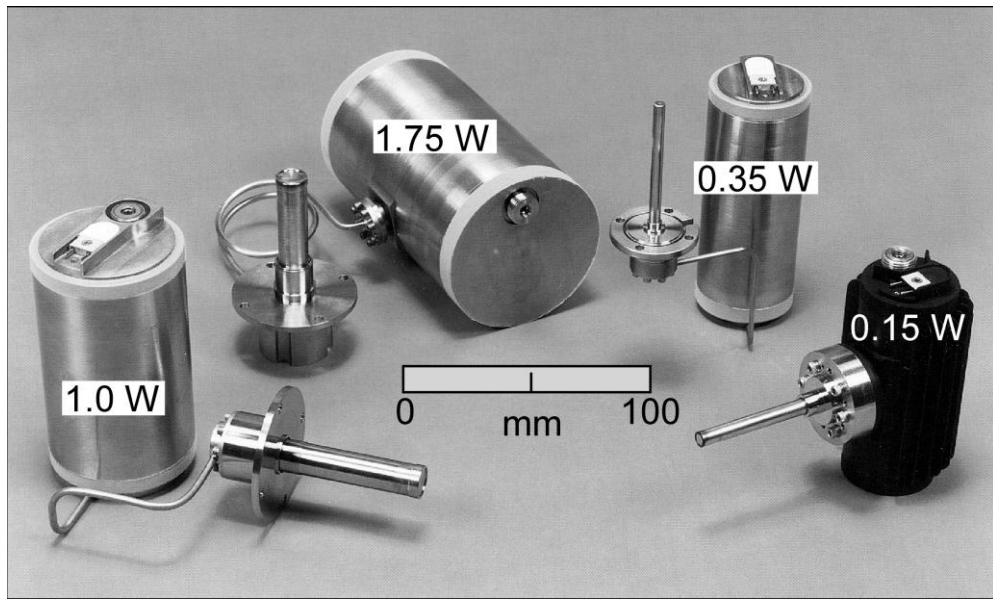


Figure 1. 3 Four sizes of Stirling cryocoolers with dual-opposed linear compressors (Radebaugh, 2000).

Worldwide, a dozen or more different companies have manufactured thousands of small, single-stage Stirling cryocoolers, whose capacities range from about 150 mW to 1 W at 80 K. Largest dimensions for the units (not including the compressor) are generally no more than 150 mm with masses less than 3 kg. Power inputs range from 40 W to 50 W per 1 W of refrigeration (Timmerhaus, 1996).

### 1.3.1 Stirling Cycle

The ideal Stirling cycle consists of four processes. These processes are shown on pressure-volume and temperature-entropy diagrams in Figure 1.4. It should be kept in mind that for the ideal Stirling Cycle the heat-exchangers, regenerator, and transfer passages are assumed to have zero volume (Haywood, 2008).

The four processes are demonstrated in Figure 1.5. The cycle consists of the following steps (Willems, 2007):

I-II Isothermal compression. The compression piston moves to the right, while the expansion piston stays at its left-most position. The gas is compressed. Because this compression is isothermal, an amount of heat ( $Q_h$ ) has to be removed from the system. The volume of the system is reduced from  $V_1$  to  $V_2$ .

II-III Isochoric displacement. Both pistons move to the right. As the gas moves through the regenerator, it is cooled down to temperature  $T_l$ . Heat ( $Q_2$ ) is transferred from the gas to the regenerator.

III-IV Isothermal expansion. The expansion piston moves to the right, while the compression piston stays in its right-most position. The volume is increased from volume  $V_2$  back to  $V_1$ . The gas is expanded. Because the expansion is isothermal, an amount of heat ( $Q_1$ ) is transferred to the gas.

IV-I Isochoric displacement. Both pistons move to the left. Upon passing through the regenerator, the gas is reheated ( $Q_4$ ) to temperature  $T_h$ . The system is now back in its original state.

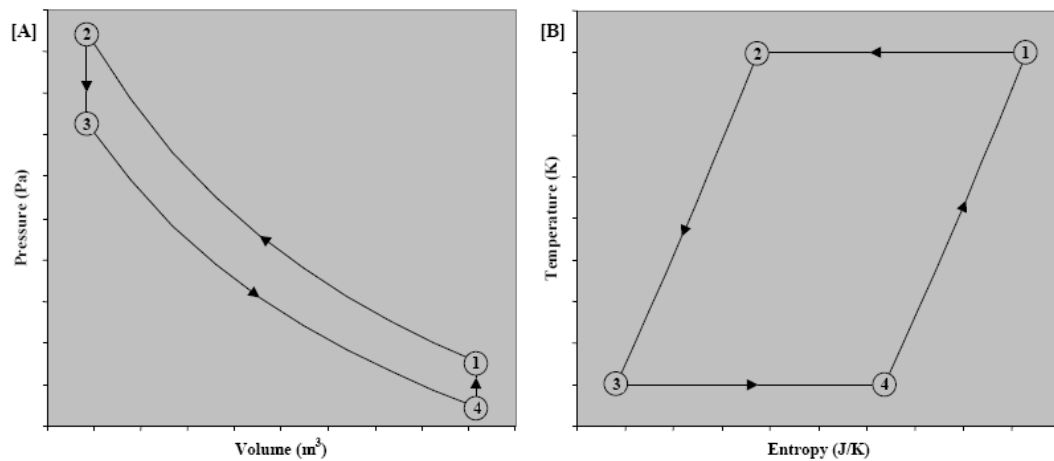


Figure 1.4 P-V and T-s diagrams of Stirling refrigerator (Haywood, 2008).

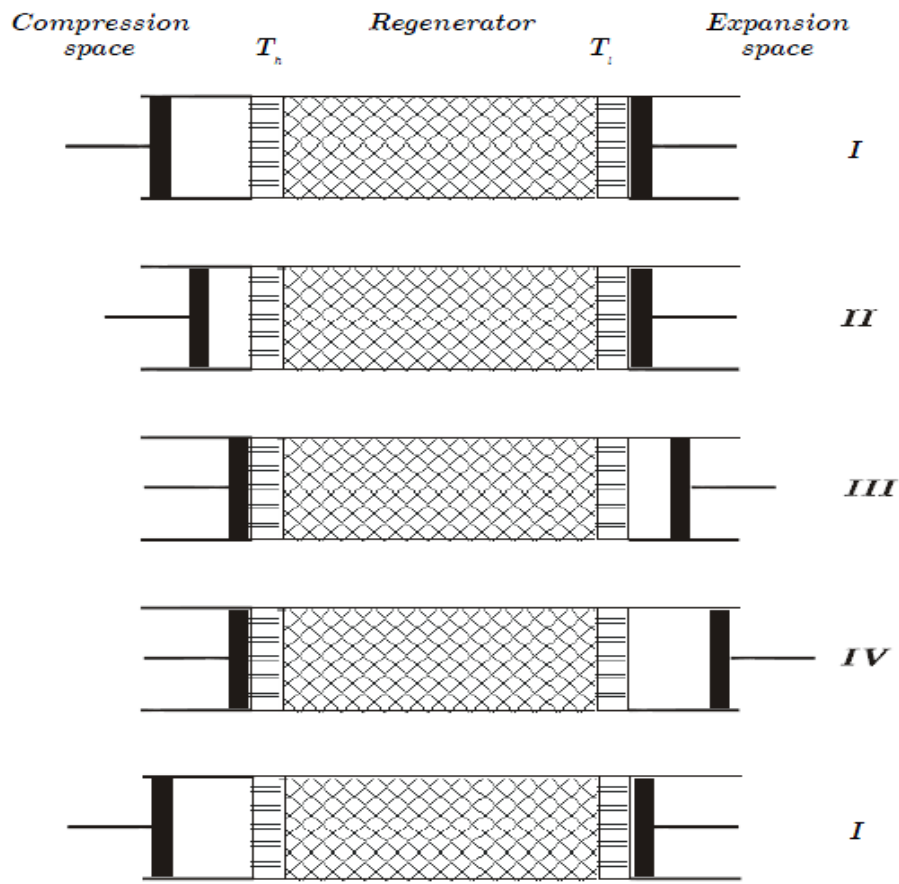


Figure 1. 5 The four steps in the Stirling Cycle (Willems, 2007).

### 1.3.1.1 Work input to an ideal Stirling-cycle refrigerator or heat-pump

The net work input of a Stirling-cycle refrigerator can be evaluated by considering the cyclic integral of pressure with respect to volume:

$$W = \oint PdV$$

This can be easily visualized as the area enclosed by the process curves on the pressure volume diagram in Figure 1.4.

To evaluate the integral we need only consider the work done during the isothermal expansion and compression processes, since there is no work done during the isochoric processes, i.e.

$$W = \int_{V_1}^{V_2} PdV + \int_{V_3}^{V_4} PdV \quad (1.1)$$

By considering the equation of state:

$$PV = mRT$$

and noting that  $T$  is constant for an isothermal process, and  $m$  is constant for a closed cycle, then an expression for work done during an isothermal process can be formulated:

$$\int_{V_A}^{V_B} PdV = \int_{V_A}^{V_B} \frac{mRT}{V} dV = mRT [\ln V]_{V_A}^{V_B} = mRT \ln \left( \frac{V_B}{V_A} \right) \quad (1.2)$$

so that by substitution of Equation 1.2. into Equation 1.1. we can evaluate the work integral:

$$W = mRT_H \ln \left( \frac{V_2}{V_1} \right) + mRT_L \ln \left( \frac{V_4}{V_3} \right) \quad (1.3)$$

where the subscripts  $H$  and  $L$  denote the high and low temperature isotherms respectively.

This equation can then be further simplified by noting that  $V_4 = V_1$  and  $V_3 = V_2$  so that a final equation for work can be obtained:

$$W = mR \ln \left( \frac{V_2}{V_1} \right) (T_H - T_L) \quad (1.4)$$

Inspection of Equation 1.3. therefore shows that the work input for a Stirling-cycle refrigerator should be increased when maximizing the temperature difference between hot and cold ends ( $T_H - T_L$ ), the compression ratio ( $V_2/V_1$ ), the gas mass (and

hence either the total volume of the machine and/or the mean operating pressure), or the specific gas constant.

Material strength/temperature considerations and practicalities such as the overall size of the machine usually limit the amount that the temperature, volume, or pressure can be increased. However, it is interesting to note that with the same work input, temperature difference or the compression ratio can be dramatically enhanced in a Stirling-cycle machine simply by selecting a working gas with a high specific gas constant.

Table 1. 2: Specific gas constants (Wyllen et al., 1994).

<b>Gas</b>	<b>Specific gas constant, R (J/kgK)</b>
Air	286.9
Ammonia	488.2
Carbon dioxide	188.9
Helium	2077.0
Hydrogen	4124.2
Nitrogen	296.8
Propane	188.6
Steam	461.5

### 1.3.1.2 Heat flow in an ideal Stirling-cycle refrigerator or heat-pump

The heat flowing into and out of a Stirling-cycle refrigerator/heat-pump can be evaluated by considering the integral of temperature with respect to entropy:

$$Q = \int TdS \quad (1.5)$$

This can be visualised as the area beneath the process curves on the temperature-entropy diagram in Figure 1.4. Since the isochoric heat transfers within the

regenerator are completely internal to the cycle, i.e.  $-Q_{2\rightarrow3} = Q_{4\rightarrow1}$ , then to evaluate the heat flows into and out of the system we need only consider the isothermal processes.

For the isothermal expansion process in a closed cycle (where  $T$  and  $m$  are constant, and where the subscripts  $H$  and  $L$  denote the high and low temperature isotherms respectively):

$$Q_H = \int_{S_1}^{S_2} T_H dS \quad (1.6)$$

This integral can be most easily evaluated by considering the First Law of Thermodynamics in the form:

$$\delta Q = dU - \delta W \quad (1.7)$$

and since:

$$\delta Q = TdS \quad (1.8)$$

$$\delta W = PdV \quad (1.9)$$

Then it can be said that:

$$TdS = dU - PdV \quad (1.10)$$

so that the heat flow during the isothermal expansion process can be expressed in terms of a change in internal energy and volume becomes:

$$Q_H = \int_{U_1}^{U_2} dU - \int_{V_1}^{V_2} PdV \quad (1.11)$$

and by considering the equation of state  $PV = mRT$  :

The pressure term can be expressed in terms of volume and temperature, and (noting that there is no change in internal energy during an isothermal process) the integral can be easily solved:

$$Q_H = \int_{U_1}^{U_2} dU - \int_{V_1}^{V_2} \frac{mRT_H}{V} dV = 0 - mRT_H \ln[V]_{V_1}^{V_2} \quad (1.12)$$

$$\text{giving:} \quad Q_H = -mRT_H \ln \left[ \frac{V_2}{V_1} \right] \quad (1.13)$$

which is a somewhat convoluted (but hopefully instructive) method of derivation. The same expression can, of course, be obtained much more easily by simple inspection of Equation 1.4., since the heat and work transfers for an isothermal expansion process are equal but opposite. The isothermal compression process can also be readily evaluated (noting that  $V_4 = V_1$  and  $V_3 = V_2$ , and where the subscripts  $H$  and  $L$  denote the high and low temperature isotherms respectively), giving:

$$Q_L = mRT_L \ln \left[ \frac{V_2}{V_1} \right] \quad 1.14$$

### 1.3.1.3 Performance of an ideal Stirling-cycle refrigerator or heat-pump

The coefficient of performance for any refrigerator/heat-pump is defined as the ratio of heating/cooling effect to work input, i.e.

$$\text{for a heat-pump, the heating coefficient of performance is:} \quad COP_H = \frac{-Q_H}{W} \quad (1.15)$$

$$\text{for a refrigerator, the refrigeration coefficient of performance is:} \quad COP_L = \frac{Q_L}{W} \quad (1.16)$$

hence equations for coefficient of performance for ideal Stirling-cycle refrigerators and heat-pumps can be developed by considering Equations 1.4, 1.13, and 1.14, giving:

$$COP_{H_{STIRLING}} = \frac{mRT_H \ln \left[ \frac{V_2}{V_1} \right]}{mR \ln \left( \frac{V_2}{V_1} \right) (T_H - T_L)} \quad (1.17) \quad COP_{L_{STIRLING}} = \frac{mRT_L \ln \left[ \frac{V_2}{V_1} \right]}{mR \ln \left( \frac{V_2}{V_1} \right) (T_H - T_L)} \quad (1.18)$$

which simplifies to:

$$COP_{H_{STIRLING}} = \frac{T_H}{T_H - T_L} \quad (1.19)$$

$$COP_{L_{STIRLING}} = \frac{T_L}{T_H - T_L} \quad (1.20)$$

so that

$$COP_{H_{STIRLING}} = COP_{H_{CARNOT}}$$

$$COP_{L_{STIRLING}} = COP_{L_{CARNOT}}$$

### 1.3.2 The Regenerator

In both Stirling engines and Stirling coolers the regenerator plays a crucial role in the cycle. The regenerator typically contains a porous matrix, the regenerator matrix, which has a very large heat transfer area and a large heat capacity, which in turn increases the power output (Jones, 1982). Regenerator matrices can be made from very thin wires, fibers, layers of dimpled or etched foil where gas can flow between and/or through the layers, or beds of small packed spheres. The main purpose of the regenerator is to act as thermal heat storage in order to minimize the amount of energy that must be added in the heater, thus increasing the thermal efficiency. The regenerator matrix must absorb heat when hot gas is blown through it in one direction and it must release the energy again when the flow direction is reversed and cold gas is blown through it in the other direction. As a result of the alternating blasts of hot and cold gas from different directions, a steep temperature gradient is build up inside the regenerator during the cycle. In a Stirling cooler the regenerator absorbs heat when the compressed gas is moved from the compression volume to the expansion volume. This reduces the amount of heat carried by the gas from the warm end of the cooler to the cold heat absorber. The heat is released to the expanded gas again when the gas is pushed towards the heat rejector. The regenerator increases the coefficient of performance, i.e. the COP, because it increases the cooling power for a given amount of work input (Andersen et al., 2006).

The requirements for an ideal regenerator are listed below (Willems, 2007):

- 1) Infinite heat capacity: the temperature of the material does not change due to the heat that is stored in and released from the matrix material;
- 2) Perfect heat transfer: heat is transferred from the gas to the regenerator and vice versa without any temperature difference. Only then the heat transfer is a reversible process;
- 3) No pressure drop: the gas can flow freely through the regenerator. This transport does not require any work;
- 4) No heat conduction in axial direction: heat conduction from the hot to the cold end of the regenerator is an irreversible process that decreases the performance of the cryocooler;
- 5) No void volume: any gas that is stored in the regenerator does not take part of the compression and expansion cycle. Expanding and compressing this gas leads to increased mass flow, which in turn might lead to additional losses;
- 6) The gas in the regenerator is ideal.

### **1.3.3 Types of Stirling Cryocoolers**

There are mainly four types of cryocoolers, which are categorized by the drive mechanisms of compressor and displacer.

#### **1.3.3.1 Rotary Compressor & Mechanically Driven Expander**

Rotary kinematic Stirling cryocooler shown in Figure 1.6 has a compressor and displacer driven by a rotating crankshaft. In this type of coolers phase angle is adjusted kinematically by connecting rods.

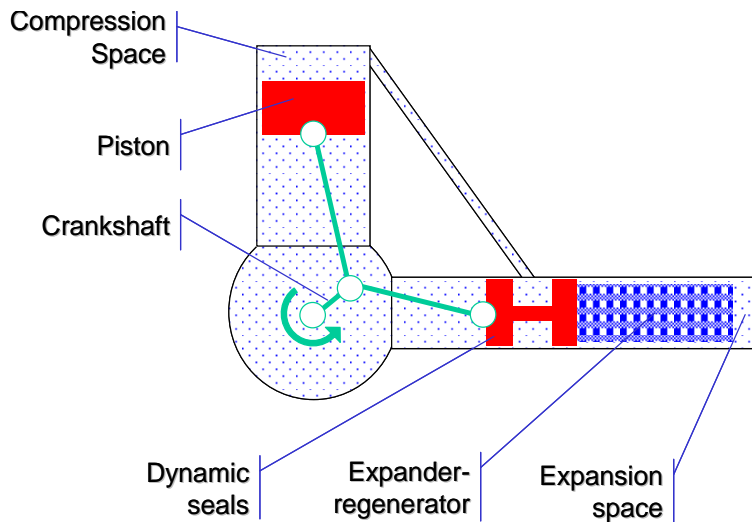


Figure 1. 6 Rotary kinematic Stirling cryocooler (Riabzev, 2002).

### 1.3.3.2 Rotary Compressor & Pneumatically Driven Expander

Rotary pneumatic Stirling cryocooler shown in Figure 1.7 has a compressor driven by a crankshaft and a displacer driven pneumatically. In this type of cryocoolers phase angle is adjusted by a spring attached to bottom of the displacer.

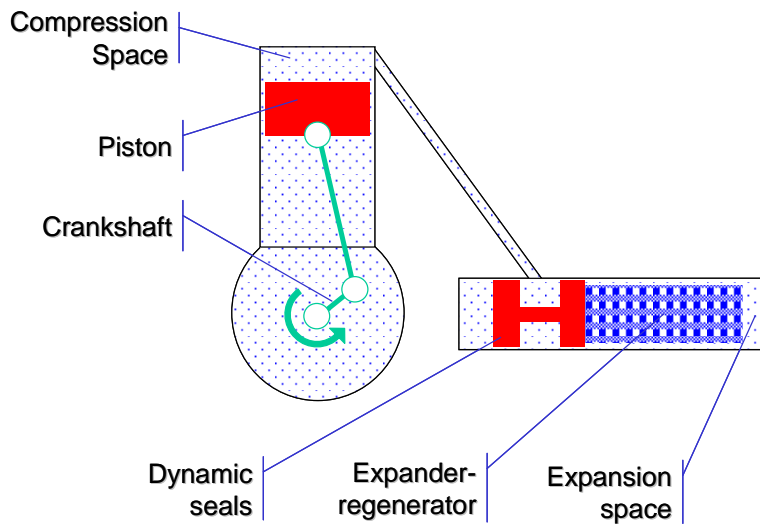


Figure 1. 7 Rotary pneumatic Stirling cryocooler (Riabzev, 2002).

### 1.3.3.3 Linear Compressor & Linear Motor Driven Expander

Linear kinematic stirling cryocooler shown in Figur 1.8 has a compressor and displacer which are driven by linear electric motors. There is an electric motor for each and phase angle is adjusted by the electronic control unit of linear motors.

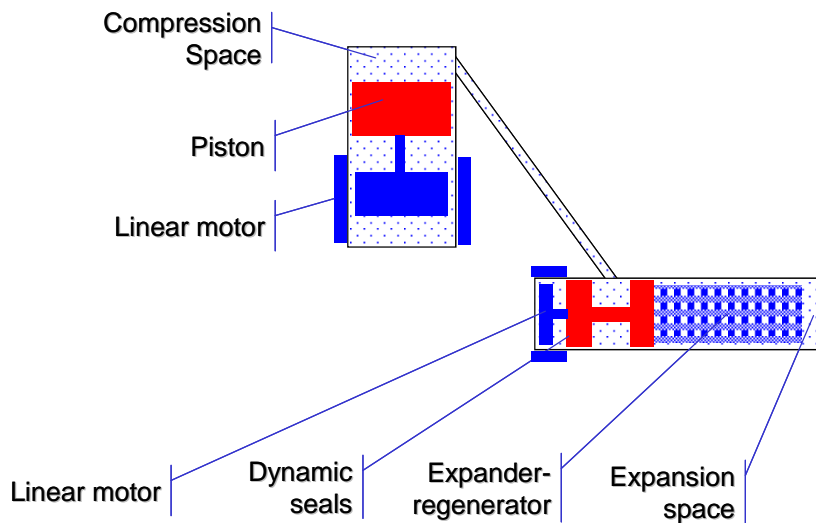


Figure 1. 8 Linear kinematic stirling cryocooler (Riabzev, 2002).

### 1.3.3.4 Linear Compressor & Pneumatically Driven Expander

Linear pneumatic stirling cryocooler shown in figure 1.9 has a compressor driven by a linear electric motor and a displacer which is driven pneumatically. This type of coolers are the most common type among all of them. Phase angle is adjusted by a spring attached to bottom of the displacer.

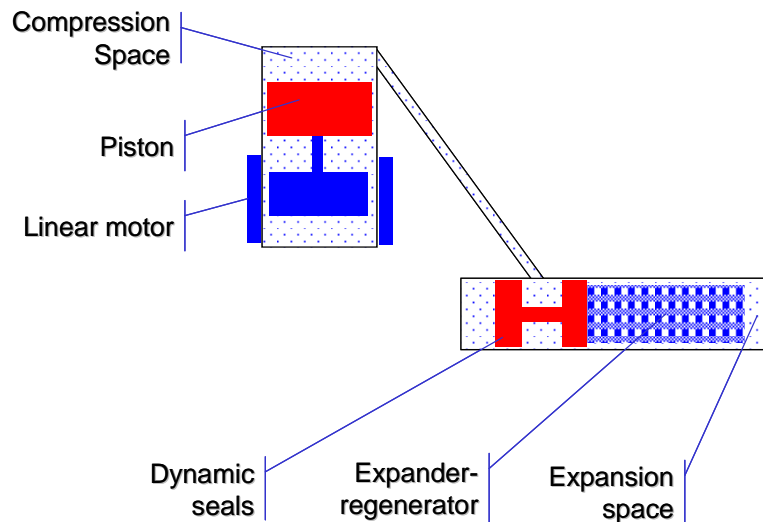


Figure 1. 9 Linear pneumatic Stirling cryocooler (Riabzev, 2002).

### 1.3.4 Theoretical Analysis of Stirling Cryocoolers

The techniques of analysis for Stirling machines can be classified with Martini's (Martini, 1983) nomenclature as zeroth, first, second and third order analysis.

#### 1.3.4.1 Zeroth Order Analysis

Zeroth order analysis is probably the simplest analysis for modeling cryocoolers. Most modern coolers perform under similar conditions of the parametric ratios, which can be counted as dead volume ratio, temperature ratio, swept volume ratio, displacer-piston phase angle advance. The experimental data available on various engines has been correlated and it is found that the following equation to represent the cooler performance (Yuan and Spradley, 1992):

$$Q_{REF} = f \cdot T_L \cdot P_{mean} \cdot V_E \cdot 10^{-4} \quad (1.21)$$

Where;

f = angular frequency,

$T_L$  = cold space temperature,

$P_{mean}$  = mean pressure of the system,

$V_E$  = volume of the expansion space.

#### **1.3.4.2 First Order Analysis**

The classical analysis of the ideal Stirling cycle was done in 1871 by Gustav Schmidt. He obtained closed-form solutions for the special case of sinusoidal volume variations and isothermal hot and cold spaces (Schmidt, 1871). He assumes ideal conditions listed below (Yutopian, 2000):

- 1) Ideal working gas
- 2) No pressure drop in the cooler
- 3) Sinusoidal piston movement
- 4) Uniform temperature inside the system
- 5) Isothermal compression and expansion
- 6) Perfect regenerator
- 7) Steady state conditions

Figure 1.11, demonstrates the model equations from the isothermal assumption shown in Figure 1.10. These can be integrated with a computer but a closed form solution is available in which sinusoidal motion is assumed. The relative volume changes can be calculated using sinusoidal motion equations and system performance is evaluated by using the schematic in Figures 1.10 and equations in Figure 1.11. This analysis is loss-free and a correction factor is normally applied in practical designs to account for the losses (Dyson et al., 2004). Detailed information about this analysis will be given in Chapter 2.

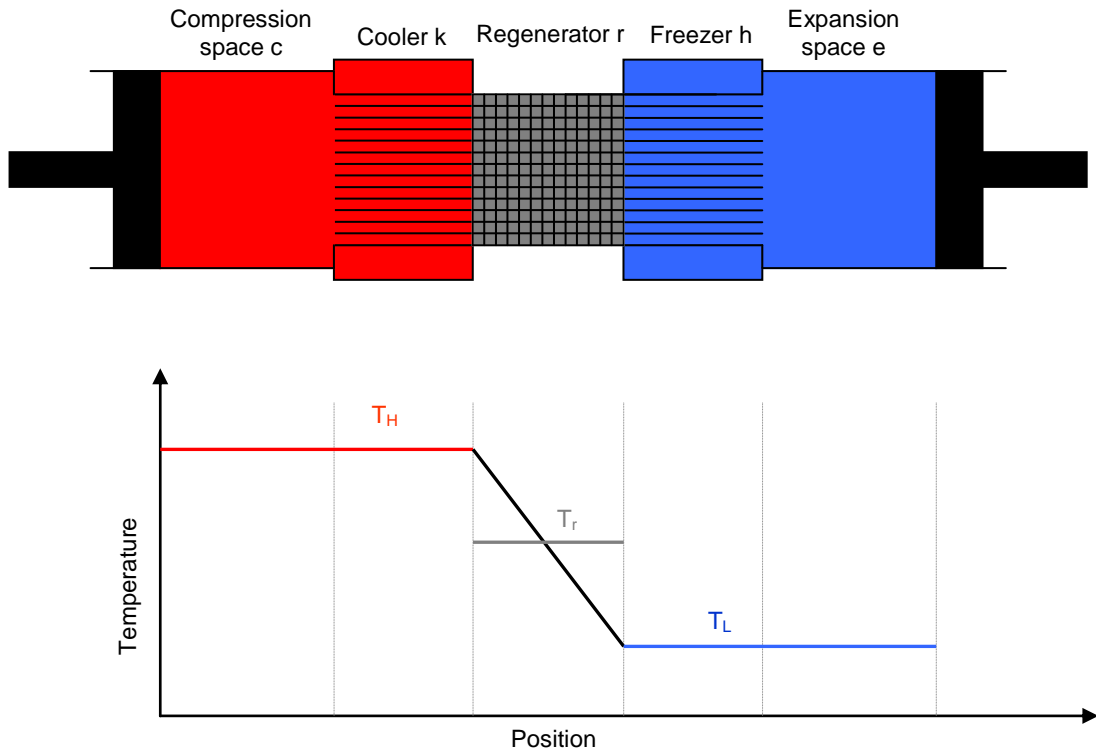


Figure 1. 10 Ideal isothermal model (Urieli) (Dyson et al., 2004).

$P = \frac{M \cdot R}{\frac{V_c}{T_H} + \frac{V_k}{T_H} + \frac{V_r \cdot \ln\left(\frac{T_L}{T_H}\right)}{T_L - T_H} + \frac{V_h}{T_L} + \frac{V_e}{T_L}}$	Pressure
$Q_L = W_e = \int P \left( \frac{dV_e}{d\theta} \right) d\theta$	Heat transferred
$Q_H = W_c = \int P \left( \frac{dV_c}{d\theta} \right) d\theta$	Work input
$W = W_c + W_e$	Work input
$COP = \frac{Q_L}{W}$	

Figure 1. 11 Closed Form Solution Process (Urieli) reproduced: ideal isothermal model set of equations (Dyson et al., 2004).

### 1.3.4.3 Second Order Analysis Methods

Second order analysis is based on application of an ideal analysis (First Order Analysis or Ideal Adiabatic analysis) plus decoupled loss terms. These lost terms include (Yuan and Spradley, 1992):

- 1) conductive heat loss
- 2) regenerator ineffectiveness
- 3) pressure drop
- 4) pumping loss

Second order analysis methods start by applying one of the ideal solutions to the system and determine the heat lifted and required power input. Afterwards losses in the cryocooler are calculated and added to the input power or subtracted from heat lifted, according to the nature of loss and consequently the efficiency of the machine is determined. Unlike first order methods these type of analysis employ heat transfer losses in the machine and allow quantifying them. These losses may include shuttle loss, losses due to imperfect heat exchangers and regenerators, conduction losses in heat exchanger walls and in regenerator axial direction, and losses due to flow friction. Second order analysis assumes that these losses are independent of each other and they are evaluated at that way. Mainly two types of second order analysis can be indicated. These types are identified according to the ideal method employed, isothermal analysis and adiabatic analysis.

Isothermal analysis: This analysis is based on the ideal analysis of Schmidt. Its main assumption is that the heat exchanger and expansion and compression volumes are isothermal, where the gas temperature in the expansion space equals to lower temperature and the temperature of the gas in the compression space equals to that of the higher temperature. Also regenerator is assumed to be perfect. All the heat transferred by the gas to the heater is transferred back to the gas when the direction of flow changes. The results of ideal Schmidt analysis imply that heat exchangers are redundant and all heat transfer occurs in compression and expansion spaces.

However when the losses are included in the second order isothermal analysis, the results can be as realistic as in second order adiabatic model.

Adiabatic analysis: This analysis assumes that there is no heat transfer in expansion and compression spaces, i.e. these sections are adiabatic. Heat transfer is into the machine in heater and out from the machine in the cooler. Again the wall temperatures of heater and cooler sections are assumed to be isothermal as in the isothermal model. This type of analysis also assumes that the regenerator is perfect. Since actual operating systems tend to have adiabatic compression and expansion spaces, this analysis is closer to practical conditions. The most common form of this analysis is Simple analysis, which is developed by Urieli (1984). Numerical methods are employed by solution of this analysis, where isothermal model has a closed form of solution. (Dyson et al., 2004).

*The Martini-Weiss program (CryoWeiss):* A Stirling machine simulation program and design aid for PC's authored by M.H Weiss, G. Walker and O.R Fauvel, Department of Mechanical Engineering, The University of Calgary (Walker et al., 1990).

The Martini-Weiss program has been used extensively and is a proven program for the simulation of Stirling engines (power systems). Martini-Weiss is a menu-driven, graphics orientated computer simulation program for Stirling machines. The main simulation program is based on the isothermal analysis of Martini and is written in FORTRAN 77. The program efficiently simulates a wide range of Stirling machine configurations, drive systems and heat exchanger types. The algorithm implemented in the main simulation is effective in providing estimates of machine performance and is well suited for parametric optimization or trade studies (Sier, 2009).

*The Urieli-Walker model:* includes complete differential equations for the adiabatic model as well as a program to simulate a three-expansion-stage Stirling cryocooler. This program forms the foundation for general computer simulation for a cryocooler as it can be applied to different configurations of multiple expansion stage Stirling cryocoolers.

*The SNAPpro software by Altman* (SNAP is an abbreviation for Stirling Numerical Analysis Program) is a commercially available Stirling simulation program by Altman (Altman, 2005). The program is based on the work of Martini (Martini, 1978; Martini 1983) is classified as a second order model. The program is being actively promoted on the internet (Altman, 2005) and at conferences (Altman, 2003).

*The PROSA software by Thomas* (PROSA is an abbreviation of Program for second order analysis.) is a commercial Stirling simulation program available from Thomas (Thomas, 2006). The versions of PROSA up to version 2.4 are second order models. *PROSA* has been successfully validated, both with and without calibration, against experimental data for a number of Stirling machines as documented in the above mentioned papers by Thomas.

#### **1.3.4.4 Third Order or Nodal Analysis Methods**

Third-order design methods, also known as nodal analyses, consist of three basic procedures: (1) Dividing the machine into a network of nodes or control volumes; (2) Setting up the differential equations for conservation of mass, momentum, and energy, plus equation of state for the working gas; (3) Solving simultaneously the system of difference equations by some adequate numerical method.

Third order models make fewer assumptions about the cycle and about the coupling of loss mechanisms to each other and to the cycle. This means that third order models may yield more accurate prediction of machine performance. Third order models do not yield closed form solutions and are much more computationally intensive than first and second order models.

Some of the first analysis at this level of fidelity was by Finkelstein (Finkelstein, 1995), Urieli (Urieli et al., 1977) and Berchowitz (Berchowitz, 1978).

A third order numerical model for Stirling refrigerators was developed by Yuan and coworkers (Yuan and Spradley, 1992) under an independent research program at Lockheed's Research and Development Division. This model has been validated against experimental results of an Oxford type Lucas Stirling refrigerator.

The codes by David Gedeon referred to as GLIMPS (Gedeon, 1992; Geng and Tew, 1992) and Sage (Gedeon, 1994; Gedeon 1999 A and B) are one dimensional and solve the governing equations implicitly in space and time.

The linearized harmonic analysis code referred to as HFAST (Huang, 1993) solved a steady-state periodic problem in the frequency domain. Again, transient behavior is not modeled.

#### **1.4 Scope of the Thesis**

This study focuses on developing a computer code for simulating a Stirling cryocooler according to the second order analysis. The main goal is to determine the performance of a cryocooler to investigate system parameters and loss mechanisms, which are crucial to understand before designing a cryocooler. This goal is achieved by following the route of Urieli (Urieli et al., 1984), which was focused on Stirling cycle engines.

Although there exist many simulation programs in second and third order analysis methods, a second order numerical analysis is performed in order to be able to investigate Stirling cryocooler characteristics without having to purchase one of these programs. With this motivation it is aimed to present a detailed knowledge on Stirling cryocoolers. Performance and behavior of a Stirling cryocooler under different operating conditions and effects of system parameters can be clearly understood by a detailed examining of this work.

## CHAPTER 2

### COMPUTATIONAL ANALYSIS OF STIRLING CRYOCOOLERS

#### 2.1 The Schmidt Analysis

The Schmidt cycle analysis (Schmidt, 1871) is a closed form of analysis of an ideal Stirling machine, based on the following assumptions

- Sinusoidal Volume Variations in the compression and expansion spaces
- The working gas in the compression space is at a constant temperature  $T_k$  and the working gas in the expansion space is at a constant temperature  $T_h$
- The regenerative process is perfect
- There is no instantaneous pressure drop or leakage
- All processes are reversible
- Working gas is ideal

Volume of the compression space  $V_c$  and the expansion space  $V_e$  are as following;

$$V_c = V_{clc} + V_{swc} \frac{(1 + \cos \theta)}{2} \quad (2.1)$$

$$V_e = V_{cle} + V_{swe} \frac{[1 + \cos(\theta + \alpha)]}{2} \quad (2.2)$$

Where;

$\theta$  = crank angle

$\alpha$  = angular phase advance of the expansion space volume variations with respect to the compression space volume variations

$V_{clc}$  = compression clearance volume

$V_{cle}$  = expansion clearance volume

$V_{swc}$  = compression piston swept volume

$V_{swe}$  = expansion piston swept volume.

The total mass of the gas in the machine shown in Figure 1.10 is constant

$$M = m_c + m_k + m_r + m_h + m_e \quad (2.3)$$

Where the subscripts c,k,r,h,e stands for compression, cooler, regenerator, freezer and expansion respectively.

Substituting ideal gas relation  $m = \frac{PV}{RT}$

$$M = \frac{P}{R} \left( \frac{V_c}{T_H} + \frac{V_k}{T_H} + \frac{V_r}{T_R} + \frac{V_h}{T_L} + \frac{V_e}{T_L} \right) \quad (2.4)$$

Substituting equation (2.2) and rearranging;

$$P = MR \left( \frac{V_c}{T_H} + \frac{V_k}{T_H} + \frac{V_r \ln(T_L/T_H)}{T_L - T_H} + \frac{V_h}{T_L} + \frac{V_e}{T_L} \right)^{-1} \quad (2.5)$$

$$P = MR \left[ \begin{array}{l} \frac{V_{swc}}{2T_H} + \frac{V_{clc}}{T_H} + \frac{V_k}{T_H} + \frac{V_r \ln(T_L/T_H)}{T_L - T_H} + \frac{V_h}{T_L} + \frac{V_{swe}}{2T_L} + \frac{V_{cle}}{T_L} + \left( \frac{V_{swe} \cos \alpha}{2T_L} + \frac{V_{swc}}{2T_H} \right) \cos \theta \\ - \left( \frac{V_{swe} \sin \alpha}{2T_L} \right) \sin \theta \end{array} \right]^{-1} \quad (2.6)$$

Rearranging;

$$P = MR [s + c \cos \beta \cos \theta - c \sin \beta \sin \theta]^{-1} \dots \dots \dots (2.7)$$

Where (considering the trigonometric substitutions in the figure 2.1)

$$s = \frac{V_{swc}}{2T_H} + \frac{V_{clc}}{T_H} + \frac{V_k}{T_H} + \frac{V_R \ln(T_L/T_H)}{T_L - T_H} + \frac{V_h}{T_L} + \frac{V_{swe}}{2T_L} + \frac{V_{cle}}{T_L} \quad (2.8)$$

$$c \sin \beta = \frac{V_{swe} \sin \alpha}{2T_L} \quad (2.9)$$

$$c \cos \beta = \frac{V_{swe} \cos \alpha}{2T_L} + \frac{V_{swc}}{2T_H} \quad (2.10)$$

$$\beta = \tan^{-1} \left( \frac{V_{swe} \sin \alpha / T_L}{V_{swe} \cos \alpha / T_L + V_{swc} / T_H} \right) \quad (2.11)$$

$$c = \frac{1}{2} \left[ \left( \frac{V_{swe}}{T_L} \right)^2 + 2 \frac{V_{swc}}{T_H} \frac{V_{swe}}{T_L} \cos \alpha + \left( \frac{V_{swc}}{T_H} \right)^2 \right]^{\frac{1}{2}} \quad (2.12)$$

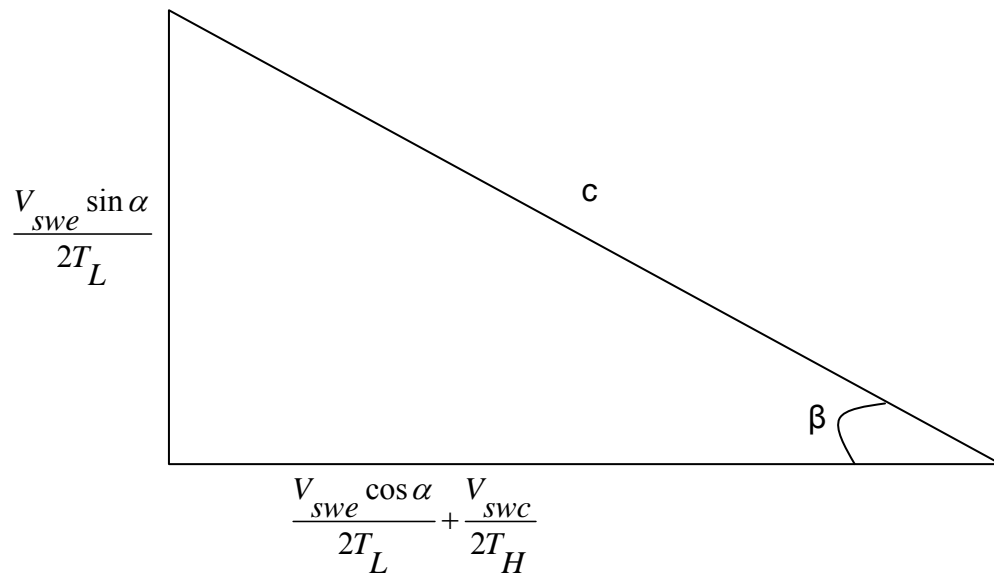


Figure 2. 1 Trigonometric substitution of  $\beta$  and  $c$  (Schmidt, 1871)

Substituting equations (2.9) and (2.10);

$$P = \frac{MR}{s(1 + b \cos \phi)} \quad (2.13)$$

Where  $\phi = \theta + \beta$   $b = \frac{c}{s}$

Minimum and maximum values can easily be evaluated;

$$P_{\max} = \frac{MR}{s(1-b)} \quad (2.14) \quad P_{\min} = \frac{MR}{s(1+b)} \quad (2.15)$$

Average pressure can be given as;

$$P_{\text{mean}} = \frac{1}{2\pi} \int_0^{2\pi} P d\phi = \frac{MR}{2\pi} \int_0^{2\pi} \frac{1}{1+b \cos \phi} d\phi \quad (2.16)$$

From tables of integrals (Dwight, 1961) (2.13) becomes;

$$P_{\text{mean}} = \frac{MR}{s\sqrt{1-b^2}} \quad (2.17)$$

Eq.(2.17) is the main relation between total mass of the working gas and mean operating pressure.

Total work done is the sum of work done by compression and expansion spaces.

$$W_c = \int_0^{2\pi} P dV_c = \int_0^{2\pi} P \frac{dV_c}{d\theta} d\theta \quad (2.18)$$

$$W_e = \int_0^{2\pi} P dV_e = \int_0^{2\pi} P \frac{dV_e}{d\theta} d\theta \quad (2.19)$$

$$W = W_c + W_e \quad (2.20)$$

Differentiating (2.1) and (2.2);

$$\frac{dV_c}{d\theta} = -\frac{1}{2} V_{swc} \sin \theta \quad (2.21)$$

$$\frac{dV_e}{d\theta} = -\frac{1}{2} V_{sve} \sin(\theta + \alpha) \quad (2.22)$$

Substituting (2.21), (2.22) and (2.17) into (2.18) and (2.19) one can obtain;

$$W_c = -\frac{V_{swc}MR}{2s} \int_0^{2\pi} \frac{\sin \theta}{1+b \cos(\beta + \theta)} d\theta \quad (2.23)$$

$$W_e = -\frac{V_{swe}MR}{2s} \int_0^{2\pi} \frac{\sin(\theta + \alpha)}{1+b \cos(\beta + \theta)} d\theta \quad (2.24)$$

The solutions of these integrals are done somewhat different from Schmidt's method by Berchowitz and Urieli (1984). They used Forier series expansion method and tables of integrals (Dwight,1961) to get the same results as those obtained by Schmidt ;

$$W_c = \pi V_{swc} P_{mean} \frac{\sin \beta (\sqrt{1-b^2} - 1)}{b} \quad (2.25)$$

$$W_e = \pi V_{swe} P_{mean} \frac{\sin(\beta - \alpha) (\sqrt{1-b^2} - 1)}{b} \quad (2.26)$$

COP of the cooler can be given as;

$$COP = \frac{Q_L}{W} = \frac{W_e}{W} \quad (2.27)$$

### *Regenerator Mean Effective Temperature*

Urieli has shown that the temperature profile for real regenerators is very nearly linear (Urieli 1980). So the regenerator can be assumed to have a linear temperature profile as in Figure 2.2.

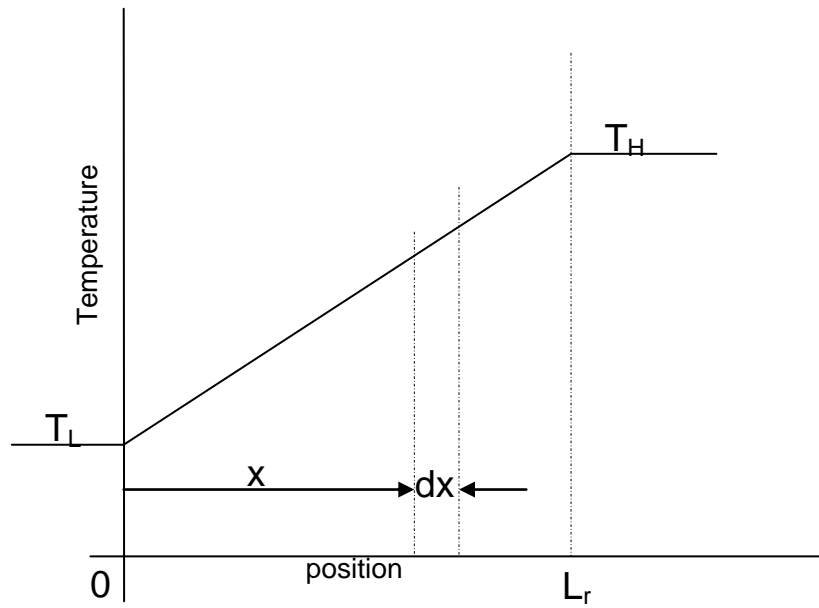


Figure 2. 2 Regenerator linear temperature profile (Creswick 1965)

From Figure 2.2,

$$T(x) = \frac{(T_L - T_H)x}{L_r} + T_H \quad (2.28)$$

Total gas in the regenerator is given as

$$m_r = \int_0^{V_r} \rho dV_r \quad (2.29)$$

Substituting  $\rho = \frac{P}{RT}$ ,  $V_r = A_r L_r$ ,  $dV_r = A_r dx$  into (2.29) one can get;

$$m_r = \frac{V_r P}{R} \int_0^{L_r} \frac{1}{(T_L - T_H)x + T_H L_r} dx \quad (2.30)$$

After performing the integration;

$$m_r = \frac{V_r P}{R} \frac{\ln(T_L / T_H)}{T_L - T_H} \quad (2.31)$$

Consider the ideal gas equation of state for the regenerator having mean effective temperature of  $T_r$ ;

$$m_r = \frac{V_r P}{RT_r} \quad (2.32)$$

From (2.22) and (2.33)

$$T_r = \frac{T_L - T_H}{\ln(T_L / T_H)} \quad (2.34)$$

Which is the mean effective regenerator temperature as a function of  $T_L$  and  $T_H$ .

## 2.2 Ideal Adiabatic Analysis

Urieli have developed an ideal adiabatic model for Stirling engines. This model is very similar to isothermal model developed by Schmidt except that the compression and expansion spaces are adiabatic rather than isothermal. Heat transfer between the surroundings and the system occurs only in the cooler and freezer.

Since the basic approach of this study is identical to Urieli's, the differential and algebraic equations developed by Urieli have been used. However some modifications were made to be more clear.

Basic assumptions are;

- The instantaneous pressure is the same throughout the system.
- The mass of working fluid in the system is constant.
- The compression and all expansion spaces are adiabatic.
- Sinusoidal Volume Variations in the compression and expansion spaces
- Heat rejector and freezer spaces are under isothermal conditions.

- Regenerator matrix have linear temperature distribution.
- Since the working gas moves back and forth in the cylinder, the mass flow changes direction accordingly, so conditional temperatures are applied;

if  $\dot{m}_{ck} > 0$  then  $T_{ck} = T_c$ , otherwise  $T_{ck} = T_H$ ;

if  $\dot{m}_{he} > 0$  then  $T_{he} = T_L$  otherwise  $T_{he} = T_e$ ;

This implies that when compression piston is moving to the cooler, gas inside the compression space moves to the cooler accordingly and the temperature of the gas in the interface between the compressor and the cooler ( $T_{ck}$ ) equals to the temperature of the gas in the compression space ( $T_c$ ). When the compression piston changes direction, i.e. piston moves away from the cooler the temperature of the gas the interface between the compressor and the cooler ( $T_{ck}$ ) equals to the temperature of the gas in the cooler ( $T_H$ ). The same process is also applied to the gas flow between the expansion space and the freezer. These conditional temperatures cause a non-linear enthalpy flow between pistons and heat exchangers and thus an analytical solution cannot be applied. Numerical solution is required in order to solve the process.

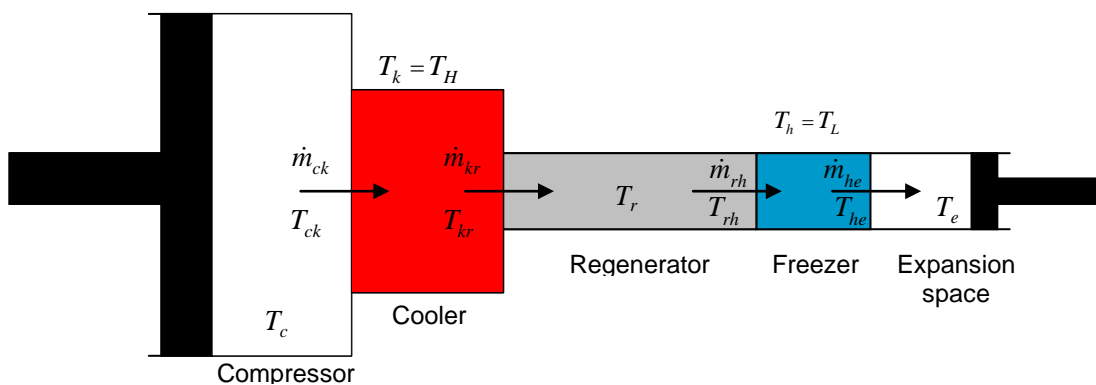


Figure 2. 3 Conditional interface temperature

The ideal adiabatic model is developed according to three main principles;

- Conservation of mass

$$\sum \dot{m}_i - \sum \dot{m}_o = dm \quad (2.35)$$

- Conservation of energy (neglecting kinetic and potential energy terms)

$$\delta Q - \delta W + \sum \dot{m}_i h_i - \sum \dot{m}_o h_o = dE \quad (2.36)$$

- Equation of state

$$PV = mRT \quad (2.37)$$

Where the subscript i stands for inlet and o stands outlet.

The internal energy of an ideal gas is given as;  $du = C_v(T)dT$  (2.38)

The enthalpy of an ideal gas is given as;  $dh = C_p(T)dT$  (2.39)

Also for an ideal gas;

$$C_p = C_v + R \quad (2.40)$$

$$\gamma = \frac{C_p}{C_v} \quad (2.41)$$

$$C_p = \frac{R\gamma}{\gamma - 1} \quad (2.42)$$

$$C_v = \frac{R}{\gamma - 1} \quad (2.43)$$

The term  $dE$  on the right-hand side of the energy equation is

$$dE = d(mu) \quad (2.44)$$

Assuming that the specific heat capacity is constant with temperature, the internal energy and enthalpy are

$$u = C_v T \quad (2.45)$$

$$h = C_p T \quad (2.46)$$

Substituting the equations (2.44) (2.45) (2.46) into the energy equation ;

$$\delta Q - \delta W + C_p T_i \dot{m}_i - C_p T_o \dot{m}_o = C_v d(mT) \quad (2.47)$$

Differentiate equation of state to get;

$$\frac{dP}{P} + \frac{dV}{V} = \frac{dm}{m} + \frac{dT}{T} \quad (2.48)$$

Volume is constant for three heat exchangers, so;

$$\frac{dP}{P} = \frac{dm}{m} \quad (2.49)$$

Equations derived above can be applied to the cryocooler. The mass of the working fluid in the system is constant;

$$m_c + m_k + m_r + m_h + m_e = M \quad (2.50)$$

Differentiate (2.50) to get;

$$dm_c + dm_k + dm_r + dm_h + dm_e = 0 \quad (2.51)$$

Substitute (2.49) into (2.51) to get;

$$dm_c + dm_e + dP \left( \frac{m_r}{P} + \frac{m_h}{P} + \frac{m_k}{P} \right) = 0 \quad (2.52)$$

Using equation of state;

$$dm_c + dm_e + \frac{dP}{R} \left( \frac{V_k}{T_H} + \frac{V_r}{T_r} + \frac{V_h}{T_L} \right) = 0 \quad (2.53)$$

On order to eliminate  $dm_c$  and  $dm_e$  terms, conservation of energy equation should be applied for expansion and compression spaces.

For compression space;

$$\delta Q_c - C_p T_{ck} \dot{m}_{ck} = \delta W_c + C_v d(m_c T_c) \quad (2.54)$$

Compression space is adiabatic  $\delta Q_c = 0$ , from conservation of mass  $dm_c = -\dot{m}_{ck}$  and the work is  $\delta W_c = PdV_c$ , so equation (2.54) becomes;

$$C_p T_{ck} dm_c = PdV_c + C_v d(m_c T_c) \quad (2.55)$$

Substituting equation (2.37) (2.40), (2.42) and (2.43) into (2.55);

$$dm_c = \frac{PdV_c + V_c \frac{dP}{\gamma}}{RT_{ck}} \quad (2.56)$$

Similarly for expansion space;

$$\delta Q_e - C_p T_{he} \dot{m}_{he} = \delta W_e + C_v d(m_e T_e) \quad (2.57)$$

Expansion space is adiabatic  $\delta Q_e = 0$ , from conservation of mass  $dm_e = -\dot{m}_{he}$  and the work is  $\delta W_e = PdV_e$ , so equation (2.57) becomes;

$$C_p T_{he} dm_e = PdV_e + C_v d(m_e T_e) \quad (2.58)$$

Substituting equation of state equation, equation (2.40), (2.42) and (2.43) into (2.58);

$$dm_e = \frac{PdV_e + V_e \frac{dP}{\gamma}}{RT_{he}} \quad (2.59)$$

Substituting equations (2.56) and (2.59) into (2.53) and rearranging;

$$dP = \frac{-\gamma P \left( \frac{dV_c}{T_{ck}} + \frac{dV_e}{T_{he}} \right)}{\frac{V_c}{T_{ck}} + \gamma \left( \frac{V_k}{T_H} + \frac{V_r}{T_r} + \frac{V_h}{T_L} \right) + \frac{V_e}{T_{he}}} \quad (2.60)$$

The masses in each section are determined by equation of state;

$$m_c = \frac{PV_c}{RT_c} \quad (2.61)$$

$$m_k = \frac{PV_k}{RT_H} \quad (2.62)$$

$$m_r = \frac{PV_r}{RT_r} \quad (2.63)$$

$$m_h = \frac{PV_h}{RT_L} \quad (2.64)$$

$$m_e = \frac{PV_e}{RT_e} \quad (2.65)$$

Substituting (2.61) to (2.65) into (2.50) and rearranging;

$$P = \frac{MR}{\frac{V_c}{T_c} + \frac{V_k}{T_H} + \frac{V_r}{T_r} + \frac{V_h}{T_L} + \frac{V_e}{T_e}} \quad (2.66)$$

In order to get the mass flow in a control volume one should apply conservation of mass to each section;

$$\dot{m}_{ck} = -dm_c \quad (2.67)$$

$$\dot{m}_{kr} = \dot{m}_{ck} - dm_k \quad (2.68)$$

$$\dot{m}_{he} = dm_e = \dot{m}_{rh} - dm_h \quad (2.69)$$

$$\dot{m}_{rh} = \dot{m}_{he} + dm_h \quad (2.70)$$

Differential temperatures can be obtained by using equation (2.48);

$$dT_c = T_c \left( \frac{dP}{P} + \frac{dV_c}{V_c} - \frac{dm_c}{m_c} \right) \quad (2.71)$$

$$dT_e = T_e \left( \frac{dP}{P} + \frac{dV_e}{V_e} - \frac{dm_e}{m_e} \right) \quad (2.72)$$

The equations for differential work are as following;

$$\delta W_c = PdV_c \quad (2.73)$$

$$\delta W_e = PdV_e \quad (2.74)$$

The total work is given as;

$$\delta W = \delta W_c + \delta W_e \quad (2.75)$$

Substituting equation (2.37) (2.40) into equation (2.47) and applying these equations to heat exchanger spaces where  $\delta W = 0$  and  $dV = 0$ ;

$$\delta Q_k = \frac{V_k dPC_v}{R} - C_p (T_{ck} \dot{m}_{ck} - T_{kr} \dot{m}_{kr}) \quad (2.76)$$

$$\delta Q_r = \frac{V_r dPC_v}{R} - C_p (T_{kr} \dot{m}_{kr} - T_{rh} \dot{m}_{rh}) \quad (2.77)$$

$$\delta Q_h = \frac{V_h dPC_v}{R} - C_p (T_{rh} \dot{m}_{rh} - T_{he} \dot{m}_{he}) \quad (2.78)$$

### 2.3. Simple analysis

In this section second order analysis of a Stirling cryocooler is described. Simple analysis, which is developed by Urieli (1984) employs ideal adiabatic analysis with regenerator, heat exchanger and pumping loss mechanisms. After performing ideal adiabatic analysis, the effect of heat transfer and flow-friction effects of the nonideal heat exchangers on the refrigerator performance have been evaluated.

This analysis starts with ideal adiabatic analysis, where the cooler and freezer are assumed to be isothermal and the regenerator is assumed to be perfect. However, when the gas flows in the system from expansion space to compression space and vice versa, the temperature of the gas is different from the temperature of the heat exchanger walls. This effect is caused by the convection between the gas and heat exchanger wall. In addition to that there is always a flow friction in the system which makes the heat transfer in the heater freezer and regenerator to deviate from ideal conditions. These facts result in a decrease in the cooling capacity of the cryocooler.

Simple analysis takes these effects into account and includes the evaluations of heat transfer losses and friction losses in the system. It is called “simple” because it enables to use the heat transfer and flow friction correlations directly by using the ideal adiabatic model and to analyze system performance in a simplified way.

This research employs simple analysis method with some modifications made on the friction factor correlations which will be described in this chapter.

### **2.3.1. Regenerator simple analysis**

Regenerator is the most crucial element in a Stirling cycle cryocooler. In a Stirling cryocooler gas flows from compression space to expansion space and from expansion space to compression space. As the gas moves from hot side to the cold side it gives or takes energy to or from the regenerator. A regenerator has a duty of storing energy of the gas and transferring it back to the gas that flows inside and by doing so regenerator increases the efficiency of the system.

In the case of an ideal regenerator, while the gas moves from the cooler to the freezer it gives heat to the regenerator and its temperature decreases to that of the freezer and while the gas flows from freezer to the cooler all the energy absorbed by the regenerator is transferred to the gas back and the gas reaches to the temperature

of the cooler. However in case of a real regenerator this scene changes. The gas that enters to the freezer has a higher temperature than the freezer and the gas that enters to the cooler has a lower temperature than the cooler. These temperatures differences should be compensated by the cryocooler, which means additional loss for cooler and freezer spaces.

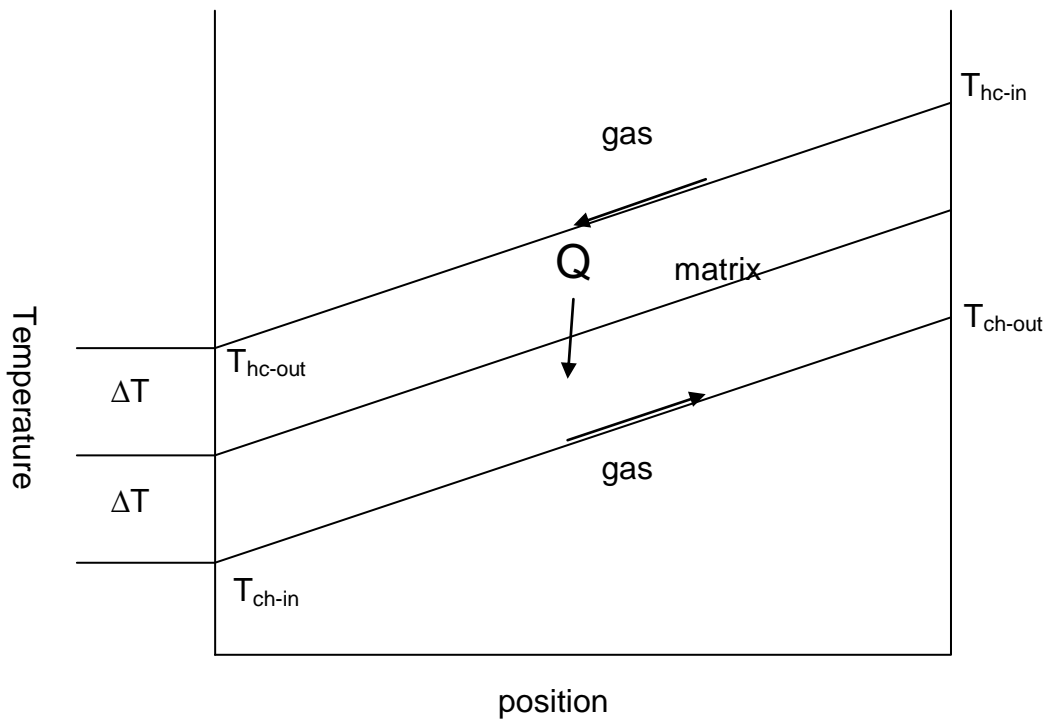


Figure 2. 4 Temperature distribution in a non-ideal regenerator

Assuming equal mass flow rates and thermal properties, the difference between the gas temperature and wall temperatures ( $\Delta T$ ) are equal in cooler and freezer. So effectiveness of the regenerator is;

$$\varepsilon = \frac{T_{hc-in} - T_{hc-out}}{T_{hc-in} - T_{ch-in}} \quad (2.79)$$

$$\Delta T = T_{hc-out} - T_{ch-in} \quad (2.80)$$

Where;

$T_{hc-in}$  : Temperature of the gas entering to the regenerator from the freezer

$T_{hc-out}$  : Temperature of the gas entering to the cooler from the regenerator

$T_{ch-in}$  : Temperature of the gas entering to the regenerator from the cooler

$T_{ch-out}$  : Temperature of the gas entering to the freezer from the regenerator

Combining the equations (2.79) (2.80);

$$\varepsilon = \frac{1}{1 + \frac{2\Delta T}{T_{hc-in} - T_{hc-out}}} \quad (2.81)$$

From conservation of energy for regenerator matrix

$$C_p \dot{m} (T_{hc-in} - T_{hc-out}) = 2hA_{wg} \Delta T \quad (2.82)$$

Substituting equation (2.82) into (2.81);

$$\varepsilon = \frac{1}{1 + \frac{C_p \dot{m}}{hA_{wg}}} \quad (2.83)$$

Substituting  $NTU = \frac{hA_{wg}}{C_p \dot{m}}$  and rearranging effectiveness equation becomes;

$$\varepsilon = \frac{NTU}{1 + NTU} \quad (2.84)$$

Now consider Stanton number;

$$ST = \frac{h}{\rho u C_p}$$

Where  $\rho$  is density of the fluid and  $u$  is the velocity, and knowing that  $\frac{\dot{m}}{A} = \rho u$

$$NTU = ST \frac{A_{wg}}{A} \quad (2.85)$$

Stanton number is defined for heat transfer from the gas to the matrix. However in stirling cryocooler heat transfer is from gas to matrix when gas flow is into the freezer and from matrix to the gas when gas flow is into the cooler, so number of transfer units become;

$$NTU = ST \frac{A_{wg}}{2A} \quad (2.86)$$

$A_{wg}$  = wetted surface area in the heat exchanger

$A$  = free flow area in the heat exchanger

Regenerator effectiveness, which is the measure of the regenerator is defined by Urieli (1984) as;

$$\varepsilon = \frac{\text{The amount of heat transferred unidirectionally to the working gas in the regenerator section over the cycle}}{\text{The equivalent amount of heat transferred in the regenerator section of the ideal adiabatic model}}$$

According to this definition the enthalpy loss due to imperfect regeneration can be calculated by the following equation;

$$Q_{R_{loss}} = Q_{R_{ideal}} (1 - \varepsilon) \quad (2.87)$$

Where  $Q_{R_{ideal}}$  is evaluated as the difference between the maximum and minimum values

Since the temperature in the cooler section is higher than the temperature of the gas flowing from the regenerator to the cooler, in the cooler section some of the heat will be transferred to the incoming gas, which will result in a decrease of the heat rejected to the environment.

$$Q_H = Q_{H_{ideal}} + Q_{R_{loss}} \quad (2.88)$$

Where  $Q_{H_{ideal}}$  has a negative value and  $Q_{R_{loss}}$  has a positive value,

Similarly the temperature in the freezer is lower than the temperature of the gas flowing from the regenerator to the freezer, so in the freezer section some heat is transferred from incoming gas to the gas in the freezer, which will result in a decrease of the heat absorbed from the environment.

$$Q_L = Q_{L_{ideal}} - Q_{R_{loss}} \quad (2.89)$$

Where  $Q_{L_{ideal}}$  and  $Q_{R_{loss}}$  are both positive values.

### 2.3.2. Heat exchanger simple analysis

In an imperfect heat exchanger the mean effective temperatures of the gas is different from that of the heat exchanger walls. In cryocoolers the mean effective temperature of the gas in the freezer is lower than the temperature of the freezer wall and similarly the mean effective temperature of the gas in the cooler space is higher than the temperature of the cooler wall. This fact causes that the cryocooler is actually operating between temperature differences which is higher than the ideal case and the efficiency of the system decreases significantly. Consider the heat transferred in the freezer;

$$Q_L = Q_{L_{ideal}} - Q_{R_{loss}} = h_h A_{wgh} (T_L - T_{gh}) \quad (2.90)$$

Where;

$T_L$  = freezer wall temperature (cold side temperature),

$T_{gh}$  = the mean effective gas temperature and in the freezer space

$h_h$  = mean heat transfer coefficient in freezer.

Rearranging;

$$T_{gh} = T_L - \left( \frac{Q_{L_{ideal}} - Q_{R_{loss}}}{h_h A_{wgh}} \right) \quad (2.91)$$

Similarly heat transferred in cooler space is;

$$Q_H = Q_{H_{ideal}} + Q_{R_{loss}} = h_k A_{wgh} (T_H - T_{gk}) \quad (2.92)$$

Where;

$T_H$  = cooler wall temperature (hot side temperature),

$T_{gk}$  = the mean effective gas temperature and in the cooler space

$h_k$  = mean heat transfer coefficient in cooler.

Rearranging;

$$T_{gk} = T_H - \left( \frac{Q_{H_{ideal}} + Q_{R_{loss}}}{h_k A_{wgh}} \right) \quad (2.93)$$

New values of mean effective temperature of the gas in the heat exchanger are calculated with the equations above by using the solutions of the ideal adiabatic model and using these new values a new ideal adiabatic solution is performed. This cycle continues until convergence is obtained.

### 2.3.3. Pressure drop simple analysis

In real systems where fluid flow exists there is always a friction, which effects the performance of the system. Although it is assumed that the pressure in the system is same throughout the cryocooler, fluid friction causes a pressure drop in heat exchanger regions.

Consider Newton's law of viscosity;

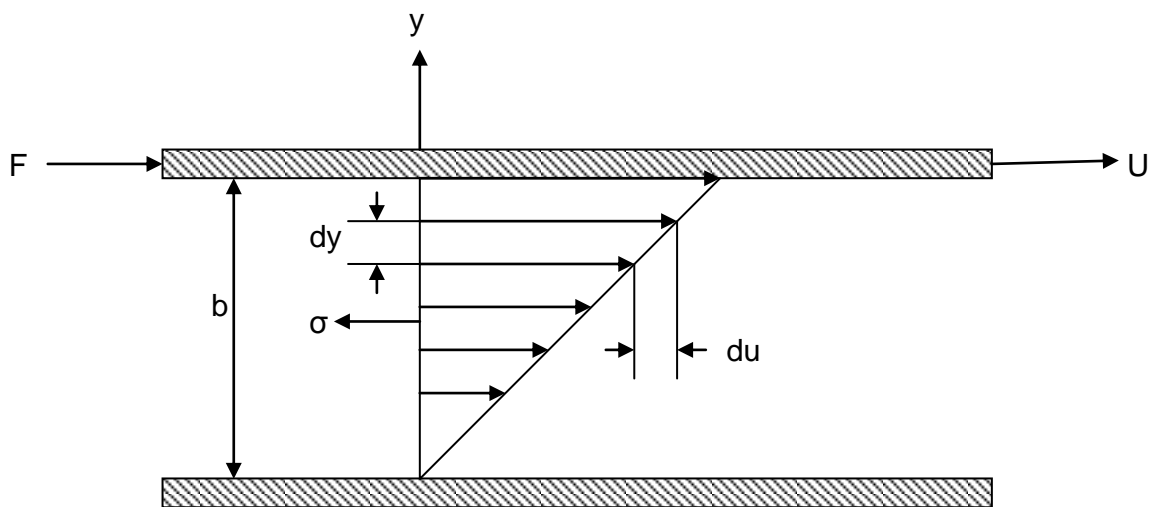


Figure 2. 5 Newton's conceptual model for defining the viscosity of a real fluid

The flow is one dimensional so;

$$\frac{F}{A_{wg}} = \mu \frac{u}{b} = \mu \frac{du}{dy} = -\sigma \quad (2.94)$$

Where

$A_{wg}$  = wetted area

$\mu$  = dynamic viscosity

$\sigma$  = shear stress in the flow field

$\frac{du}{dy}$  = slope of the velocity profile

Wetted area can be obtained by using the hydraulic diameter which can be defined for a circular pipe as;

$$d_H = \frac{4V}{A_{wg}} \quad (2.95)$$

Where  $V$  is void volume.

Substituting equation (2.94) into (2.95) drag force can be obtained as;

$$F = \sigma A_{wg} = \frac{4\sigma V}{d_H} \quad (2.96)$$

Fanning friction factor is defined as the ratio of shear stress to the dynamic head;

$$f_f = \frac{2\sigma}{\rho u^2}$$

Where  $\rho$  is the density

Since  $u = \frac{\phi}{\rho}$  Fanning friction factor becomes  $f_f = \frac{2\rho\sigma}{\phi^2}$  and substituting this into

(2.96) flow friction force can be found as;

$$F = \frac{2f_f V \phi^2}{d_H \rho} \quad (2.97)$$

It is known that the sum of the flow friction and the force caused by the pressure drop equals zero;

$$F + \Delta P \cdot A_w = 0 \quad (2.98)$$

However it can be concluded that the term  $F$  is always positive, which means violation of conservation of momentum, so Urieli found a solution to that problem by including the Reynolds number and defining friction factor  $f_R$ ;

$$f_R = f_f \cdot RE \quad (2.99)$$

Where  $RE = \frac{\rho \cdot u \cdot d_H}{\mu}$

Substituting Reynolds number,  $u = \frac{\phi}{\rho}$  and  $\rho = \frac{m}{V}$  into flow friction force  $F$ ;

$$F = \frac{2f_R V^2 \phi \mu}{d_H^2 m} \quad (2.100)$$

So force equation becomes;

$$\frac{2f_R V^2 \phi \mu}{d_H^2 m} + \Delta P A = 0 \quad (2.101)$$

Dividing both sides by  $A$  pressure can be obtained as;

$$\Delta P = \frac{-2f_R V L \phi \mu}{d_H^2 m} \quad (2.102)$$

Where  $L$  is length and  $m$  is mass.

Pressure drop equation in the final form obeys to the conservation of momentum, since mass flux term  $\phi$  takes both positive and negative values according to the direction of mass flow.

Total input work in one cycle can be expressed as the sum of the input work calculated by ideal adiabatic analysis and the losses due to pressure drop in the heat exchangers.

$$W_{in} = W_{in_{ideal}} + \Delta W \quad (2.103)$$

Where  $\Delta W$  is calculated as;

$$\Delta W = (dP_H + dP_R + dP_K)dV_E \quad (2.104)$$

### 2.3.4. Correlations used in simple analysis

Reynolds number is defined as the ratio of inertia forces to viscous forces in a system. In this study Reynolds number is used to determine if the flow is turbulent or laminar and it is used for calculating the flow friction and heat transfer losses in the cryocooler. Reynolds number for flow in a tube or pipe is expressed as

$$RE = \frac{\rho u d_H}{\mu} \quad (2.105)$$

Gas mass flux can be given as

$$\phi = \rho u \quad (2.106)$$

Substituting (2.106) into (2.91), the final form of the Reynolds number in this study is obtained as;

$$RE = \frac{\phi d_H}{\mu} \quad (2.107)$$

After calculating The Reynolds number the type of the flow is determined according to that number;

*if*  $RE < 2000 \Rightarrow$  laminar

*if*  $2000 < RE < 4000 \Rightarrow$  transition to turbulence

*if*  $RE > 4000 \Rightarrow$  turbulence

Stanton number is defined as the ratio of heat transferred into a fluid to the thermal capacity of fluid and in this study it is obtained in terms of Reynolds number. This number is used for determining effectiveness of the regenerator as described in

section 2.3.1. The regenerator in the cryocooler contains woven wire matrix and for this type of configuration the correlations of GLIMPS user manual (1992) are used.

$$ST = \frac{p \cdot RE^{-m}}{Pr} \quad (2.108)$$

Where ;

$\psi$  =porosity

$$m = 0.43 \cdot \psi + 0.15$$

$$p = 0.537 \cdot \psi \quad \text{if } \psi < 0.39$$

$$p = 1.54 - 6.36 \cdot \psi + 7.56 \cdot \psi^2 \quad \text{if } \psi \geq 0.39$$

$$Pr = \frac{C_p \cdot \mu}{k} = \text{Prandtl number}$$

Friction factor, which includes Fanning friction factor is described in section 2.3.3. As in the case with the Stanton number, for calculating the Fanning friction factor correlations of GLIMPS user manual (1992) are used;

$$\left. \begin{aligned} f_f &= \frac{16}{RE} && \text{if } RE < 2000 \\ f_f &= 0.015 - 3.5 \cdot 10^{-6} \cdot RE && \text{if } 2000 < RE < 4000 \\ f_f &= 0.079 \cdot RE^{-0.25} && \text{if } RE > 4000 \end{aligned} \right\} \quad (2.109)$$

### 2.3.4. Performance of the cryocooler

Performance of a refrigeration cycle is the ratio of heat removed to total work input, which can be shown as;

$$COP = \frac{\text{Heat lifted}}{\text{Work input}} = \frac{Q_L}{W_{in}} \quad (2.110)$$

As previously described actual heat transfer in the freezer spaces is evaluated by adding the regenerator losses to the heat transfer value found by ideal adiabatic analysis. There are additional loss, regenerator wall heat leakage, which should also be included in the performance analysis. Regenerator wall heat leakage is a conduction loss. Since the regenerator is working between two different temperatures, the wall, carrying the regenerator mesh, encounters conductive heat transfer from cooler to freezer. Loss by the regenerator wall heat leakage can be quantified as;

$$Q_{Leak} = k_{rw} \cdot A_{rw} (T_{wh} - T_{wk}) \quad (2.111)$$

Where;

$k_{rw}$  = Thermal conductivity of the regenerator wall

$A_{rw}$  = Cross-sectional area of the regenerator wall

$T_h$  = Temperature of the freezer wall

$T_k$  = Temperature of the cooler wall

So the final form of the coefficient of performance can be shown as;

$$COP = \frac{Q_{H_{ideal}} + Q_{Leak} - Q_{R_{loss}}}{W_{in_{ideal}} + \Delta W_P} \quad (2.112)$$

## **2.4 Solution method**

The system of equations derived in the previous sections require a numerical solution. Urieli (1984) developed an algorithmic approach to solve these equations and this approach is used also in this study. Mathcad is employed for numerical simulation, where Runge Kutta 4<sup>th</sup> order algorithm is used in solving non-linear equations derived above. In Appendix A developed set of MathCAD functions and sub functions are provided. In Figure 2.6 the algorithm of the numerical simulation is presented.

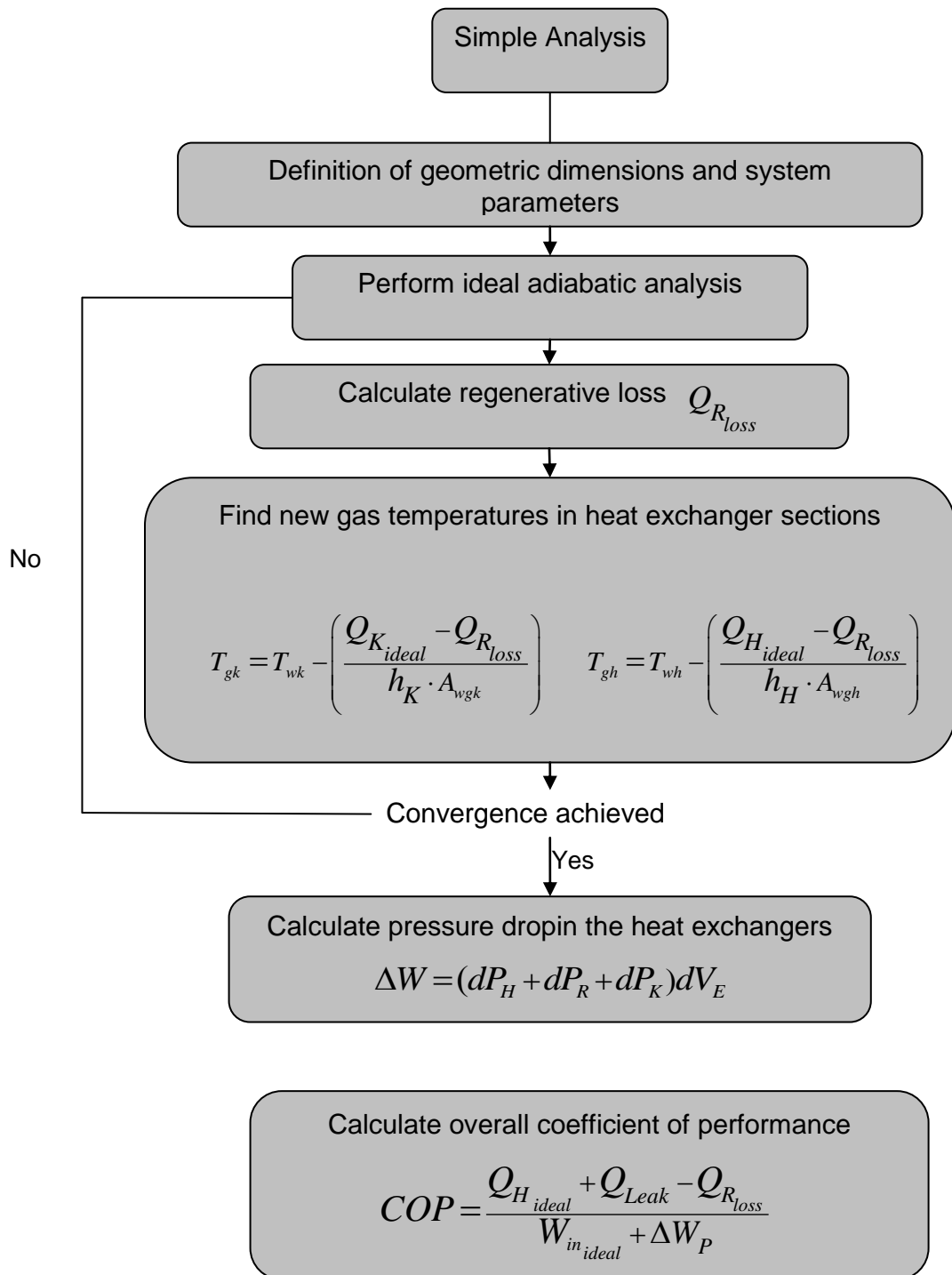


Figure 2. 6 Algorithm of numerical simulation by simple analysis

## CHAPTER 3

### ANALYSIS AND RESULTS

#### 3.1. Cryocooler dimensions and operational data used in the analysis

In this research dimensions and operating conditions of the cryocooler are assumed in such a way that they are as realistic as possible. These realistic values are obtained by inspection of a commercial cryocooler used in military applications. Since it is a commercial product internal dimensions of the cryocooler are not shared by manufacturer. However main objective of this study is to analyze the effects of operating parameters on the cryocooler and assumed data serve the purpose.

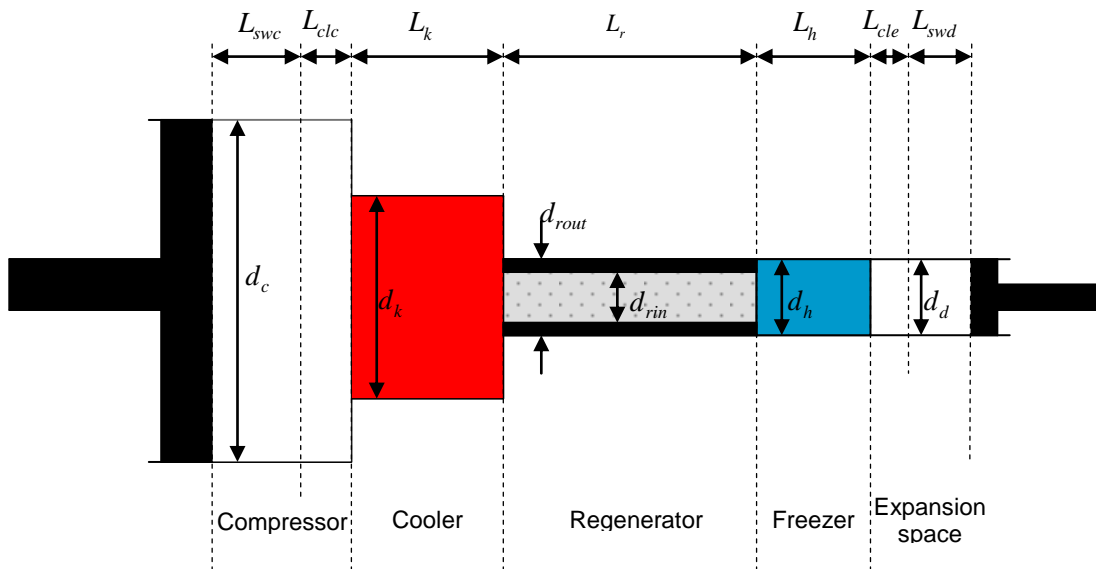


Figure 3. 1 Cryocooler schematics

Table 3. 1 Cryocooler dimensions and operating parameters

Compressor piston diameter, $d_c$	8mm
Compression piston swept distance, $L_{swc}$	6mm
Compression space clearance distance, $L_{clc}$	2mm
Displacer diameter, $d_d$	5mm
Displacer swept distance, $L_{swd}$	1mm
Expansion space clearance distance, $L_{cle}$	0.1mm
Cooler diameter, $d_k$	10mm
Length of the cooler $L_k$	10mm
Freezer diameter, $d_h$	5mm
Length of the freezer, $L_h$	2mm
Regenerator housing outer diameter, $d_{rout}$	5mm
Regenerator housing inner diameter, $d_{rin}$	4mm
Length of the regenerator, $L_r$	55mm
Porosity of the regenerator, $\psi$	0.6
Mesh wire diameter, $d_{wire}$	0.005mm
Cooler wall temperature, $T_k$	300K
Freezer wall temperature, $T_h$	80K
Mean operating pressure, $P_{mean}$	3Mpa
Operating frequency, $f$	60Hz
Phase angle, $\alpha$	90
Working gas	Helium

### 3.2. Schmidt Analysis Results

As described before, Schmidt analysis is a highly idealized method to investigate the performance of the Stirling machines. Assumptions are far from real conditions, which means that this method can only be used as an introduction to real Stirling machines. At the operating conditions tabulated in section 3.1, Schmidt analysis gives a coefficient of performance value of 0.364, which is a high value considering the real cryocoolers, whose coefficient of performance values are commonly between 0.03 and 0.06. Coefficient of performance is dependent only on the temperature. Changing the frequency or mean pressure does not have any effect on the COP. However the values of input work and heat removed change directly when these parameters are changed. With the given operating conditions heat removed is evaluated as 0.496W while the input power is 1.363W. The mass of the working gas is found to be 8.712mg and it is used in ideal adiabatic analysis.

Resulting PV diagram is as shown in figure 3.2, when the PV diagram of the ideal cycle is considered there is a significant difference between the ideal PV diagram and Schmidt PV diagram. This is a result of sinusoidal volume variations.

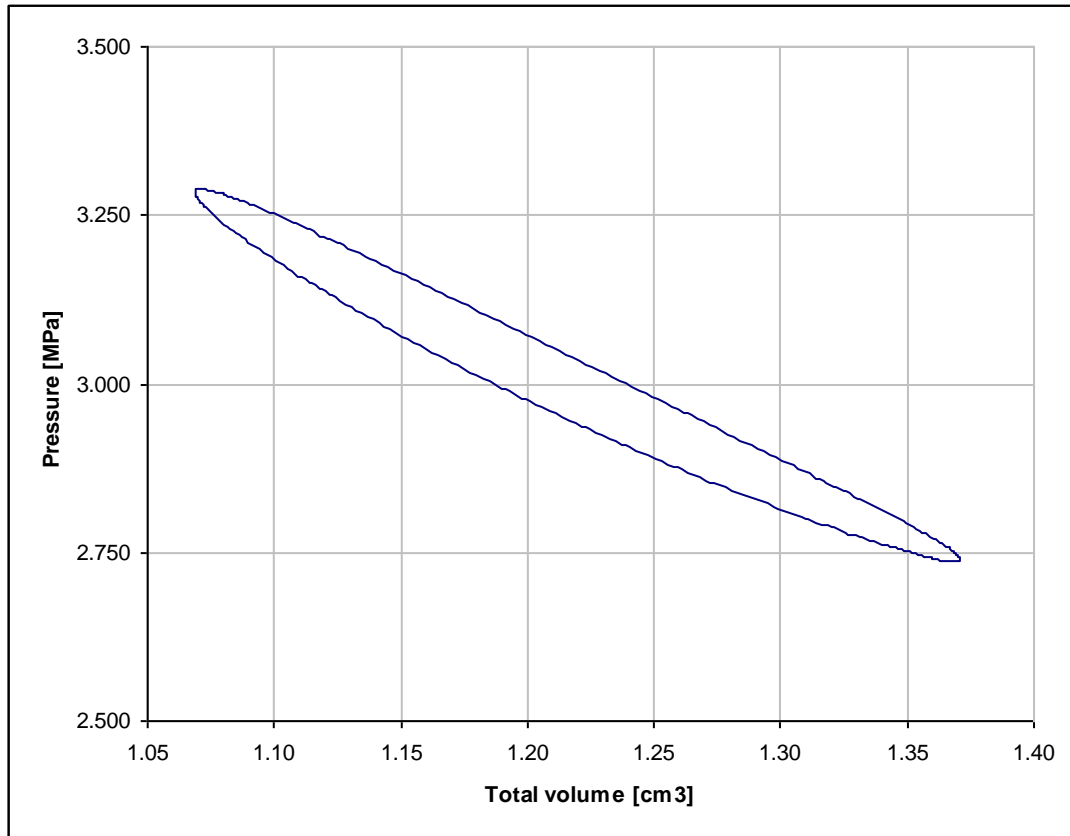


Figure 3.2 PV diagram obtained by Schmidt analysis

Volume variations, shown in figure 3.3, is same for Schmidt analysis, ideal adiabatic analysis and simple analysis, since piston motions are assumed to be sinusoidal in each case. Phase angle between the compression end expansion pistons can easily be distinguished. It can also be observed that the variation of the total volume is similar to the variations in the compression space volume which shows that the change in the total volume is driven by the compression space volume. The difference between total volume and compression volume is caused by the constant volume heat exchangers.

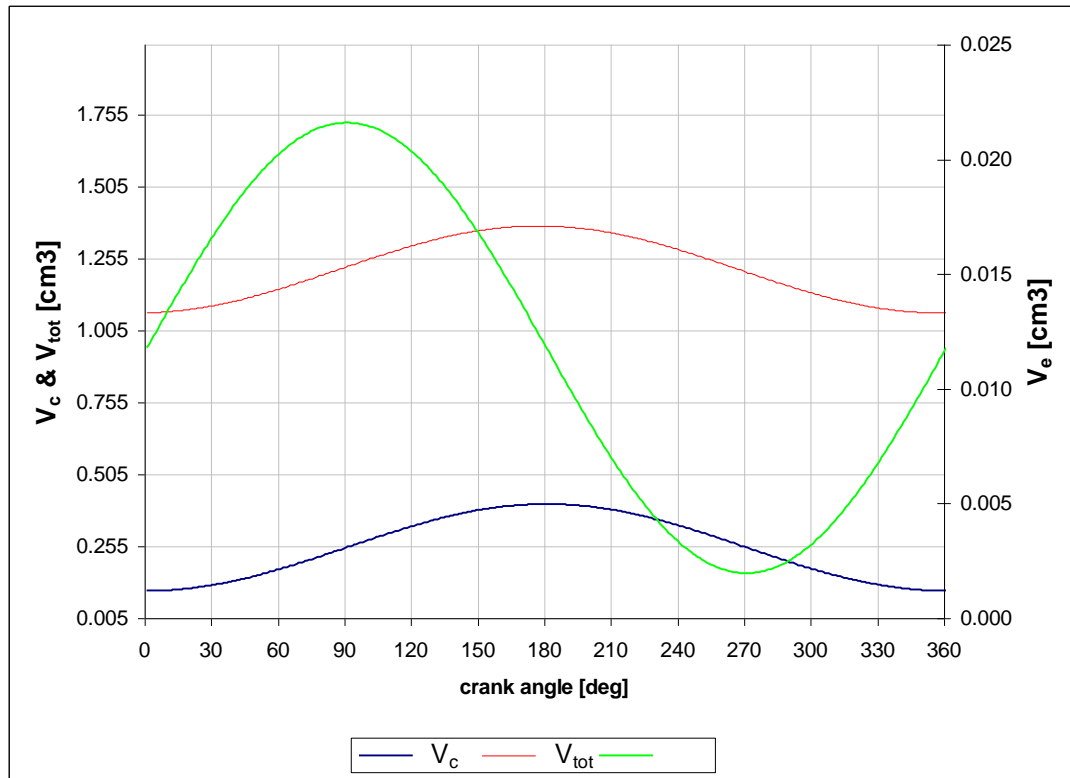


Figure 3. 3 Volume variations with respect to crank angle

In Schmidt analysis a closed form solution is employed where the final values of input work and heat removed are calculated, so these values cannot be demonstrated with respect to the crank angle.

### 3.3. Ideal adiabatic Analysis Results

Ideal adiabatic model does not include the imperfections in the system as in the case with the Schmidt analysis. However this method is more realistic when compared to Schmidt analysis, since in real systems compression and expansion spaces tend to be adiabatic and the heat transfer in the system occurs in the heat exchangers mainly.

The resulting PV diagram can be shown as in figure 3.4, which is slightly different than that of the Schmidt analysis. This difference is because of the difference in the calculation of temperatures.

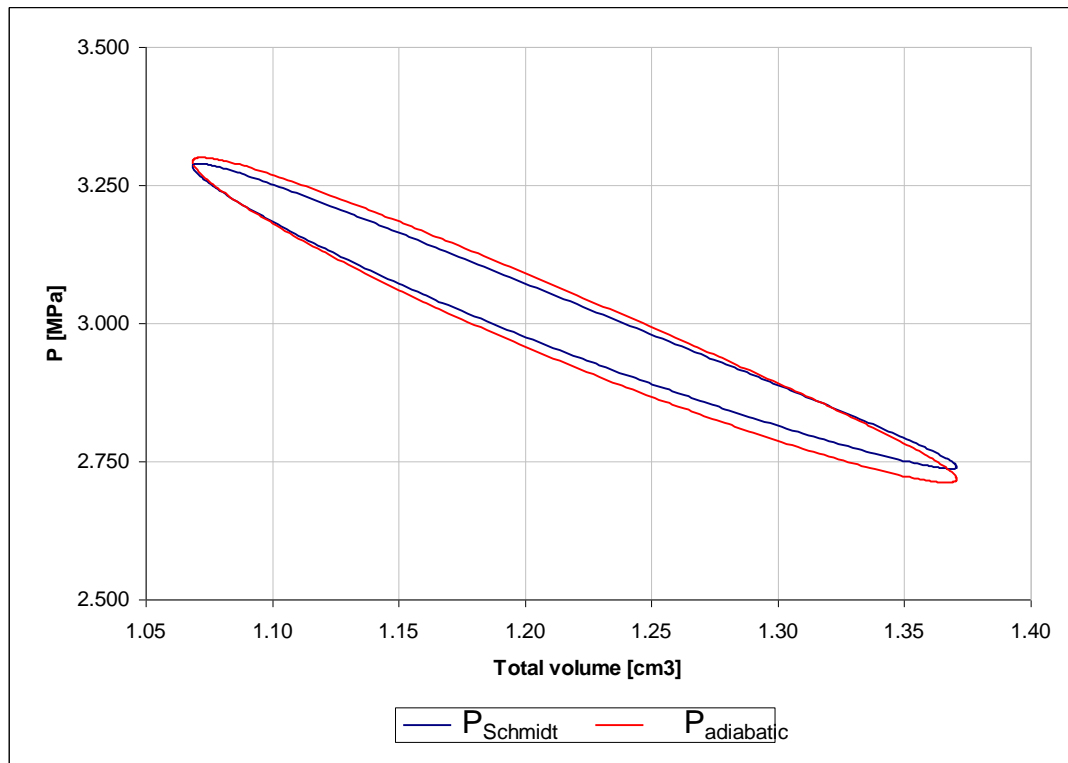


Figure 3.4 PV diagram obtained by ideal adiabatic analysis

In figure 3.5 plot of pressure vs. crank angle can be seen, which shows that cycle starts with expansion. It can be observed that there is a slight difference in pressure variations between ideal Schmidt and adiabatic analysis. This difference is in accordance with the PV diagram given in Figure 3.4.

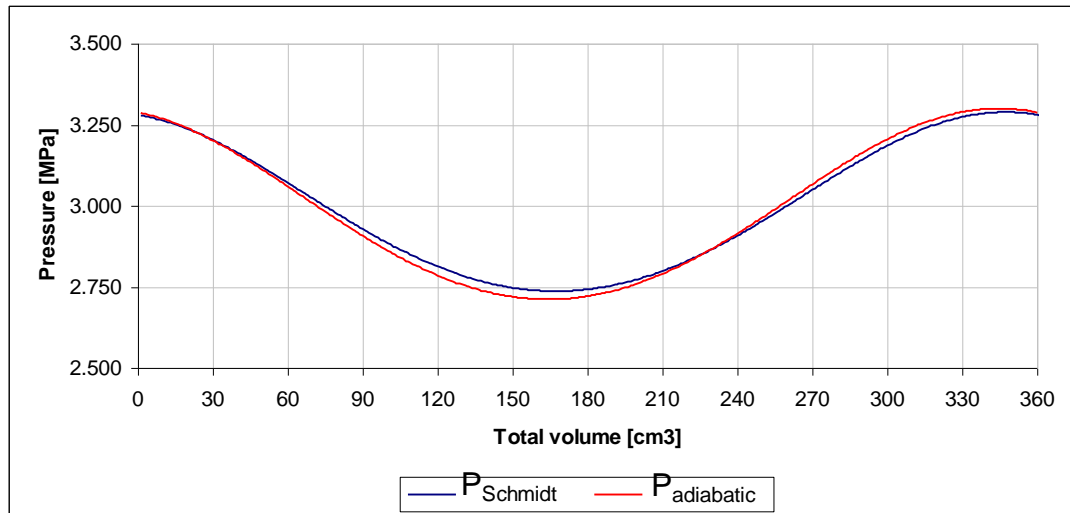


Figure 3.5 Pressure by ideal adiabatic analysis with respect to crank angle (j)

Figure 3.6 shows masses in five components of the cryocooler vs. crank angle. As expected the mass in the regenerator section is highest, since it has second highest volume in the cryocooler and its temperature lower compared to cooler and compression sections. Although it has the highest temperature in the system, expansion space has minimum fraction of the gas, since its volume is very small.

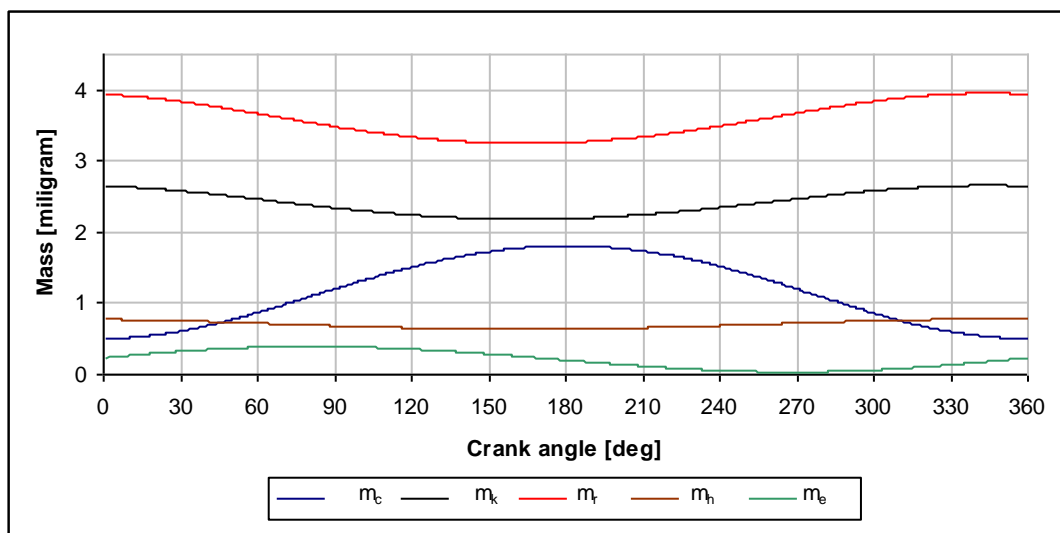


Figure 3.6 Mass variations with respect to crank angle in compression space(c), expansion space(e), regenerator(r), freezer(h), and cooler(k) sections.

The temperature in the compression  $T_C$  and expansion volume  $T_e$  vs. crank angle is given in Figure 3.7. It can be seen that  $T_C$  oscillates between 290.4K and 314.4K while  $T_e$  changes between 80.6K and 74.6K.

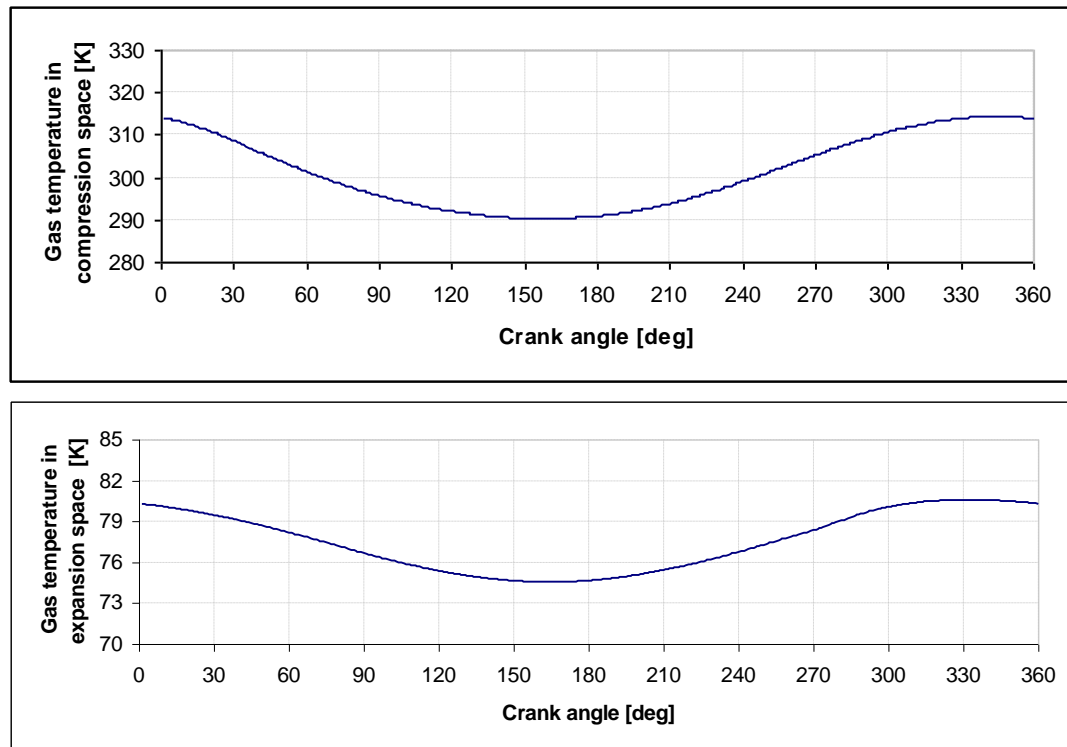


Figure 3. 7 Temperature with respect to crank angle in compression (c) and expansion (e) spaces.

Heat transfer and work done vs. crank angle plot of the cryocooler is shown in Figure 3.8. As it can be seen considerable heat transfer occurs in the regenerator  $Q_R$  and at the end net heat transferred to the regenerator becomes zero, which is the case for ideal regenerators. In the cooler section heat  $Q_H$  is transferred to the cooler until the compression starts and after that instant cooler rejects heat to environment and at the end it has a negative net value. Total work  $W$  and the compression work  $W_c$  are very close to each other, which shows that major part of the total work is compressor work.

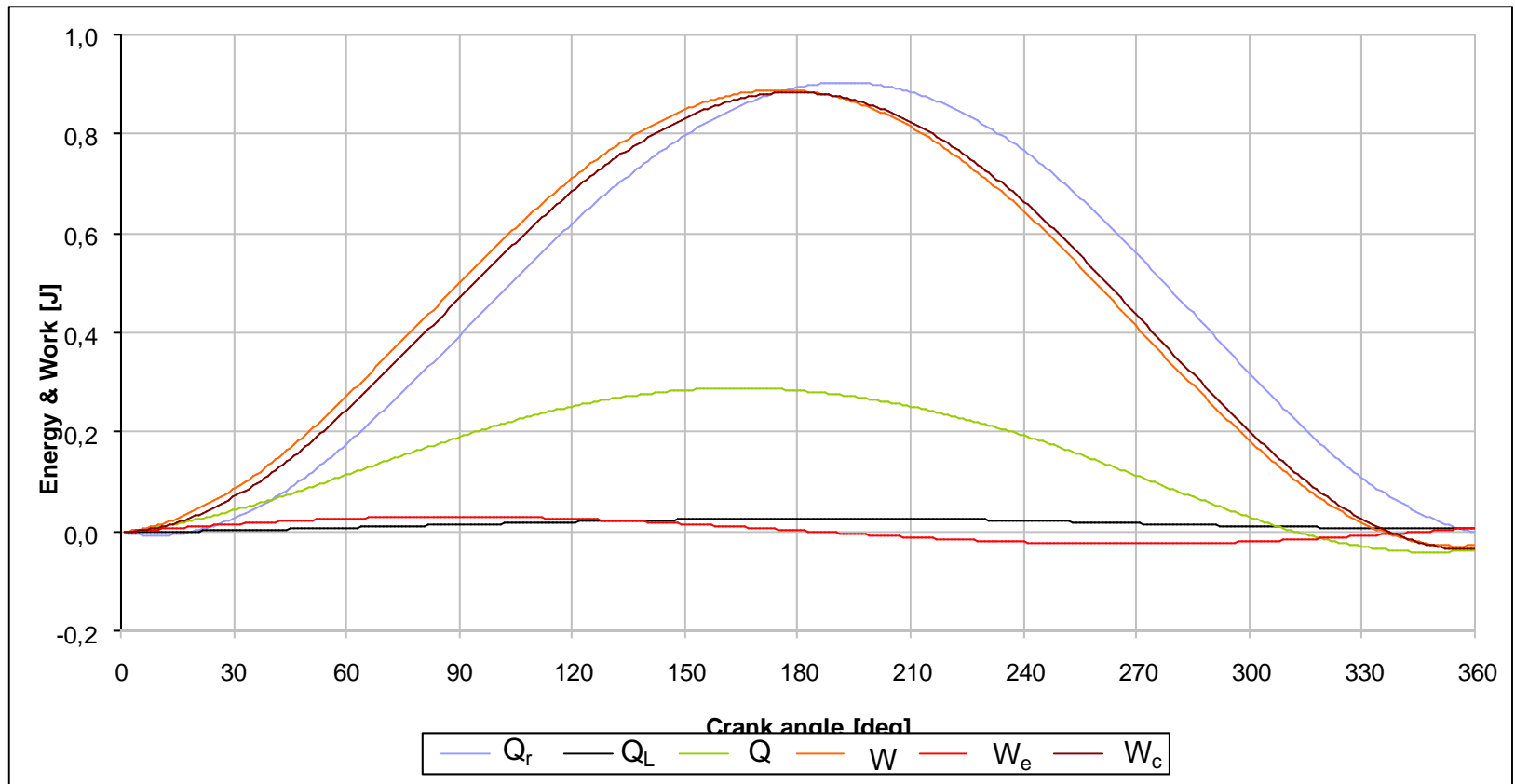


Figure 3. 8 Heat transfer in the cooler ( $Q_H$ ), freezer ( $Q_L$ ), regenerator ( $Q_r$ ) and expansion work ( $W_e$ ), compression work ( $W_c$ ) and total work input ( $W$ ) with respect to crank angle.

Figure 3.9 shows a closer look to heat rejected  $Q_H$ , heat removed  $Q_L$  and expansion work  $W_e$ . It is clear that  $Q_L$  and  $W_e$  are equal at the end of the cycle although they follow very different paths. When the expansion starts  $Q_L$  starts to increase and continue to increase until compression starts. After that point due to compression, it starts to decrease. However at the end of the cycle it is positive meaning net heat transfer is the gas.

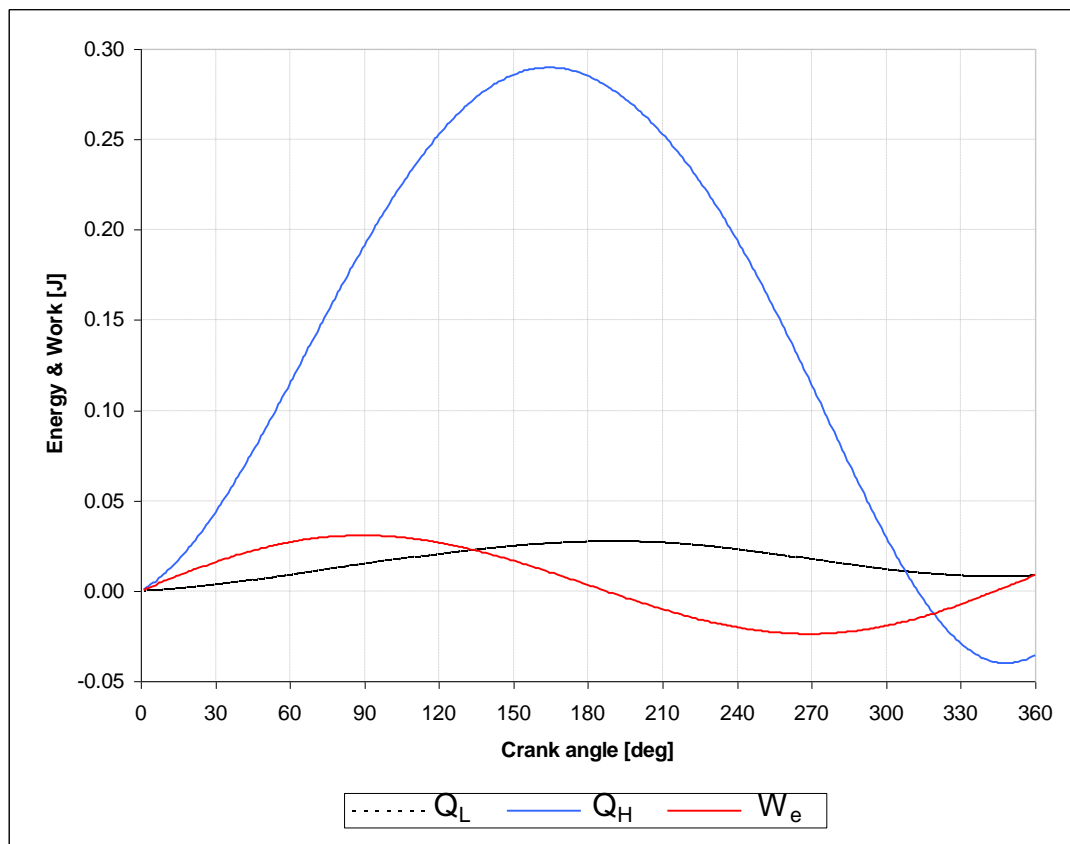


Figure 3.9 Heat transfer in the cooler (K), freezer (H) and expansion work (e), with respect to crank angle

Ideal adiabatic analysis returned a coefficient of performance of 0.331 with a heat removal of 0.526W and input power of 1.59W. Although COP has a lower value than the ideal adiabatic analysis, still it is a high value for a real Stirling cryocooler

### 3.4. Simple Analysis Results

The values found in the previous section are used in Simple analysis as a start point for evaluation of losses due to imperfection of the components. Using the correlations derived in Chapter 2 new values of gas temperatures in the cooler and freezer sections are obtained and with these new temperature values a new ideal adiabatic analysis is performed until convergence is obtained.

By following this procedure the temperature of the gas in the freezer is obtained as 51.5K and the temperature of the gas in the cooler section is obtained as 361.3K. Using these final temperature values, ideal adiabatic analysis is performed and following PV diagram in Figure 3.10 is obtained. However PV diagram for simple analysis is obtained decoupled from the system.

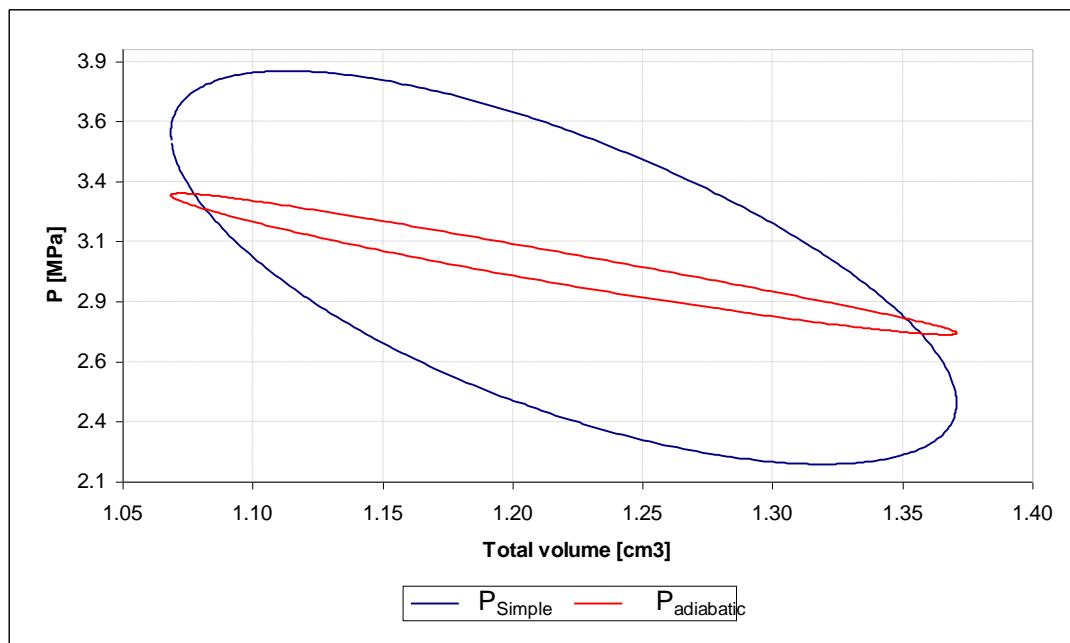


Figure 3.10 PV diagram obtained by simple analysis and ideal adiabatic analysis

Pressure drop in the regenerator  $\Delta P_r$ , in the cooler  $\Delta P_k$  and in the heater  $\Delta P_h$  vs. crank angle can be obtained as in Figure 3.11. There is considerable pressure drop in the regenerator, which seriously affect the performance of the system. Pressure drop in the heater and cooler section is negligible when compared to pressure drop in the regenerator. Low values of pressure drop in the freezer and cooler is mainly due to small wetted area of these sections

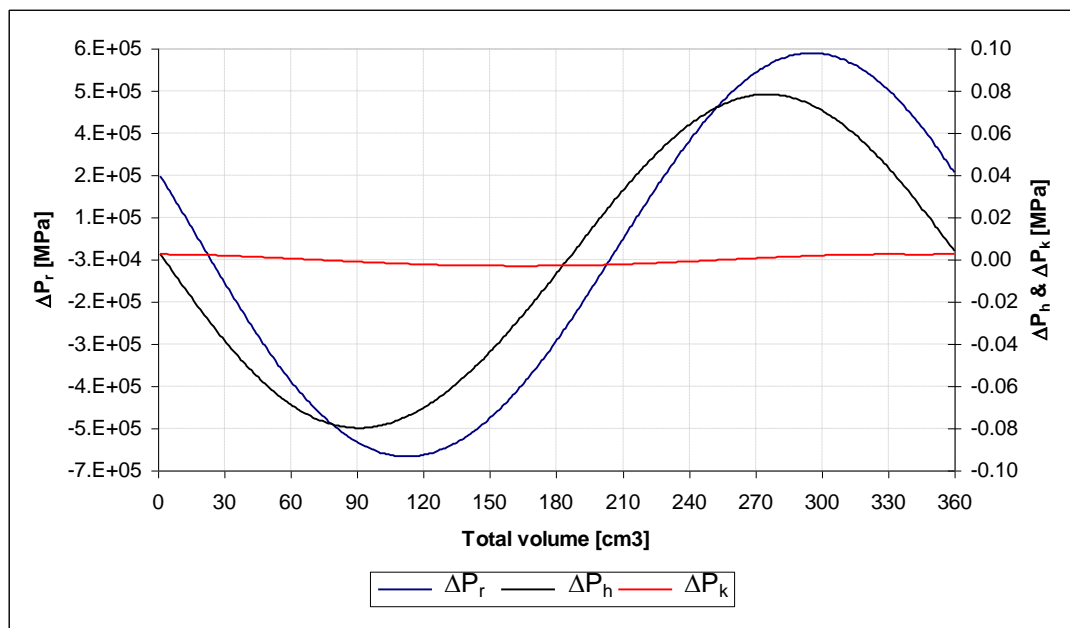


Figure 3.11 Pressure drop variations with respect to crank angle in regenerator (r), in cooler (k) and in freezer(h)

The pressure drop in the regenerator mainly occurs due to existence of regenerator matrix, effects of which will be investigated in the following section.

Although the initial conditions changed in the final adiabatic analysis, final temperatures vs. crank angle of the compression and expansion spaces are nearly the same with ideal adiabatic analysis.

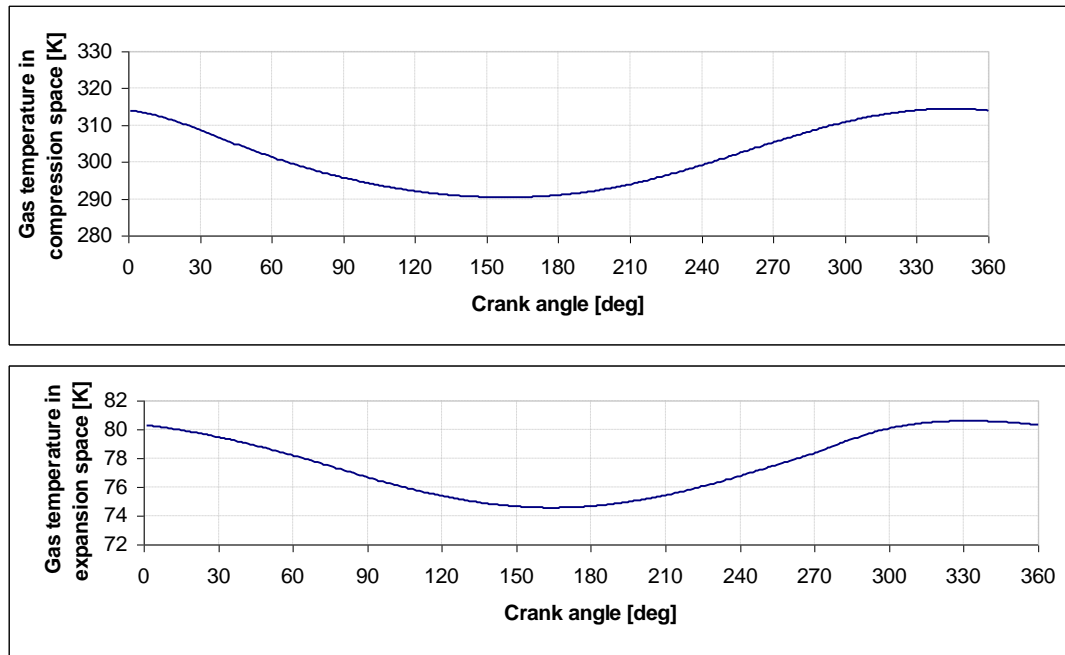


Figure 3.12 Temperature variation with respect to crank angle (i) in expansion (e) and in compression (c) spaces after simple analysis.

Simple analysis returned a coefficient of performance of 0.134, which is very low compared to Schmidt and ideal adiabatic analysis. This shows significance of the losses in a Stirling cryocooler. Heat removal and input work are evaluated as 0.526W and 1.59 W respectively by the ideal adiabatic analysis. Regenerative loss due to regenerator imperfection is calculated by the equations given in chapter two and found to be 0.012W, where the effectiveness of the regenerator is 0.999. As expected, main losses are caused by pressure drop and by regenerator wall heat leakage, values of which are 0.471W and 0.239W respectively. Not surprisingly regenerator wall heat leakage causes a 45.4% decrease in the freezer performance and pressure drop losses cause 29.6% increase in the input work and consequently a heat removal of 0.276 W and a work input of 2.06 W are evaluated.

The summary of the results obtained by three analysis methods can be tabulated as in Table 3.2.

Table 3. 2 Comparison of three analysis methods

<b>Analysis</b>	<b>Work input [W]</b>	<b>Heat removed [W]</b>	<b>COP</b>
Ideal Schmidt analysis	0.496	1.363	0.364
Ideal adiabatic analysis	1.59	0.526	0.331
Simple analysis	2.06	0.276	0.134

### **3.5. Effect of system parameters on the performance**

In this section effects of operating parameters to the overall engine performance are investigated in a detailed manner. As it is seen in the previous section heat transfer and flow friction losses have a considerable effect on the system performance. Investigation of system parameters may be very helpful for understanding the loss mechanisms and make it possible to take precautions before designing a working cryocooler.

#### **3.5.1. Effect of porosity**

Porosity is defined as the ratio of void volume to total volume in the regenerator. As it is seen in the previous sections, regenerator has crucial effect on the performance. The value of the heat transfer in the regenerator is almost equal to the compressor work, which shows the importance of the regenerator. Absence of the regenerator means loss of this energy.

Since porosity is main parameter in a regenerator, it is mandatory to investigate its effect in the performance. Figure 3.13 shows the variation of regenerator effectiveness  $\varepsilon$  with respect to porosity  $\psi$ . As porosity increases, the effectiveness of the regenerator decreases. Main cause of this effect is total area of heat transfer. As porosity increases void volume in the regenerator increases and as a consequence total area of heat transfer decreases.

This fact can lead us to another conclusion about the diameter of the mesh wire. It can be said that, as the diameter of the mesh matrix wire decreases the effectiveness of the regenerator increases as a result of increasing heat transfer area.

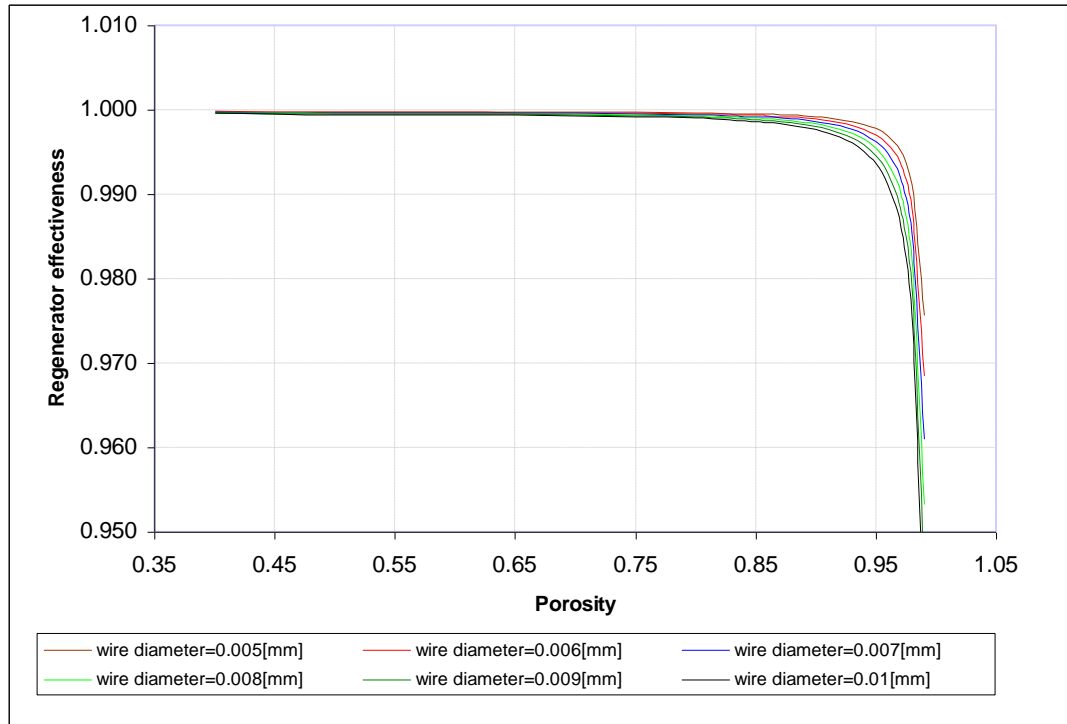


Figure 3.13 Regenerator effectiveness  $\epsilon$  versus porosity  $\psi$  at different mesh wire diameters plot

While considering the effect of porosity on the regenerator effectiveness, total efficiency of the engine should also be considered. Figure 3.14 shows efficiency vs. porosity plot of the cryocooler. Efficiency first increases and then decreases as porosity increases. This can lead us to two important conclusions. At low values of porosity, where the void volume in the regenerator is low pressure drop effects the system performance in a negative way and at high values of porosity, regenerative effects become smaller and heat loss due to regenerator effectiveness increases, causing a decline in total efficiency.

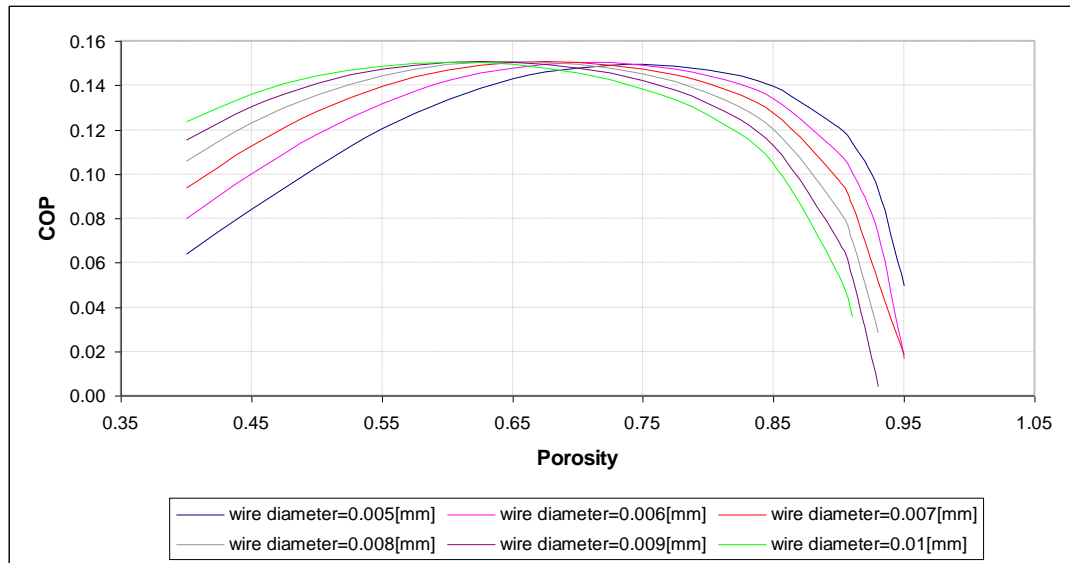


Figure 3.14 Coefficient of performance COP versus porosity  $\psi$  at different mesh wire diameters plot

Pressure drop losses increases and the efficiency of the cryocooler decreases. In Figure 3.15 effect of porosity on pressure drop is demonstrated. Two porosity values are chosen and regenerator pressure drop is evaluated while other parameters are same. As it can be seen pressure drop due to friction is much higher when porosity is 0.5. This explains the effect of porosity on pressure drop and on efficiency of the system consequently.

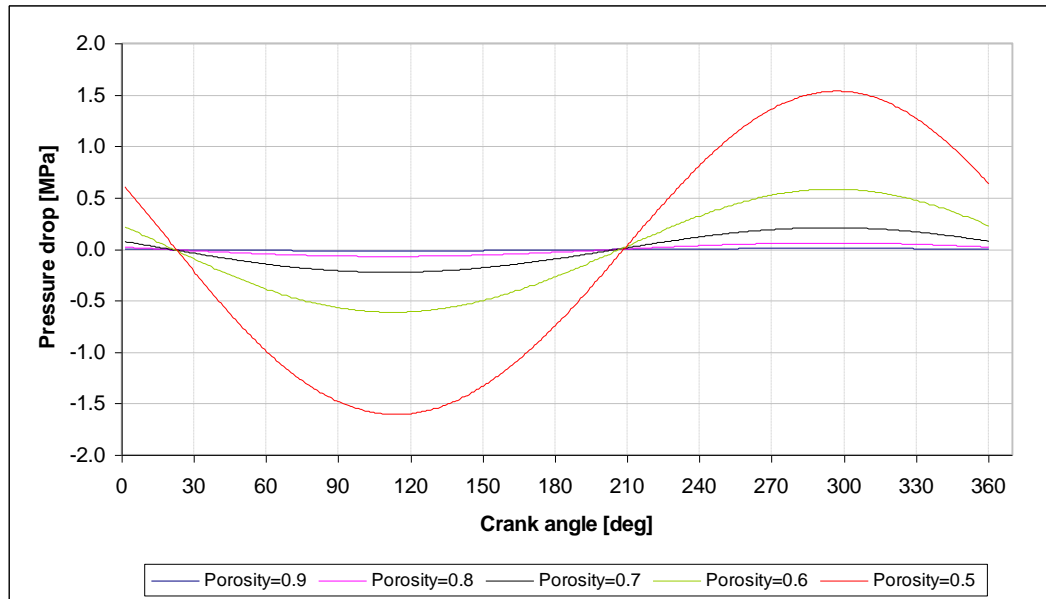


Figure 3.15 Pressure drop in the regenerator with respect to crank angle at porosity values between 0.5 and 0.9

In Figure 3.16 effect of porosity in losses of the system is presented. It is in agreement with the regenerator effectiveness vs. porosity graph. As porosity increases the regenerative losses increases

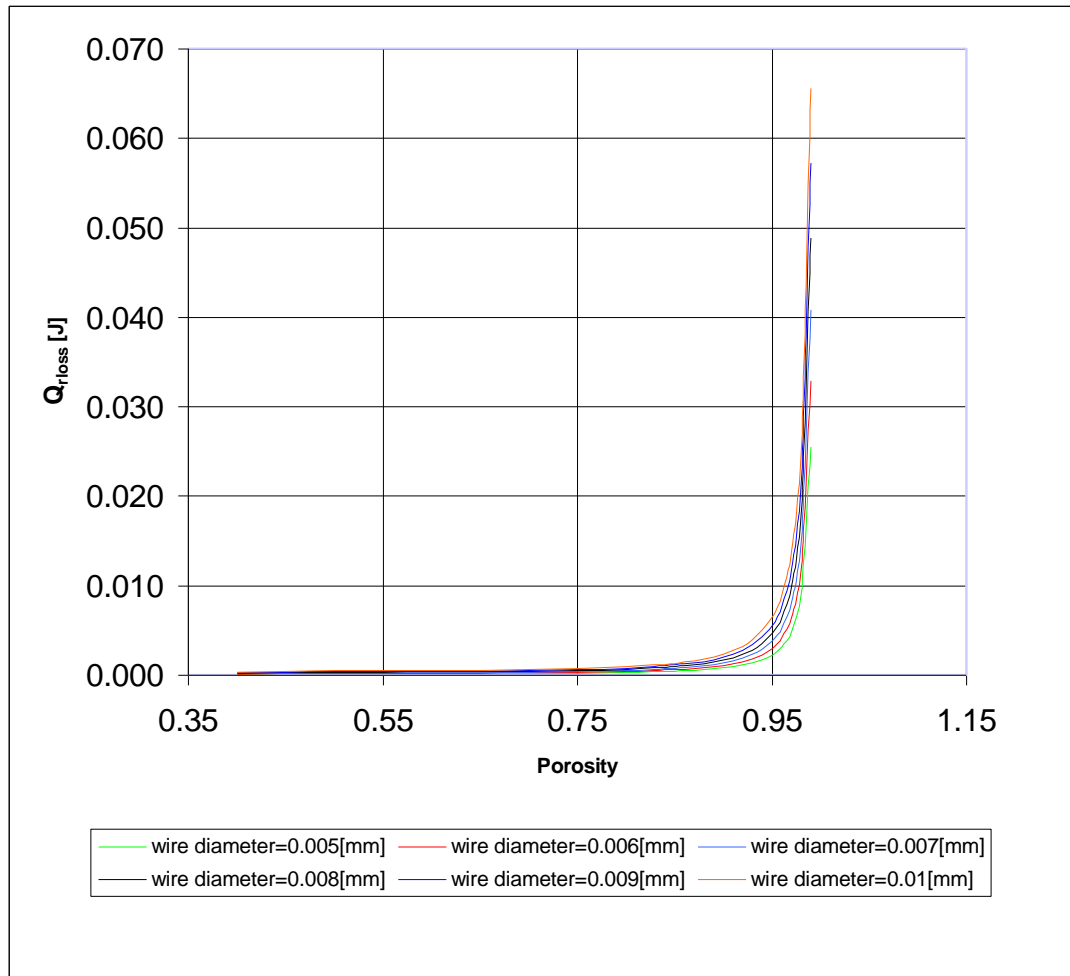


Figure 3.16 Regenerator loss  $Q_{Rloss}$  versus porosity  $\psi$  plot at different mesh wire diameters.

Considering the plots demonstrated above, an efficient cryocooler having an acceptable capacity of heat removal can be designed for a porosity value of 0.7. At this point both efficiency of the system and losses due to flow friction losses have an acceptable value.

### 3.5.2. Effect of operating frequency

Frequency is a system parameter which can be changed after design and production phase. It is arranged by the electronics which drive the cooler and can be regulated

easily. Usually in design process of a cryocooler working frequency is determined after production of cryocooler and it is not uncommon to have two similar cryocoolers operating at two different frequencies, since the dynamics of the system is affected by the production significantly. In addition to that requirement of the application of cryocooler is another criterion when determining the operating frequency. Where a high efficiency is required, cryocooling system works at the point of highest frequency. However another application may require a high cooling capacity and ignore the efficiency of the cryocooler. Since designing a new cryocooler for each application is not preferred, usually similar cryocoolers with different operating frequencies are employed for different applications.

In Figure 3.17 efficiency versus operating frequency can be observed. As the frequency increases the efficiency increases up to a point and it starts do decrease. This decrease is mainly caused by the losses due to flow friction. Velocity of the working gas in the system becomes larger, as the frequency increases and consequently this increase cause pressure drop losses due to friction to increase. Furthermore it is expected that the temperature in the cooler gets higher and the device become hot. In Figure 3.18 losses due to pressure drop vs. frequency plot is presented, which supports these observation.

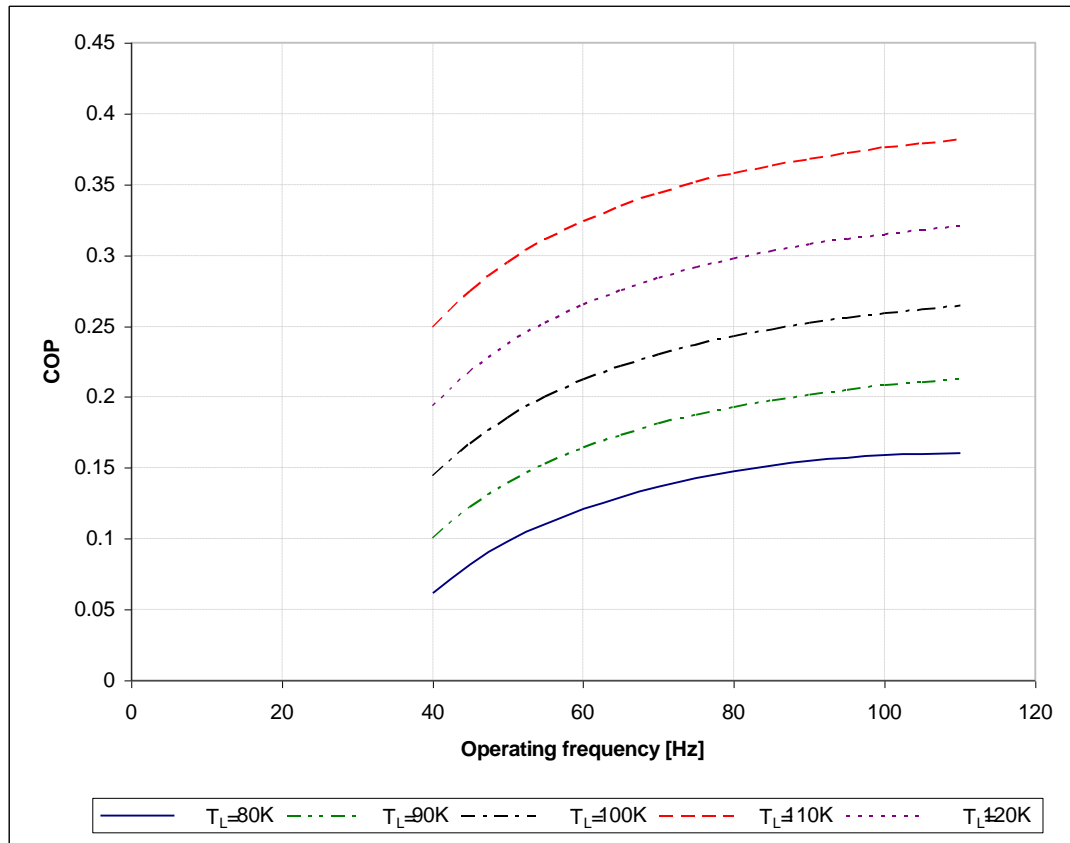


Figure 3.17 Coefficient of performance at different cold side temperatures versus operating frequency at different cold side temperatures plot

In Figure 3.19 gas temperature in the heater vs. frequency and in Figure 3.20 heat rejected from the system vs. frequency are demonstrated. According to these plots it can be concluded that when operating frequency increases heat rejected from the system increases, which is followed by an increase in the gas temperature. Heat exchangers in the cooler section become very important when this fact is considered. At the point where this heat couldn't be rejected, cryocooler become inoperable at that frequency.

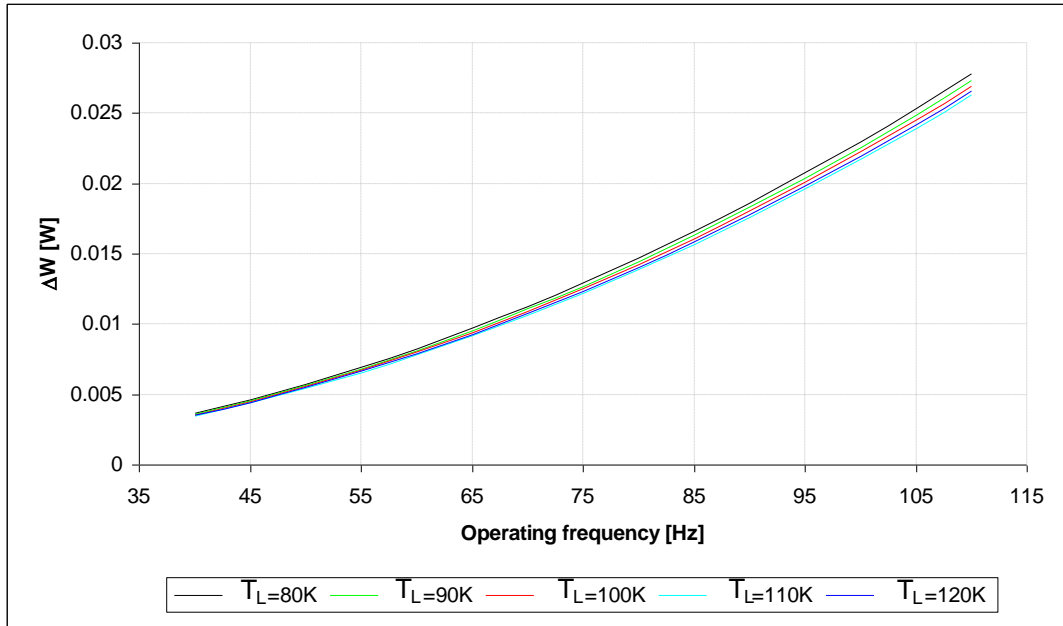


Figure 3.18 Loss due to pressure drop  $\Delta W$  [W] at different cold side temperatures versus operating frequency plot

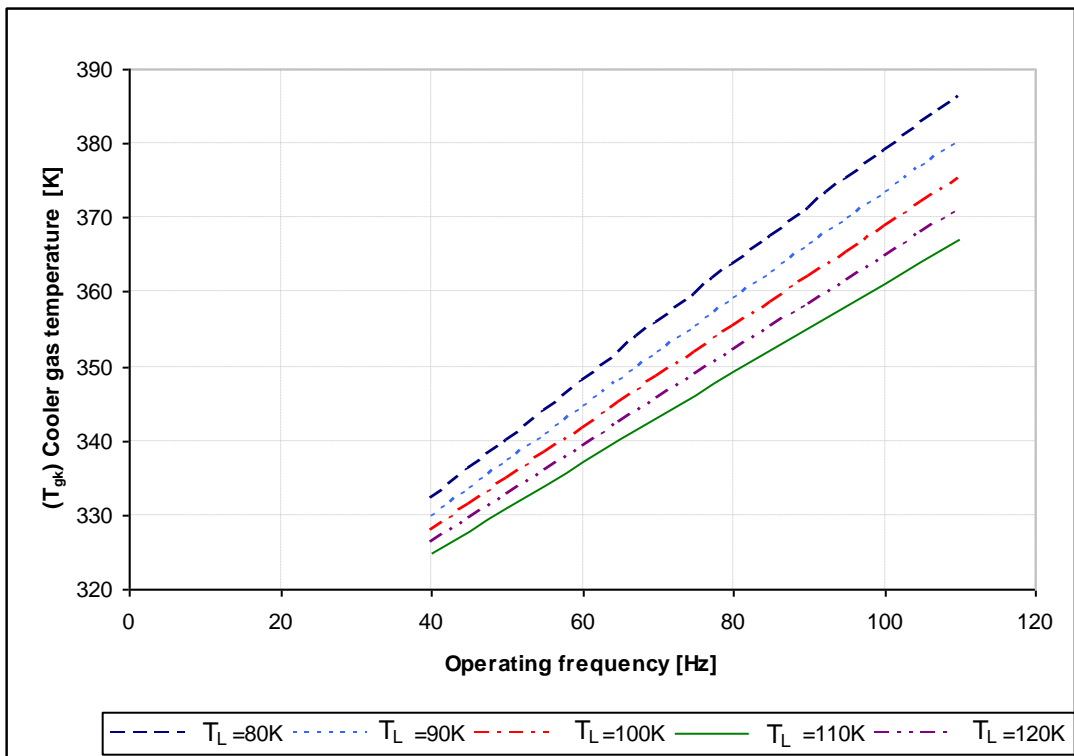


Figure 3.19 Cooler gas temperature at different cold side temperatures versus frequency plot

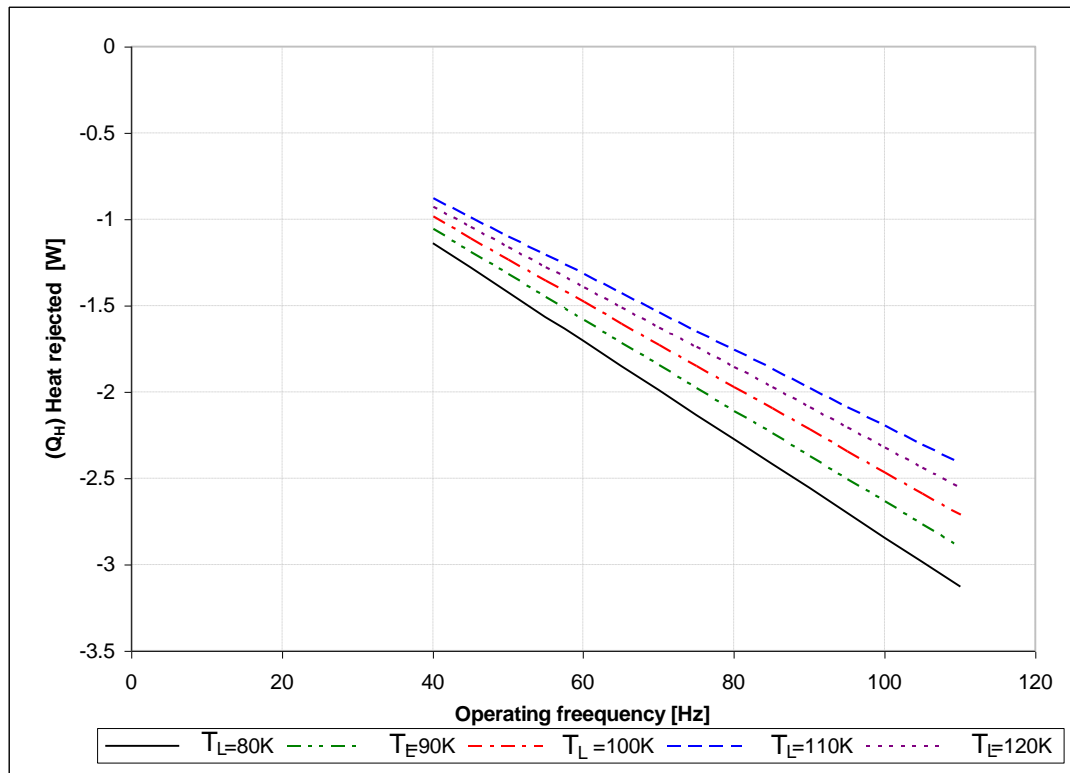


Figure 3.20 Heat rejected at different cold side temperatures vs frequency plot

### 3.5.3. Effect of operating temperatures

One of the major operating parameters of a cryocooler is the cold side temperature which is dependent on the application. For cryocoolers used in cooling of infrared detectors common working temperatures change between 77K to 120K. It is obvious that this parameter changes the efficiency significantly. Figure 3.21 shows efficiency versus freezer wall temperature while cooler temperature is changed from 290K to 310 K, which are usual cold side temperatures. Not surprisingly efficiency increases as the temperature difference where the cryocooler works decreases.

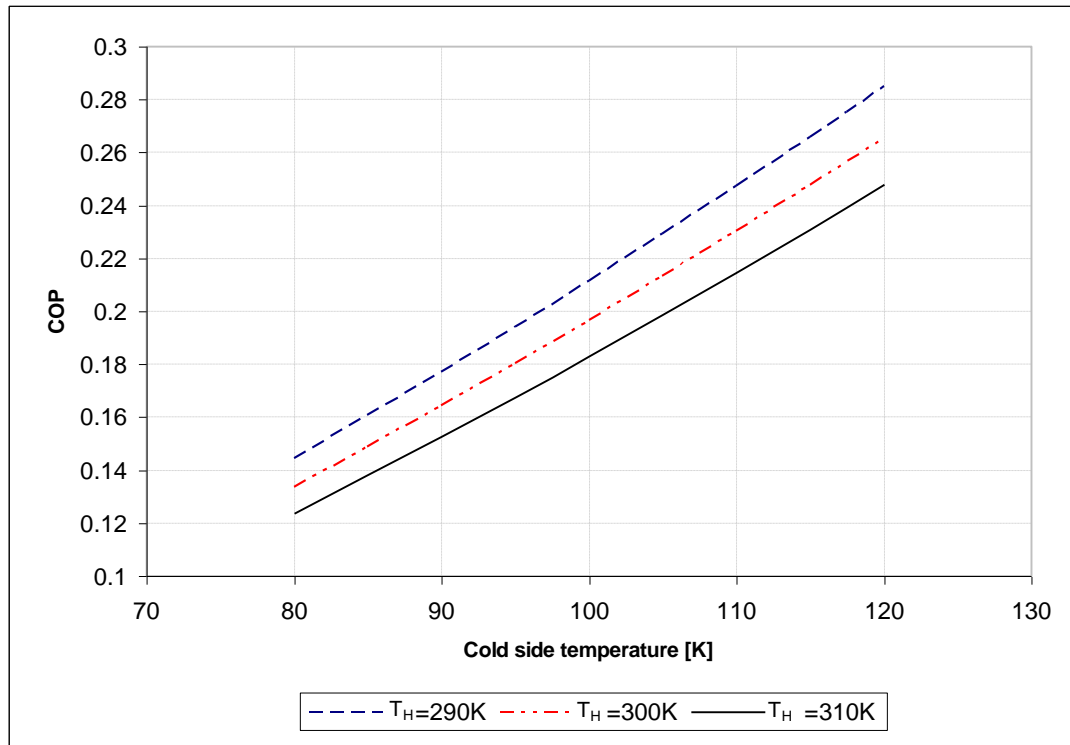


Figure 3.21 Coefficient of performance at different hot side temperatures versus freezer wall temperature

Figure 3.22 shows the heat absorbed in the freezer vs freezer wall temperature. Cooling capacity follows the efficiency graph. Cryocooler has a higher cooling capacity at low temperature differences.

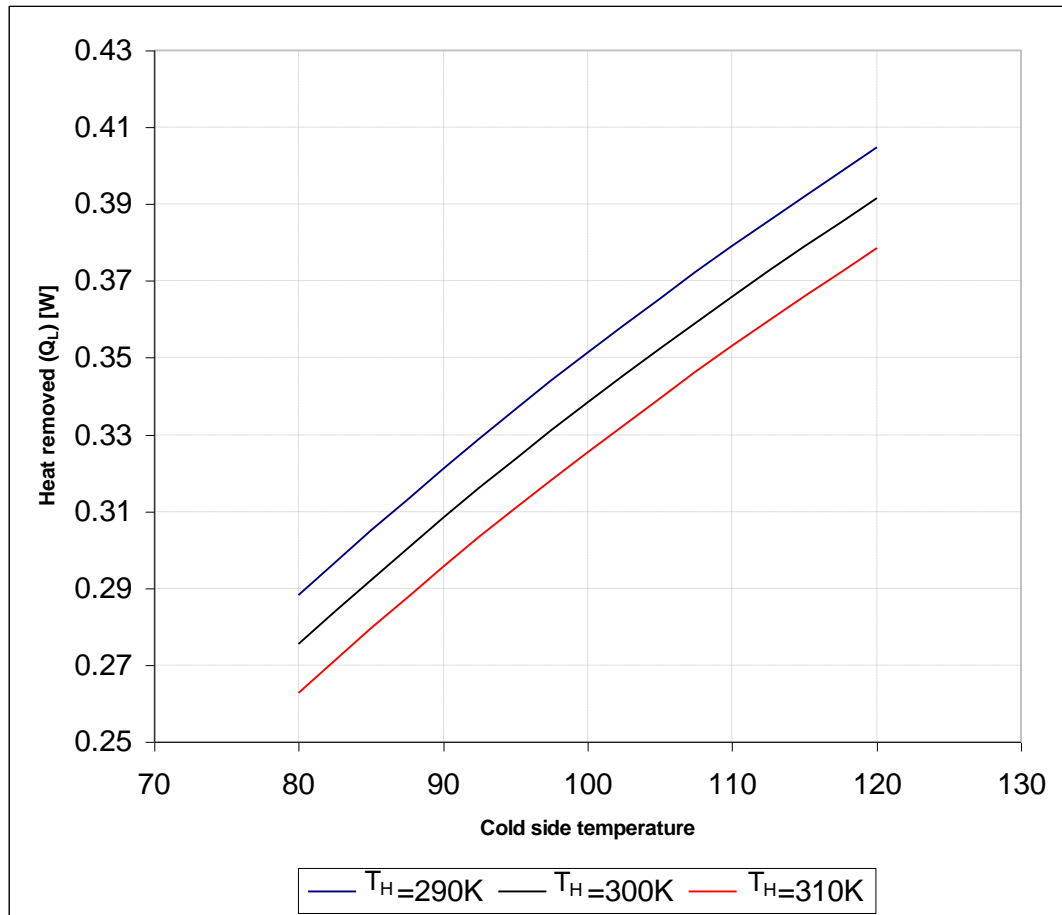


Figure 3.22 Heat removed at different temperatures versus freezer wall temperature

### 3.5.3. Effect of charging pressure

As in the case with the operating temperature difference, pressure also has direct effect on the system performance. In Figure 3.23 efficiency vs. charging pressure and in Figure 3.24 heat removed removed vs. pressure plots are given. These plots indicate that increasing pressure has positive effect on the system performance.

In practical applications pressure is dependent on the materials and on the production techniques. Since at higher values of pressure gas leakage from the cryocooler increases. These leakage results in deviation of the cryocooler performance from the designed values and a decrease in the performance occur.

Therefore, common design pressure range for cryocoolers changes between 2 to 4 MPa.

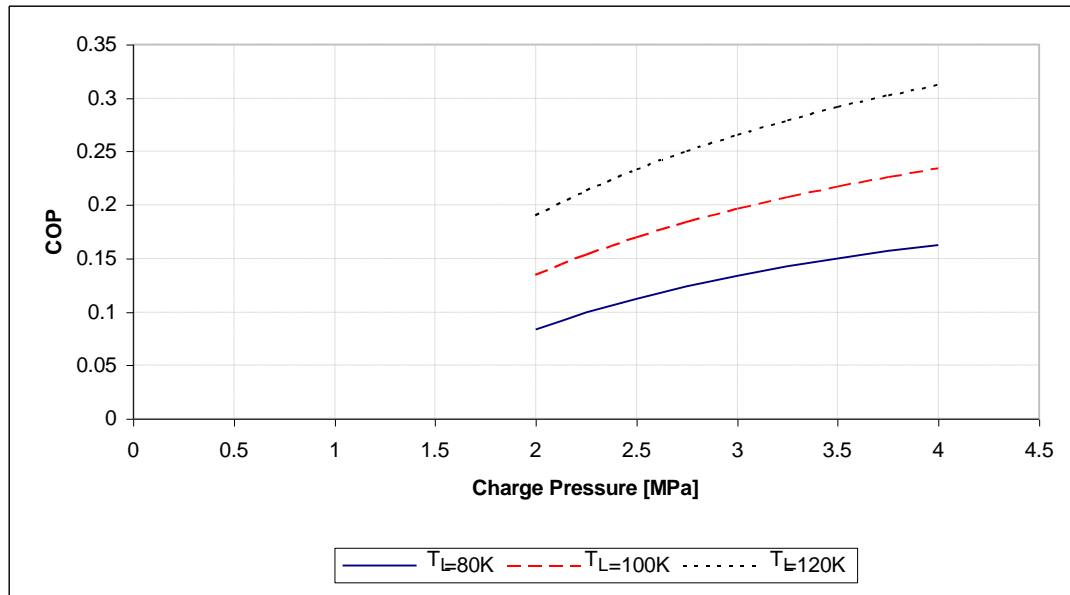


Figure 3.23 Coefficient of performance at different cold side temperatures versus charge pressure plot

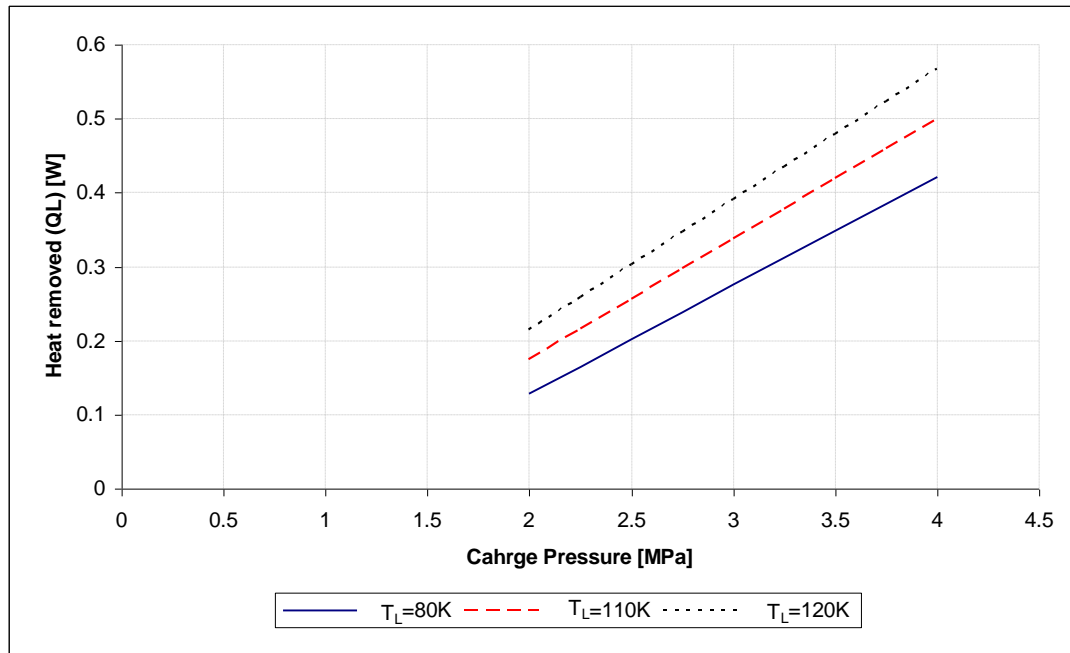


Figure 3. 24 Heat removed at different cold side temperatures versus charge pressure plot

### 3.5.4. Effect of phase angle

Phase angle is the differential angle between compression and expansion pistons and it has a considerable effect on the performance of the system as seen in Figure 3.25. As the phase angle decreases the efficiency of the system increases up to a point. However it can be observed that when phase angle decreases cooling capacity also decreases. At about  $70^\circ$  optimum point can be achieved where cooling capacity and efficiency curves intersect.

In figure 3.26 it is shown that the work input is strongly related to phase angle. In actual cryocoolers phase angle is adjusted accurately according to the dimensions of the machine, since optimum phase angle is effected by pressure drops in the machine.(Otaka 2002)

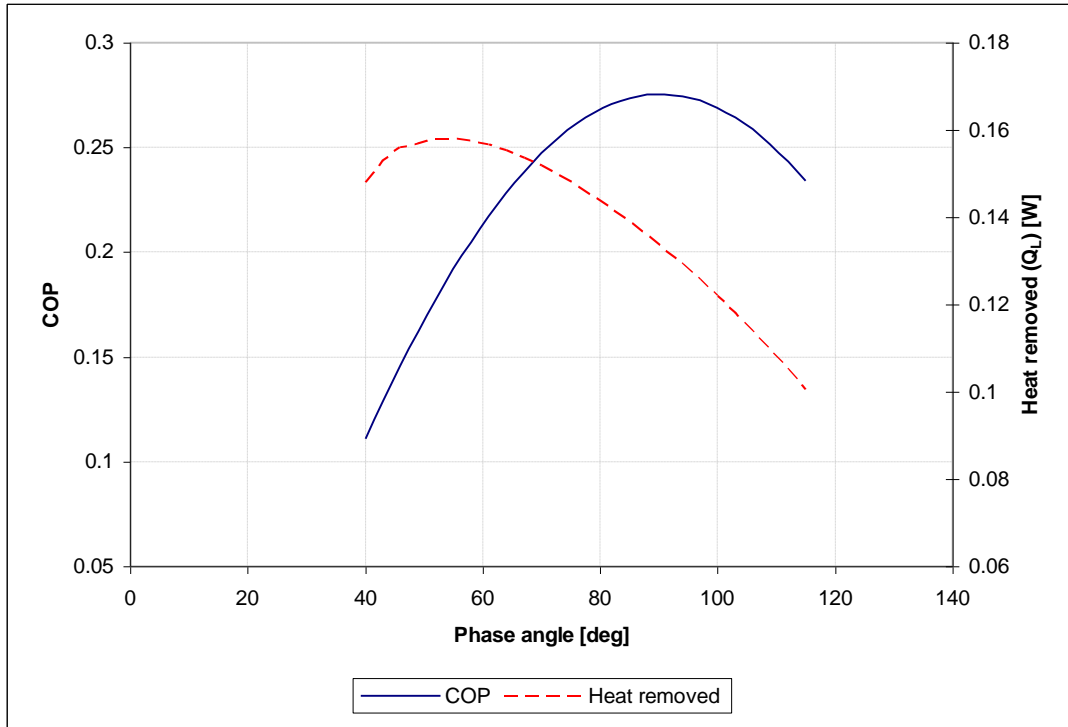


Figure 3.25 Coefficient of performance and heat removed [W] versus phase angle plot

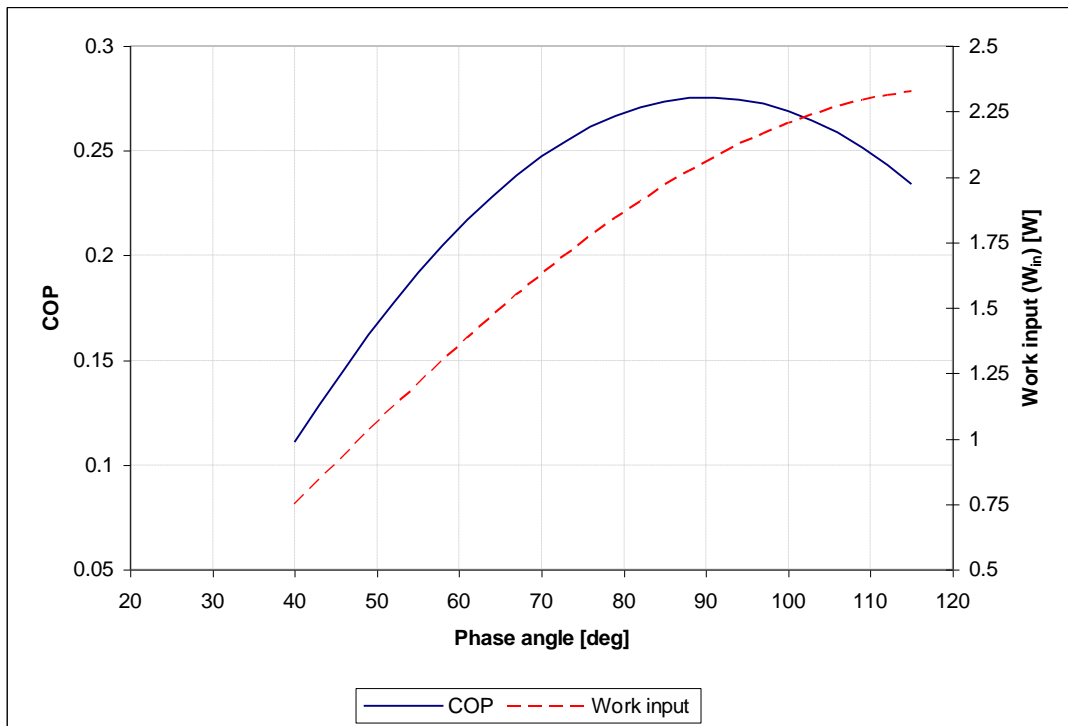


Figure 3.26 Coefficient of performance and work input [W] versus phase angle plot

## **CHAPTER 4**

### **CONCLUSION**

#### **4.1 Interpretation of the results of the three analysis**

In this research three different methods of analysis of Stirling cryocoolers are employed. The results presented in previous chapter indicate that Schmidt analysis and ideal adiabatic analysis give optimistic predictions. However they are useful for an initial consideration of the cryocooler performance. Simple analysis is more realistic in terms of performance prediction. This analysis allows to analyze system parameters in a detailed manner. Especially to be able to predict the regenerator performance is crucial in a cryocooler design.

By performing simple analysis, the effects of losses in the system due to non-ideal components are quantified. Regenerative losses, flow friction losses and conduction losses are obtained decoupled from the system by employing ideal adiabatic analysis. By using these loss values the gas temperature in the cooler and freezer are predicted. It is emphasized that these losses have a significant effect on the system performance and it can be concluded an analysis excluding these losses is far from realistic values.

The results of the simple analysis indicate that the regenerator porosity is a very important design parameter. It should be adjusted by considering both its negative and positive effects. A high or a low value can result in increased regenerative losses or increased flow friction losses respectively. This fact should be considered in the optimization process. Although the regenerator has a massive effect, regenerator do not solely determine the overall performance. Other parameters such as working

pressure, operating temperature difference pressure and phase angle difference has significant effect, which should be included in the optimization.

#### **4.2 Future work and recommendations**

In this research dimensions and operating parameters employed have assumed values. Although it is attempted to be as realistic as possible, employing practical values may be useful, where it could be possible to compare the results with a real cryocooler and verify the results obtained by numerical analysis. By comparing the results, numerical model could be modified and adjusted to give better results.

The losses evaluated by simple analysis may also include losses in the regenerator section due to conduction in mesh material, shuttle loss, which is caused by the gap between the displacer and the cold finger and radiation losses between the cold tip and the environment.

The main drawback of the simple analysis other than the losses it doesn't include is the assumption that the regenerator is at a constant temperature, mean effective temperature. In the regenerator, the temperature of the gas has highest temperature gradient, which shows that constant temperature assumption is a very poor approach to the solution. The results of the simple analysis can be improved by dividing the regenerator into a finite number of volumes and solving the equations for regenerator for each volume as if there are multiple regenerators in the cryocooler. By doing so the effects of the regenerator can be included in a more realistic way.

Moreover further studies may include a third order numerical analysis. Third order analysis employs dividing the cryocooler into control volumes and solving conservation equations for each segment, which could yield to more precise results

## REFERENCES

Aerospace.2009. Cryogenic Systems Overview <<http://www.aero.org/publications/donabedian/donabedian-1.html>> Last accessed date: 2010, August 29.

Altman A. 2003. SNAPpro Stirling Numerical Analysis Program, In: Proc. of the 11th International Stirling Engine Conference, Rome, University of Rome “La Sapienza” p. 166-172.

Altman A. 2005. SNAPpro. <<http://home.comcast.net/~snapburner>> Last accessed date: 2010, August 30.

Andersen ST, Carlsen H and Thomsen PG. 2006. Numerical study on optimal Stirling engine regenerator matrix designs taking into account the effects of matrix temperature oscillations Energy Conversion and Management 47: 894–908.

Berchowitz DM. 1978. A computer and experimental simulation of stirling cycle machines. [MS Thesis] University of Witwatersrand.

Butterworth-Heinemann (2006) in hisbook “ Cryogenic technology and applications

Creswick FA. 1965. Thermal design of Stirling cycle machines. Int. Auto. Eng. Congr. Detroit, SAE 650079.

Dunmire H. 1998. U. S. Army cryocooler status update,” Military and commercial applications for low cost cryocoolers. Electronic Industries Association (EIA), Arlington, VA.

Dwight HB. 1961. Tables of integrals and other mathematical data 4th edn (New York: Macmillan).

Dyson RW, Wilson SD and Tew RC. 2004. Review of computational Stirling. Analysis Methods [gltrs.grc.nasa.gov/reports/2004/TM-2004-213300.pdf](http://gltrs.grc.nasa.gov/reports/2004/TM-2004-213300.pdf) Last accessed date: 2010, August 30.

Finkelstein T. 1975. Computer Analysis of Stirling Engines. Proc. 10th IECEC.

Gedeon D. 1992. GLIMPS Version 4: User's Manual. Gedeon Associates.

Gedeon D. 1994. Sage - Object-oriented software for Stirling machine design", AIAA Paper 94-4106.

(A) Gedeon D. 1999. Sage:Stirling-Cycle Model-Class Reference Guide, Third Ed.", Gedeon Associates.

(B) Gedeon D. 1999. Sage:User's Guide, Third Edition" Gedeon Associates.

Geng SM, Tew RC. 1992. Comparison of GLIMPS and HFAST Stirling Engine Code Predictions with Experimental Data. NASA TM-105549, 27th IECEC.

Haywood D. 2008. An introduction to Stirling cycle machines. <http://www.docstoc.com/docs/2688629/AN-INTRODUCTION-TO-STIRLING-CYCLE-MACHINES> Last accessed date: 2010, August 30.

Hu Z. 2007. Thermoacoustic expansion valve: a new type of expander to enhance performance of recuperative cryocooler systems. <http://minds.wisconsin.edu/bitstream/handle/1793/21648/57.pdf.txt?sequence=2> Last accessed date: 2010, August 29.

Huang SC. 1993. HFAST Version 2.00: User Manual", Mechanical Technology, Inc., NASA Contract NAS3-25330.

Jha AR. 2006. Cryogenic technology and applications. Elsevier Inc. p. 147

Jones JD. 1982. A new regenerator theory. In: Proceedings of the 17th Intersociety energy conversion engineering conference, p. 1656–61.

Kosov BV. 2003. In: Low temperature and cryogenic Refrigeration. Ed. Kakaç SH, Avelino MR. Kluwer Academic publishers p. 9

Martini WR. 1978. Stirling Engine Design Manual. DOE/NASA Technical report DOE/NASA/3152-78/1 (NASA CR-135382), Joint Center For Graduate Study.

Martini WR. 1983. Stirling Engine Design Manual Second Edition. DOE/NASA Technical report DOE/NASA/3194-1 (NASA CR-168088 and/or CR-158088), NASA Lewis Research Center.

Martini WR. 1983. Stirling engine design manual. 2nd Ed.", NASA CR-168088.

Radebaugh R. 1991. In: Applications of cryogenic technology, 10th Ed. Ed. Kelley JP. Plenum Press. p. 15.

Otaka T. 2002 Study of Performance Characteristics of a Small Stirling Refrigerator, Heat Transfer Asian Research, 2002

Radebaugh R. 1995. Recent developments in cryocoolers. Proc. Int Cong Refrigeration, Vol IIIb, Paris, p. 973.

Radebaugh R. 2000. Pulse Tube Cryocoolers for Cooling Infrared Sensors. Proceedings of SPIE, The International Society for Optical Engineering, Infrared Technology and Applications Vol 26. 4130, p. 363-379.

Radebaugh R. 2003. In: Low temperature and cryogenic refrigeration. Ed. Kakaç S, Smirnov HF, Avelino MR. Kluwer Academic publishers p: 417.

Riabzev S. 2002. Stirling cycle machine. [www.ricor.com/Uploads/58Stir-pt.pps](http://www.ricor.com/Uploads/58Stir-pt.pps)  
Last accessed date: 2010, August 30.

Sahu AB. 2010. CFD simulation of a small stirling cryocooler. [BS Thesis]. Rourkela: National Institute of Technology.

Schmidt G. 1871. The theory of Lehmann's calorimetric machine Z. Ver. Dtsch Ing. Vol. 15, Part 1.

Schmidt G. 1871. The Theory of Lehmann's Calorimetric Machine Z. ver. Dtsch. Ing. 15 part I.

Sier R. 2009. Computer programs for simulating Stirling engines <<http://www.stirlingengines.org.uk/simulation/simulat.html>> Last accessed date: 2010, August 30.

Thomas, B. 2006. Web page of Prof. Dr.-Ing. Bernd Thomas at the Reutlingen University. <<http://userserv.fh-reutlingen.de/~thomas>> Last accessed date: 2010, August 30.

Timmerhaus KD. 1996. Cryocooler development: 1995 AIChE Institute lecture. AIChE Journal Vol 42 No: 11.

Urieli I .1980. A general purpose program for Stirling engine simulation Proe. 15th IECEC, Seattle, Washington Paper 809336 p 1701-5.

Urieli I, Berchowitz DM. 1984. Stirling cycle engine analysis. Adam Hilger Ltd., Bristol.

Urieli I, Rallis CJ, Berchowitz DOM. 1977. Computer simulation of stirling cycle machines. Proc. 12th IECEC.

Urieli I, Rallis CJ, Berchowitz DOM.1977. Computer Simulation of Stirling Cycle Machines. Proc. 12th IECEC.

Urieli I. and Walker G. 1990. An ideal adiabatic analysis of a stirling cryocooler with multiple expansion stages. Southampton, England, UK. Low Temperature Engineering and Cryogenics Conference.

Ventura G and Risegari L. 2008. The art of cryogenics: low-temperature experimental techniques. 1st Ed. Elsevier Ltd, p. 37.

Walker G, Weiss MH, Fauvel R, Reader G. 1990. Adventures with MarWeiss: A summary Of experience with stirling simulation. In: Proc. of the 25th Intersociety Energy Conversion Engineering Conference, Reno Nevada, American Institute of Chemical Engineers., p. 342-345.

Willems DWJ. 2007. High power cryocooling. [PhD Thesis] Eindhoven: Technische Universiteit Eindhoven.

Wylen V, Sonntag RE and Borgnakke C. 1994. Fundamentals of Classical Thermodynamics. John Wiley & Sons Inc., New York.

Yuan SWK and Spradley IE. 1992. A third order computer model for stirling refrigerators. Advances in Cryogenic Engineering Vol 37 Part B Ed. RW Past Plenum Press.

Yuan SWK and Spradley IE. 1992. A third order numerical model for stirling refrigerators. Advances in cryogenic engineering. 37 B.

Yutopian Online. 2000. Numerical modeling of cryocoolers (Cryogenics, refrigerators, coolers, engines) <<http://www.yutopian.com/Yuan/MCooler.html>>  
Last accessed date: 2010, August 30.

## APPENDIX A

### NUMERICAL SIMULATION CODE DEVELOPED IN MATHCAD

#### Cryocooler dimensions and operating conditions

$\text{comp\_diam} := \frac{8}{1000}$	Compression piston diameter
$\text{comp\_swept\_dist} := \frac{6}{1000}$	Compression piston swept distance
$\text{comp\_clear\_dist} := \frac{2}{1000}$	Compression piston clearance distance
$\text{disp\_diam} := \frac{5}{1000}$	Displacer piston diameter
$\text{disp\_swept\_dist} := \frac{1}{1000}$	Displacer swept distance
$\text{disp\_clear\_dist} := \frac{.1}{1000}$	Displacer clearance distance
$v_{\text{comp\_clear}} := \text{comp\_clear\_dist} \cdot \frac{\text{comp\_diam}^2}{4} \cdot \pi$	Compression space clearance volume
$v_{\text{exp\_clear}} := \text{disp\_clear\_dist} \cdot \pi \cdot \frac{\text{disp\_diam}^2}{4}$	Expansion space clearance volume
$v_{\text{comp\_swept}} := \text{comp\_swept\_dist} \cdot \frac{\text{comp\_diam}^2}{4} \cdot \pi$	Compression space swept volume
$v_{\text{exp\_swept}} := \text{disp\_swept\_dist} \cdot \pi \cdot \frac{\text{disp\_diam}^2}{4}$	Expansion space swept volume
$\text{phase\_angle} := 90$	Phase angle between compressor and displacer
$\alpha := \text{phase\_angle} \cdot \frac{\pi}{180}$	

$dk := \text{comp\_diam}$	Cooler internal diameter
$lk := \frac{10}{1000}$	Cooler length
$ak := \pi \cdot \frac{dk^2}{4}$	Cooler internal cross-sectional area
$vk := ak \cdot dk$	Cooler volume
$awgk := \pi \cdot dk \cdot lk$	Cooler wetted area
$dh := \text{disp\_diam}$	Freezer internal diameter
$lh := \frac{2}{1000}$	Freezer length
$ah := \pi \cdot \frac{dh^2}{4}$	Freezer internal cross-sectional area
$vh := ah \cdot lh$	Freezer volume
$awgh := \pi \cdot dk \cdot lk$	Freezer wetted area
$r_{\text{out\_d}} := \text{disp\_diam}$	Regenerator wall outer diameter
$r_{\text{in\_d}} := \text{disp\_diam} - \frac{1}{1000}$	Regenerator wall inner diameter
$lr := \frac{55}{1000}$	Length of the regenerator
$awgr0 := \pi \cdot r_{\text{in\_d}} \cdot lr$	Regenerator wetted area excluding matrix
$a_{\text{matrix}} := \pi \cdot \frac{r_{\text{in\_d}}^2}{4}$	Matrix area in the regenerator
$awr := \pi \cdot \frac{(r_{\text{out\_d}}^2 - r_{\text{in\_d}}^2)}{4}$	Wall area of the regenerator
$kwr := 6$	Thermal conductivity of stainless steel for cryogenic applications
$kawr := kwr \cdot \frac{awr}{lr}$	Thermal conductance of regenerator wall
$\text{porosity} := 0.80$	Fractional void volume in the regenerator

$\text{wire}_d := \frac{0.005}{1000}$	Mesh wire diameter
$\text{ar} := \text{a}_{\text{matrix}} \cdot \text{porosity}$	Free flow area in the regenerator
$\text{vr} := \text{ar} \cdot \text{lr}$	Void volume in the regenerator
$\text{dr} := \frac{\text{wire}_d \cdot \text{porosity}}{1 - \text{porosity}}$	Hydraulic diameter of regenerator
$\text{awgr} := 4 \cdot \frac{\text{vr}}{\text{dr}} + \text{awgr0}$	Total wetted area in the regenerator
$\text{gama} := 1.67$	Cp/Cv for Helium
$\text{rgas} := 2078.6$	Gas constant of helium
$\text{mu0} := 18.8510^{-6}$	Dynamic viscosity of helium
$\text{t0} := 300$	Environment temperature
$\text{Suth} := 80$	Sutherland constant
$\text{prandtl} := 0.71$	Prandtl number
$\text{cv} := \frac{\text{rgas}}{\text{gama} - 1}$	Constant pressure specific heat of helium
$\text{cp} := \text{gama} \cdot \text{cv}$	Constant volume specific heat of helium
$\text{pmean} := 3000000$	Charging pressure
$\text{tk} := 300$	Cooler wall temperature
$\text{th} := 80$	Freezer wall temperature
$\text{tr} := \frac{\text{th} - \text{tk}}{\ln\left(\frac{\text{th}}{\text{tk}}\right)}$	Regenerator mean temperature
$\text{freq} := 60$	Operating frequency
$\text{omega} := 2 \cdot \pi \cdot \text{freq}$	

### Sinusoidal volume variations

$$\text{vc}(\text{theta}) := \text{v}_{\text{comp\_clear}} + \frac{1}{2} \cdot \text{v}_{\text{comp\_swept}} \cdot (1 + \cos(\text{theta} + \pi))$$

$$\text{ve}(\text{theta}) := \text{v}_{\text{exp\_clear}} + \frac{1}{2} \cdot \text{v}_{\text{exp\_swept}} \cdot (1 + \cos(\alpha + \text{theta} + \pi))$$

$$\text{dvc}(\text{theta}) := -\frac{1}{2} \cdot \text{v}_{\text{comp\_swept}} \cdot \sin(\text{theta} + \pi)$$

$$\text{dve}(\text{theta}) := -\frac{1}{2} \cdot \text{v}_{\text{exp\_swept}} \cdot \sin(\alpha + \text{theta} + \pi)$$

## Schmidt Analysis

$$c := \sqrt{\left(\frac{v_{\text{exp\_swept}}}{t_h}\right)^2 + \left(\frac{v_{\text{comp\_swept}}}{t_k}\right)^2 + 2 \cdot \left(\frac{v_{\text{exp\_swept}}}{t_h}\right) \cdot \left(\frac{v_{\text{comp\_swept}}}{t_k}\right) \cdot \cos(\alpha) \cdot \frac{1}{2}}$$

$$s := \frac{\left(\frac{v_{\text{comp\_swept}}}{2} + v_{\text{comp\_clear}} + v_k\right)}{t_k} + \frac{v_r}{t_r} + \frac{\left(\frac{v_{\text{exp\_swept}}}{2} + v_{\text{exp\_clear}} + v_h\right)}{t_h}$$

$$b := \frac{c}{s}$$

$$\text{sqrtb} := \sqrt{1 - b^2}$$

$$\text{bf} := 1 - \frac{1}{\text{sqrtb}}$$

$$\text{beta} := \text{atan} \left( \frac{\frac{v_{\text{exp\_swept}} \cdot \sin(\alpha)}{t_h}}{\frac{v_{\text{exp\_swept}} \cdot \cos(\alpha)}{t_h} + \frac{v_{\text{comp\_swept}}}{t_k}} \right)$$

$$\text{mgas} := \frac{\text{pmean} \cdot s \cdot \text{sqrtb}}{r_{\text{gas}}}$$

$$\text{wc} := \frac{\pi \cdot v_{\text{comp\_swept}} \cdot \text{mgas} \cdot r_{\text{gas}} \cdot \sin(\text{beta}) \cdot \text{bf}}{c}$$

$$\text{we} := \frac{\pi \cdot v_{\text{exp\_swept}} \cdot \text{mgas} \cdot r_{\text{gas}} \cdot \sin(\text{beta} - \alpha) \cdot \text{bf}}{c}$$

$$w := \text{wc} + \text{we}$$

$$\text{power} := w \cdot \text{freq}$$

$$\text{eff} := \left| 100 \frac{\text{we}}{w} \right|$$

## Derivations of the equations used in the ideal adiabatic analysis

$$\begin{aligned}
 \text{deriv\_adiab}(\theta, y) := & \quad y_{VC} \leftarrow v_c(\theta) \\
 & \quad y_{VE} \leftarrow v_e(\theta) \\
 & \quad dy_{VC} \leftarrow dv_c(\theta) \\
 & \quad dy_{VE} \leftarrow dv_e(\theta) \\
 & \quad v_{ot} \leftarrow \frac{v_k}{t_k} + \frac{v_r}{t_r} + \frac{v_h}{t_h} \\
 & \quad y_P \leftarrow \frac{m_{gas} \cdot r_{gas}}{\frac{y_{VC}}{y_{TC}} + v_{ot} + \frac{y_{VE}}{y_{TE}}} \\
 & \quad dy_P \leftarrow \frac{-y_P \left( \frac{dy_{VC}}{y_{TCK}} + \frac{dy_{VE}}{y_{THE}} \right)}{\frac{y_{VC}}{y_{TCK} \cdot \gamma} + v_{ot} + \frac{y_{VE}}{y_{THE} \cdot \gamma}} \\
 & \quad y_{MC} \leftarrow \frac{y_P \cdot y_{VC}}{r_{gas} \cdot y_{TC}} \\
 & \quad y_{MK} \leftarrow \frac{y_P \cdot v_k}{r_{gas} \cdot t_k} \\
 & \quad y_{MR} \leftarrow \frac{y_P \cdot v_r}{r_{gas} \cdot t_r} \\
 & \quad y_{MH} \leftarrow \frac{y_P \cdot v_h}{r_{gas} \cdot t_h} \\
 & \quad y_{ME} \leftarrow \frac{y_P \cdot y_{VE}}{r_{gas} \cdot y_{TE}} \\
 & \quad dy_{MC} \leftarrow \frac{y_P \cdot dy_{VC} + \frac{y_{VC} \cdot dy_P}{\gamma}}{r_{gas} \cdot y_{TCK}} \\
 & \quad dy_{ME} \leftarrow \frac{y_P \cdot dy_{VE} + \frac{y_{VE} \cdot dy_P}{\gamma}}{r_{gas} \cdot y_{THE}} \\
 & \quad dy_{MK} \leftarrow \frac{y_{MK} \cdot dy_P}{y_P} \\
 & \quad dy_{MR} \leftarrow \frac{y_{MR} \cdot dy_P}{y_P} \\
 & \quad dy_{MH} \leftarrow \frac{y_{MH} \cdot dy_P}{y_P}
 \end{aligned}$$

$$\begin{aligned}
y_{GACK} &\leftarrow -dy_{MC} \\
y_{GAKR} &\leftarrow y_{GACK} - dy_{MK} \\
y_{GARH} &\leftarrow y_{GAKR} - dy_{MR} \\
y_{GAHE} &\leftarrow dy_{ME} \\
y_{TCK} &\leftarrow \begin{cases} y_{TC} & \text{if } y_{GACK} > 0 \\ tk & \text{otherwise} \end{cases} \\
y_{THE} &\leftarrow \begin{cases} th & \text{if } y_{GAHE} > 0 \\ y_{TE} & \text{otherwise} \end{cases} \\
dy_{TC} &\leftarrow y_{TC} \cdot \left( \frac{dy_P}{y_P} + \frac{dy_{VC}}{y_{VC}} - \frac{dy_{MC}}{y_{MC}} \right) \\
dy_{TE} &\leftarrow y_{TE} \cdot \left( \frac{dy_P}{y_P} + \frac{dy_{VE}}{y_{VE}} - \frac{dy_{ME}}{y_{ME}} \right) \\
dy_{QK} &\leftarrow \frac{vk \cdot dy_P \cdot cv}{rgas} - cp \cdot (y_{TCK} \cdot y_{GACK} - tk \cdot y_{GAKR}) \\
dy_{QR} &\leftarrow \frac{vr \cdot dy_P \cdot cv}{rgas} - cp \cdot (tk \cdot y_{GAKR} - th \cdot y_{GARH}) \\
dy_{QH} &\leftarrow \frac{vh \cdot dy_P \cdot cv}{rgas} - cp \cdot (th \cdot y_{GARH} - y_{THE} \cdot y_{GAHE}) \\
dy_{WC} &\leftarrow y_P \cdot dy_{VC} \\
dy_{WE} &\leftarrow y_P \cdot dy_{VE} \\
dy_W &\leftarrow dy_{WC} + dy_{WE} \\
y_W &\leftarrow y_{WC} + y_{WE} \\
AA_{1,1} &\leftarrow y \\
AA_{1,2} &\leftarrow dy \\
AA &
\end{aligned}$$

## 4th order Runge Kutta Routine

```

rk4(n, x, dx, y) :=
  x0 ← x
  y0 ← y
  dy1 ← deriv_adiab(x0, y)1,2
  y ← deriv_adiab(x0, y)1,1
  for i ∈ 1..n
    yi ← y0i + 0.5 dx · dy1i
  xm ← x0 + 0.5 dx
  dy2 ← deriv_adiab(xm, y)1,2
  y ← deriv_adiab(xm, y)1,1
  for i ∈ 1..n
    yi ← y0i + 0.5 dx · dy2i
  dy3 ← deriv_adiab(xm, y)1,2
  y ← deriv_adiab(xm, y)1,1
  for i ∈ 1..n
    yi ← y0i + dx · dy3i
  x ← x0 + dx
  dy ← deriv_adiab(x, y)1,2
  y ← deriv_adiab(x, y)1,1
  for i ∈ 1..n
    
$$\begin{cases} dy_i \leftarrow (dy1_i + 2 \cdot dy2_i + 2 dy3_i + dy_i) \cdot \frac{1}{6} \\ y_i \leftarrow y0_i + dx \cdot dy_i \end{cases}$$

  AA1,1 ← x
  AA1,2 ← y
  AA1,3 ← dy
  AA

```

max\_iteration = 20

ninc := 360

dt\_heta :=  $2 \cdot \frac{\pi}{ninc}$

epsilon := 0.01

terror := 1

```

adiabatic(n, theta, dtheta, y, th, tk) :=
  iter ← 0
  yTHE ← th
  yTCK ← tk
  yTE ← th
  yTC ← tk
  for i ∈ 1..max_iteration
    theta ← 0
    tc0 ← yTC
    te0 ← yTE
    yQK ← 0
    yQR ← 0
    yQH ← 0
    yWC ← 0
    yWE ← 0
    yW ← 0
    for i ∈ 1..ninc
      theta ← rk4(n, theta, dtheta, y)1,1
      y ← rk4(n, theta, dtheta, y)1,2
      dy ← rk4(n, theta, dtheta, y)1,3
      for j ∈ 1..22
        varj,i ← yj
      for j ∈ 1..16
        dvarj,i ← dyj
      terror ← |tc0 - yTC| + |te0 - yTE|
      iter ← iter + 1
      break if terror < epsilon
  AA1,1 ← theta
  AA1,2 ← y
  AA1,3 ← dy
  AA1,4 ← iter
  AA1,5 ← var
  AA1,6 ← dvar
  AA1,7 ← terror
  AA

```

## Evaluation of Reynolds Number

$$\text{reynold}(t, g, d) := \left\{ \begin{array}{l} \mu \leftarrow \mu_0 \frac{(t_0 + S_{\text{uth}})}{(t + S_{\text{uth}})} \cdot \left(\frac{t}{t_0}\right)^{1.5} \\ k_{\text{gas}} \leftarrow \frac{c_p \cdot \mu}{\text{prandtl}} \\ \text{re} \leftarrow \frac{|g| \cdot d}{\mu} \\ \text{re} \leftarrow 1 \text{ if } \text{re} < 1 \\ \text{AA}_1 \leftarrow \mu \\ \text{AA}_2 \leftarrow k_{\text{gas}} \\ \text{AA}_3 \leftarrow \text{re} \\ \text{AA} \end{array} \right.$$

## Evaluation of Stanton number

$$\text{stanton}(\text{porosity}, \text{re}) := \left\{ \begin{array}{l} m \leftarrow 0.43\text{porosity} + 0.15 \\ p \leftarrow 0.537\text{porosity} \text{ if } \text{porosity} < 0.39 \\ p \leftarrow 1.54 - 6.36\text{porosity} + 7.56\text{porosity}^2 \text{ if } \text{porosity} \geq 0.39 \\ \text{st} \leftarrow p \cdot \frac{\text{re}^{-m}}{\text{prandtl}} \\ \text{st} \end{array} \right.$$

## Evaluation of friction factor $Fr = Re \cdot Ff$

$$\text{frictionfac}(d, \mu, \text{re}) := \left\{ \begin{array}{l} \text{fr} \leftarrow 16 \text{ if } \text{re} < 2000 \\ \text{fr} \leftarrow \text{re} \left[ \frac{0.008(\text{re} - 4000)}{-2000} + \frac{0.001(\text{re} - 2000)}{2000} \right] \text{ if } 2000 < \text{re} < 4000 \\ \text{fr} \leftarrow 0.0791\text{re}^{0.75} \text{ if } \text{re} > 4000 \\ \text{ht} \leftarrow \frac{\text{fr} \cdot \mu \cdot c_p}{2 \cdot d \cdot \text{prandtl}} \\ \text{AA}_1 \leftarrow \text{fr} \\ \text{AA}_2 \leftarrow \text{ht} \\ \text{AA} \end{array} \right.$$

## Evaluation of regenerator losses due to imperfection

```

regenloss(tr, var) :=
  sumre ← 0
  remax ← 0
  qqee ← var
  for i ∈ 1..360
    gari ←  $\frac{(qqee_{GAKR,i} + qqee_{GARH,i}) \cdot \omega}{2}$ 
    gr ←  $\frac{gar_i}{ar}$ 
    mu ← reynold(tr, gr, dr)1
    kgas ← reynold(tr, gr, dr)2
    rei ← reynold(tr, gr, dr)3
    sumre ← sumre + rei
    remax ← rei if rei > remax
    qregi ← qqeeQR,i
  reavg ←  $\frac{sumre}{360}$ 
  st ← stanton(porosity, reavg)
  fr ← 54 + 1.43reavg0.78
  ntu ←  $\frac{st \cdot awgr}{2 \cdot ar}$ 
  effect ←  $\frac{ntu}{ntu + 1}$ 
  qrmin ← min(qreg)
  qrmax ← max(qreg)
  qrloss ← (1 - effect) · (qrmax - qrmin)
  qrloss

```

## Evaluation of new gas temperature in the freezer after regenerator losses

```

freezertem(twh, qrloss, var, tr) :=
  sumre ← 0
  remax ← 0
  qqee ← var
  for i ∈ 1..360
    |
    |   (qqeeGARH,i + qqeeGAHE,i) · omega
    |   _____
    |   2
    |
    |   ghi
    |   _____
    |   ah
    |
    |   mu ← reynold(th, gh, dh)1
    |   kgas ← reynold(th, gh, dh)2
    |   re1 ← reynold(th, gh, dh)3
    |   sumre ← sumre + re1
    |   remax ← re1 if re1 > remax
    |   qregi ← qqeeQR,i
    |
    |   sumre
    |   _____
    |   360
    |
    |   fr ← frictionfac(dh, mu, reavg)1
    |   ht ← frictionfac(dh, mu, reavg)2
    |
    |   tgh ← twh - (qqeeQH,360 - regen loss(tr, var)) ·  $\frac{freq}{ht \cdot a_{gh}}$ 
    |
    |   tgh
  
```

## Evaluation of new gas temperature in the cooler after regenerator losses

```

coolertemp(twk, qrloss, var, tr) :=
  sumre ← 0
  remax ← 0
  qqee ← var
  for i ∈ 1..360
    |
    | 
$$gak_i \leftarrow \frac{(qqee_{GACK,i} + qqee_{GAKR,i}) \cdot \omega}{2}$$

    |
    | 
$$gk \leftarrow \frac{gak_i}{ak}$$

    |
    | 
$$\mu \leftarrow \text{reynold}(tk, gk, dk)_1$$

    |
    | 
$$k_{gas} \leftarrow \text{reynold}(tk, gk, dk)_2$$

    |
    | 
$$re_i \leftarrow \text{reynold}(tk, gk, dk)_3$$

    |
    | 
$$\text{sumre} \leftarrow \text{sumre} + re_i$$

    |
    | 
$$\text{remax} \leftarrow re_i \text{ if } re_i > \text{remax}$$

    |
    | 
$$qreg_i \leftarrow qqee_{QR,i}$$

    |
  reavg ← 
$$\frac{\text{sumre}}{360}$$

  fr ← frictionfac(dk, mu, reavg)1
  ht ← frictionfac(dk, mu, reavg)2
  tgk ← 
$$twk - (qqee_{QK,360} + \text{regenloss}(tr, var)) \cdot \frac{\text{freq}}{ht \cdot awgk}$$

  tgk

```

## Evaluation of flow friction losses

```

frictionloss(var, dvar) :=
  dwork ← 0
  qqee ← var
  dqqee ← dvar
  for i ∈ 1..ninc
    gk ←  $\frac{(qqee_{GACK,i} + qqee_{GAKR,i}) \cdot \omega}{2 \cdot ak}$ 
    rei ← reynold(tk, gk, dk)3
    mu ← reynold(tk, gk, dk)1
    fr ← frictionfac(dk, mu, re)1
    dpkoli ←  $\frac{2 \cdot fr \cdot \mu \cdot vk \cdot gk \cdot lk}{qqee_{MK,i} \cdot dk^2}$ 
    gr ←  $\frac{(qqee_{GAKR,i} + qqee_{GARH,i}) \cdot \omega}{2 \cdot ar}$ 
    rei ← reynold(tr, gr, dr)3
    mu ← reynold(tr, gr, dr)1
    fr ← frictionfac(dr, mu, re)1
    dpregi ←  $\frac{2 \cdot fr \cdot \mu \cdot vr \cdot gr \cdot lr}{qqee_{MR,i} \cdot dr^2}$ 
    gh ←  $\frac{(qqee_{GARH,i} + qqee_{GAHE,i}) \cdot \omega}{2 \cdot ah}$ 
    rei ← reynold(th, gh, dh)3
    mu ← reynold(th, gh, dh)1
    fr ← frictionfac(dh, mu, re)1
    dphoti ←  $\frac{2 \cdot fr \cdot \mu \cdot vh \cdot gh \cdot lh}{qqee_{MH,i} \cdot dh^2}$ 
    dpi ← dpkoli + dpregi + dphoti
    dwork ← dwork + dpi · dtheta · dqqeeVE,i
    pcomi ← qqeeP,i
    pexpi ← pcomi + dpi
  dummy1 ← dpkol
  dummy2 ← dpreg
  dummy3 ← dphot
  dummy4 ← dwork
  dummy

```

## Simple analysis

```

simple := |
  error ← 10·epsilon
  for iter ∈ 1..20
    |
    var ← adiabatic(7, theta, dtheta, y, th, tk)1,5
    dvar ← adiabatic(7, theta, dtheta, y, th, tk)1,6
    qrloss ← regenloss(tr, var)
    tgh ← freezertemp(twh, qrloss, var, tr)
    tgk ← coolertemp(twk, qrloss, var, tr)
    error ← |th - tgh| + |tk - tgk|
    break if error < 0.00001
    th ← tgh
    tk ← tgk
    tr ←  $\frac{th - tk}{\ln\left(\frac{th}{tk}\right)}$ 
  qrwall ← kawr ·  $\frac{(th - tk)}{freq}$ 
  dummy1 ← qrwall
  dummy2 ← var
  dummy3 ← th
  dummy4 ← tk
  dummy5 ← error
  dummy6 ← frictionloss(var, dvar)4
  dummy7 ← frictionloss(var, dvar)3
  dummy8 ← frictionloss(var, dvar)2
  dummy9 ← frictionloss(var, dvar)1
  dummy10 ← iter
  dummy11 ← qrloss
  dummy

```